Title

Photoselective Shade Films Mitigate Effects of Climate Change on Grapevine (Vitis vinifera L.) and Provide Insight to Trellis Adaptation in Hot Climates

Author

Marigliano, Lauren Elizabeth

Publication Date

2023

Peer reviewed|Thesis/dissertation

Photoselective Shade Films Mitigate Effects of Climate Change on Grapevine (*Vitis vinifera* L.) and Provide Insight to Trellis Adaptation in Hot Climates

By

LAUREN MARIGLIANO
DISSERTATION

Submitted in partial satisfaction of the requirements for the degree of

DOCTOR OF PHILOSOPHY

in

Horticulture and Agronomy

in the

OFFICE OF GRADUATE STUDIES

of the

UNIVERSITY OF CALIFORNIA

DAVIS

Approved:

Dario Cantù, Chair

Megan Bartlett

Daniele Zaccaria

Committee in Charge

2023

ACKNOWLEDGEMENTS

To start, I would like to thank Dr. Kaan Kurtural for his outstanding role as my major professor and mentor through my doctorate program. I came to UC Davis at the height of a global pandemic with very few connections in California. In what was already an isolating cross-country move, Kaan opened his arms and his home to a welcome a bright-eyed master's student from New York looking to make her mark on viticulture research. When I approached Kaan with the idea to pursue my Ph.D., he offered only his enthusiastic support. Few mentors are like Kaan. He wishes only the best for his students and will do everything in his power to ensure that they succeed. There aren't enough words to express my gratitude.

The skills I acquired over my time at Oakville Station can be attributed to the wonderful mentorships of Dr. Cliff Yu and Dr. Nazareth Torres. When I arrived at Oakville Station, Cliff and Nazareth dedicated themselves to ensuring that I had a toolbox of skills and knowledge that would last long after our time together. They strived to make work fun, whether it be blasting music in the lab or making delicious lunches during the somewhat grueling summer months. After they moved on to pursue their own careers, Cliff and Nazareth continued to cheer me on from afar, celebrating the major milestones of my degree process. Not only were they both incredible mentors, but also amazing friends with whom I share many fond memories. I am forever grateful to have learned from two extraordinary scientists.

Experiments are almost never the sole work of one person, but rather a culmination of the time and dedication of many. In my time at UC Davis, I have had the opportunity to work with a great group of people: Chris Gilmer, Maria Zumkeller, Dimitrios Mainos, Georgios Ampelas and Justin Tanner. Thank you for all your help and friendship. Our lab outings to baseball and basketball games are among my favorite memories.

I would like to thank all the faculty who provided advising and support throughout my time at UC Davis. Thank you to all my QE committee members for challenging me to look past the initial interpretation of my research. The QE is incredibly stressful in every aspect of the word. Yet, the experience was made only slightly less stressful knowing I had friendly faces in front of me. I would especially like to thank Dr. Anita Oberholster and Dr. Daniele Zaccaria for their guidance throughout my QE preparation. Additionally, I would like to thank my academic advisor Dr. Dario Cantu for filling whatever role I asked of him.

Without financial support, research is impossible. Thank you to the UC Davis Horticulture and Agronomy Graduate Group, the UC Davis Department of Viticulture and Enology, the American Society for Enology and Viticulture and Daios Plastics for their generous financial support over the years.

To David, my boyfriend and best friend. There is no one else on this planet who was lucky enough to experience the day-to-day of my Ph.D. adventure. You dutifully provided consistent love and emotional support throughout this entire undertaking. I wasn't sure you were going to make it through three months of QE prep. But alas, you made it! I am excited to see what comes next for us.

The biggest "Thank You" goes to my parents and family. Mom and Dad, my path to where I am today started with you. You encouraged me to be independent and strive for success. Despite the distance between us, there was never a time when I didn't know you were by my side. This achievement is as much yours as it is mine. You should be proud of the fantastic parents you are. I love you with all my heart.

ABSTRACT

This study was conducted to evaluate the efficacy of using photoselective shade films as a climate change impact mitigation practice in microirrigated vineyard systems in 2020 and 2021. Four photoselective shade films with varying transmission spectra (D1, D3, D4, D5) were compared to a control treatment (C0) consisting of uncovered grapevines. Net carbon assimilation and stomatal conductance were unaffected by shade films despite the photosynthetically active radiation (PAR) being reduced approximately by 20%. Additionally, fruit yield, total soluble solids, pH and titratable acidity were unaffected by shade films in either experimental year. Ultimately, shade films which reduced near infrared radiation increased anthocyanin concentration by 27% in 2020, the hotter of the two experimental years due to cluster temperature reduction of 9°C. Improved flavonoid profiles observed in grapes at harvest was directly transmitted to resultant wines. Additionally, wines obtained from the D4 treatment exhibited a more fruity and pleasant aroma profile than wines from the C0 treatment.

To segue from artificial shading vineyard interventions to utilizing the vine's natural shading capacity via canopy architecture, the water footprint of six trellis systems under three irrigation amounts was evaluated from 2020 to 2022, as there is a lack of information surrounding vine water requirements for various trellis systems commonly used in hot wine grape production regions. Vine water use efficiency was improved with reductions in applied water amounts. Additionally, single high wire (SH) trellis systems had the highest crop water use efficiency in all experimental years due to increased yield. Applied water amounts and trellis systems effected total water footprint and its components. The 25% ET_c treatment had lower blue water footprint in all three years but greater WF_{grey} and WF_{total} compared to 50% and 100% ET_c treatments. In 2020, SH trellis systems had the lowest WF_{blue}. In 2021, WF_{total} and its

components were reduced in single high wire and high quadrilateral (HQ) trellis systems. Ultimately, there was no significant effect of trellis on WF_{total} and its components in 2022. Under severe drought conditions, vines grown with single high wire trellis systems under irrigation regimes corresponding to replacement of 50-100% ET_c were able to sustain yields and carbohydrate allocation. In light of a climate that is increasingly variable and the reduction of an available and trainable labor force, SH irrigated to 50-100% of ET_c provided adequate fruit yield as well as a reduction of WF_{total} and amelioration of WUE_c.

Overall, this study provided information to support the need for heat mitigation strategies under future climate change conditions in hot viticulture regions. Shade films proved to be viable option for premium grape and wine producers to maintain and improve fruit and wine quality against increasing frequency and severity of heat wave events. Subsequently, reduced water availability, either by drought or increasingly stringent environmental regulations, will require adaptation measures to restore vineyard water balance. Our study provided information supporting the application of deficit irrigation strategies and trellis systems to improve vineyard water use efficiency. In conclusion, single high wire trellis systems irrigated with a water amount corresponding to at least 50% ET_c replacement can reduce the total water footprint of the vineyard system without compromising profitable fruit yield and composition, thus providing a viable solution to mitigate the effects of both increasing air temperatures and reduced water supply that result from an increasingly variable and changing climate.

Table of Contents

Introduction

A changing climate is threatening the sustainability of the vineyard itself as well as the quality of its outputs. More frequent heat waves result in a dissociation of primary and secondary metabolism in the grape berries due to reduced biosynthesis and thermal degradation of secondary metabolites. This decoupling between primary and secondary metabolites led to decreases in vintage quality in historical premium wine production regions. Thus, temperature mitigation strategies for wine grape vineyards in hot viticulture regions appear necessary under climate change conditions. Ultimately, artificial shading may provide a viable solution for premium grape growing regions. As this is a relatively expensive measure, utilizing the vine's canopy volume and architecture to shade the fruit zone may also be a viable solution. However, changes in precipitation patterns resulting in more frequent droughts reduce the water supply necessary to irrigate larger vine canopies at profitable levels. Therefore, the water footprint of various vine canopy architectures must be quantified prior to adoption of larger vine canopies at wide scale in wine grape production areas as a heat mitigation strategy.

The essential hypothesis for this study was that a reduction in grapevine canopy temperature achieved by decreasing the near-infrared component of incoming solar radiation would optimize berry and wine flavonoid and aroma profiles in hot wine grape production regions by reducing thermal degradation of these compounds. To test such hypothesis, partial exclusion of solar radiation was achieved using photoselective overhead shade films. There were two specific objectives for this study, the first being to understand the mode of action of photoselective overhead shade films on the leaf and vine physiological responses under climate change conditions. The second objective was to assess the effect of using photoselective shade films in vineyards on wine chemistry and flavonoid profile. Subsequently, this work led to

investigating the water footprint of different trellises, as grapevine training systems can provide a viable alternative to overhead shade films for achieving reduced canopy temperature and shaded clusters. Therefore, the third specific objective was to quantify the grapevine's water use efficiency and water footprint for six different trellis systems commonly used in hot viticultural areas.

This study was conducted in two vineyard blocks at the Oakville Experimental Vineyard Station in Napa County, California from 2020-2022. This Ph.D. dissertation comprises three chapters. Chapter 1 describes research work conducted during 2020 and 2021 which investigated the effects of photoselective shade films on grapevine physiology and grape berry quality. Ultimately, reduction in the near infrared component of the incoming solar radiation resulted in reduced cluster temperatures, which mitigated flavonoid degradation in the grape berry. Grapes from the film-shaded trials were collected and vinified. Chapter 2 reports the chemical properties of wines resultant from the different experimental treatments, including flavonoid and aroma profiles. Wines from film-shaded treatments produced better flavonoid and aromatic profiles compared to wines obtained from uncovered vines. While shade films are effective at mitigating effects of high temperatures resulting from climate change in wine grapes, they are a costly investment for large scale grape production. Adapting trellis systems to unconstrained and sprawling canopies is becoming more common as a method to shade clusters; however, such larger canopies have relatively higher water demands. Chapter 3 provides information from appraising the water use efficiency and water footprints of grapevine grown with six trellis systems under three regimes of applied water to provide some recommendations to growers about appropriate trellis system to adopt for long-term sustainable strategy for mitigating the adverse impacts of climate change.

A scientific article drawn from Chapter 1 was published in Frontiers in Agronomy, DOI: 10.3389/fagro.2022.898870. Another scientific article was drawn fromChapter 2 was published in Frontiers in Plant Science, DOI: 10.3389/fpls.2023.1085939. Chapter 3 is under internal review and currently being prepared to be submitted to Frontiers in Plant Science.

Chapter 1: Photoselective Shade Films Mitigate Heat Wave Damage by Reducing Anthocyanin and Flavonol Degradation in Grapevine (Vitis vinifera L.) Berries

This chapter was previously published in Frontiers in Agronomy.

Citation:

Marigliano, L. E., Yu, R., Torres, N., Tanner, J. D., Battany, M., and Kurtural, S. K. (2022). Photoselective shade films mitigate heat wave damage by reducing anthocyanin and flavonol degradation in grapevine (*Vitis vinifera* L.) berries. Front. Agron. 4. doi: 10.3389/fagro.2022.898870

Keywords: climate change, heat wave, kaempferol, photosynthesis, plant water status, stomatal conductance, anthocyanin

Abstract

Wine grape production is challenged by forecasted increases in air temperature and droughts due to climate change and photoselective overhead shade films are promising tools in hot viticulture areas to overcome climate change related factors. The aim of this study was to evaluate the vulnerability of 'Cabernet Sauvignon' grape berries to solar radiation overexposure, optimize shade film use for preserving berry composition. An experiment was conducted for two years with four shade films (D1, D3, D4, D5) with differing solar radiation spectra transmittance and compared to an uncovered control (C0). Integrals for leaf gas exchange and mid-day stem water potential were unaffected by the shade films in both years. At harvest, berry primary metabolites were not affected by treatments applied in either year. Despite precipitation exclusion during the dormant seasons in shaded treatments, and cluster zone temperatures reaching 58^{o}C in C0, yield was not affected. Berry skin anthocyanin and flavonol composition and content were measured by C18 reversed-phase HPLC. In 2020, total skin anthocyanins (mg·berry^{-1}) in the shaded treatments were 27% greater than C0 during berry ripening and at harvest. Conversely, flavonol content in 2020 decreased in partially shaded grapevines compared to C0. Berry flavonoid content in 2021 increased until harvest while flavonol degradation was apparent from veraison to harvest in 2020 across partially shaded and control grapevines. Untreated control showed lower di- to tri-hydroxylated flavonol ratios closer to harvest. Our results provided evidence that overhead partial shading of vineyards mitigate anthocyanin degradation by reducing cluster zone temperatures and is a useful tool in combatting climate change in hot climate regions.

Introduction

Grapevine (*Vitis. vinifera* L.) is a resilient and lucrative crop with a vast global distribution (Kurtural and Gambetta, 2021). Historically, climate and cultivar associations have developed regional wine identities that are commercially and culturally valued. However, steady increases in air temperature across the world's most famous growing regions have been observed since 1980, threatening to shift appropriate climatic growing conditions to regions located in higher latitudes and altitudes in search for cooler climates (Kurtural and Gambetta, 2021). Concern for shifting regional climates is based in the understanding that certain grape cultivars thrive in specific optimum air temperature regimes where wine quality is optimized. At the onset of global air temperature shift during the 1980s, wine quality ratings increased, presumably due to increased berry sugar concentration and riper flavors (Adelsheim et al., 2016; Kurtural and Gambetta, 2021). However, during the 2010s there was a marked plateau in wine quality ratings, indicating that there may be a tipping point at which wine quality will suffer as air temperatures continually increase (Kurtural and Gambetta, 2021). Consequently, for a region to adapt to ever-warming air temperatures without detrimental decreases in wine composition, mitigation strategies need to be developed.

Among grape berry secondary metabolites, flavonoids play important roles in berry and wine composition. Anthocyanins are responsible for berry and wine color (Savoi et al., 2017), while flavonols act as photoprotectants in plants, scavenging free oxygen radicals and preventing enzymatic reactive oxygen species, while also contributing to wine color through co-pigmentation with anthocyanins (Waterhouse et al., 2016). Flavonoids are produced through the phenylpropanoid pathway (Castellarin et al., 2007), which is responsive to environmental conditions, including solar radiation. It is understood that UV-B radiation induces flavonol

biosynthesis (Martínez-Lüscher et al., 2014a) by activating *MYBF1*, the key transcription factor responsible for the regulation of flavonol biosynthesis enzymes including two *flavonol synthase (FLS*) genes, VvFLS4 and VvFLS5. This occurs via a signaling cascade derived from the photoreception of UV-B radiation by Ultraviolet Resistance Locus 8 (UVR8) homodimers(Matus, 2016). Likewise, selectively screening out excessive UV-A and UV-B with overhead shade films would result in appropriate molecular signaling for flavonoid biosynthesis (Matus, 2016). Previous work (Martínez-Lüscher et al., 2019; Torres et al., 2020, 2021a, 2022) determined that flavonol profile in red skinned grape berry was a reliable biomarker for canopy architecture. In warm climates, net accumulation of flavonols might be impeded by flavonol temperature sensitivity (Martínez-Lüscher et al., 2019). Therefore, selectively removing NIR spectrum from berries would result in less flavonoid degradation due to reduced heat gain by the berry. If the grape berry was subjected to solar radiation overexposure and subsequent heat wave damage soon after sugar translocation into the berry, flavonol degradation occurred and kaempferol molar abundance in grape skins exceeded 8.6% (Martínez-Lüscher et al., 2019). Kaempferol molar abundance is the ratio of the molecule to the total flavonols in berry skin. Subsequently, kaempferol molar abundance exceeded this threshold between 540-570 $MJ \cdot m^{-2}$ of accumulated global radiation post-veraison (Martínez-Lüscher et al., 2019).

Grape berry composition is derived from a balance between primary and secondary metabolites (Castellarin et al., 2007). Ultimately, in hot climate viticulture regions, the clear sky days and concomitant berry temperature gains result in decoupling of sugar and flavonoid in grape berries (Spayd et al., 2002). Under optimal growing conditions, there is a direct relationship between sugar content and anthocyanin synthesis in grape, as some flavonoid synthesis genes such as LDOX and DFR, possess ‘sucrose boxes’ in their promoters, resulting in

sugar-regulated gene expression (Vitrac et al., 2000; Gollop et al., 2001, 2002). However, like flavonols, anthocyanins are also susceptible to chemical or enzymatic degradation at high temperatures while sugar accumulation is unaffected. Mohaved et al.(Movahed et al., 2016) described a putative peroxidase gene VviPrx31 which may be responsible for anthocyanin degradation under high temperatures. The effect of sugar and anthocyanin decoupling on berry and wine composition was investigated where 'Cabernet Sauvignon' berries subject to leaf removal and shoot removal treatments were harvested at 24°Brix and vinified (Torres et al., 2020, 2021a). Compared to untreated control, wines from leaf and shoot removal treatments had reduced color stability due to less anthocyanin hydroxylation as a function of higher temperatures and solar radiation exposure.

Efforts to reduce berry heat gain and through solar radiation exposure in vineyards with overhead and partial shading have been attempted but remain controversial in commercial wine grape vineyards. Cartechini and Palliotti(Cartechini and Palliotti, 1995) demonstrated that average within-canopy temperatures in 'Sangiovese' grapevines decreased by approximately 2°C when covered with shade cloth transmitting 30% and 60% photosynthetically active radiation (PAR). Similarly, thin netting and plastic films covering 'Italia' grapevines reduced mid-day temperatures within the canopy at fruit height by about 6°C below air temperature.(Rana et al., 2004) Martínez-Lüscher et al. (Martínez-Lüscher et al., 2017) partially excluded solar radiation with colored polyethylene shade nets. They concluded that partial shading of the canopy produced quantifiable differences in berry microclimate by reducing canopy temperature by 4°C on the SW-facing side of the canopy. The authors attributed the highest anthocyanin content in the Black-40% shade net lessened anthocyanin degradation from lower canopy temperature. However, partial shading in these experiments failed to selectively omit harmful solar radiation

from the fruit, but rather reduced total solar radiation exposure by 40% of the total radiation. The objective of this study was to selectively remove portions of solar radiation spectrum using overhead shade films in the vineyard, to mitigate the vulnerability of 'Cabernet Sauvignon' grape berry to solar radiation overexposure and optimize berry composition at harvest with desirable sugar accumulation and minimized flavonoid degradation.

Materials and Methods

Meteorological Variables. Air temperature, and precipitation data were obtained from an onsite California Irrigation Management Information System (CIMIS, station #77, Oakville, CA) weather station 160 m away from the experimental site. Seasonal air temperature accumulation was recorded as growing degree days (GDD). GDD were calculated as summation of GDD at each day from 1 April to 1 October as (daily maximum temperature - daily minimum temperature)/2 – 10, disregarding negative values (Figure 1). The number of days above 34°C and 40°C were counted for the 2020 and 2021 growing seasons (Figure S1).

Experimental Site and Plant Materials. The study was conducted at the University of California Davis, Oakville Experimental Vineyard using "Cabernet Sauvignon" (*Vitis vinifera* L.) clone FPS08 grafted onto 110 Richter rootstock. The grapevines were trained to bilateral cordons, vertically shoot positioned, and pruned to 30-single bud spurs. The grapevines were planted at 2.0 m × 2.4m (vine × row) and oriented NW to SE. Irrigation was applied uniformly from fruit set to harvest at 25% ET_c.

Experimental Design. The experiment was arranged in a randomized complete block with four replications. Four photoselective shade films (Daios S.a. Naousa, Greece) and an untreated

control were installed in 3 adjacent rows on 12 September 2019. The shade films remained suspended over the vineyard until 20 October 2021. The shade films were 2 m wide and 11m long and were secured on trellising approximately 2.5 m above the vineyard floor. Each experimental unit consisted of 15 grapevines in 3 adjacent rows. Measurements were taken in the middle row, from three adjacent grapevines, leaving the distal plants as borders. The shade films had specific photoselective properties as indicated in (Figure 2, Table 1). The photoselective properties of the overhead shade films were measured with a spectroradiometer as previously reported (Martínez-Lüscher et al., 2017).

Cluster Microclimate. To characterize the maximum temperature gain of the clusters *in situ*, HOBO Pendant MX Temp/Light (MX2202) data loggers (Onset Computer Corp., Pocasset, MA, USA) were placed on the west side of the canopy and the data were collected every 15 minutes. After a sustained heat wave event, temperature data was downloaded from each treatment replicate and processed. The sensors were mounted on wooden stakes and placed at fruit zone height (96 cm above vineyard floor) at the middle vine of each experimental unit. Canopy temperature data was measured from fruit set 7 and 10 June 2020 and 2021 until harvest (9 September 2020, and 7 September 2021, respectively).

Canopy Architecture. Leaf area index (LAI) was measured using the smartphone-based application VitiCanopy coupled with an IOS system (Apple Inc., Cupertino, CA, USA)(De Bei et al., 2016). A 'selfie-stick' was used for ease to place the device approximately 75 cm below the canopy. The device was placed beneath the canopy perpendicular to the cordon. Leaf area was then derived to calculate the leaf area to fruit ratio.

Leaf Gas Exchange and Plant Water Status. Leaf net carbon assimilation (A_{net}), stomatal conductance (g_s) and intrinsic water use efficiency (WUE_i) were measured bi-weekly from anthesis to harvest using a portable infrared gas analyzer CIRAS-3 (PP Systems, Amesbury, MA, USA). The gas analyzer was set to a relative humidity of 40% and the reference CO_2 concentration was 400 μmol $CO_2 \cdot mol^{-1}$. One sun-exposed leaf from the main shoot axis of each experimental vine was selected and measured. Gas exchange measurements were taken at saturating light conditions.

Plant water status was measured as mid-day stem water potential (Ψ_{stem}) bi-weekly from anthesis until harvest each year. The Ψ_{stem} was measured at solar noon from 13:00 to 14:00 h. One leaf from the main shoot axis in the shade was selected and placed inside a pinch-sealed Mylar® bag 2 h prior to taking measurements. Measurements were taken using a pressure chamber (Model 615, PMS Instrument Company, Albany, OR, USA). The integrals for A_{net}, g_s, WUE_i and Ψ_{stem} were calculated by natural cubic splines for each parameter and calculating the area. The area divided by the number of days elapsed between the first measurement date and the last measurement date is the resulting integral values.

Yield Components. Grapes were harvested when they reached 25° Brix, as based on industry standards. Clusters from the three middle vines in each treatment replicate were removed by hand, counted, and weighed on a top-loading scale. The average cluster weight was calculated by dividing the crop weight by cluster number.

Fruit Sample Collection and Preparation. Seventy berries were collected each year at the following developmental stages: green berry, veraison, mid-ripening and at harvest and

processed the same day. Berry weight was determined as the average of 70 berries. Fifty berries were separated for measuring berry primary chemistry parameters. The berries were crushed, and the resulting juice was used to measure total soluble solids (TSS) as degrees Brix using a digital refractometer (Atago PR-32, Bellevue, WA, USA). Titratable acidity (TA) and pH were measured using an autotitrator (862 Compact TitroSampler, Metrohm, Switzerland). Juice TA was expressed as g of tartaric acid per L of juice after titration to pH 8.3 with NaOH. Twenty berries were set aside and skinned by hand as previously reported (Martínez-Lüscher et al., 2019). Grape skins were collected and freeze-dried (Centrivap, Labcono, Kansas City, MO, USA). Once dried, the skins were ground into powder and 50 g of powder was extracted overnight at 4^{o}C with methanol: water: 7M hydrochloric acid (70:29:1) for anthocyanin and flavonol quantification. Samples were centrifuged for 10 mins at 4000RPM. Supernatants were filtered (0.45µm; VWR, Seattle, WA, USA) and transferred to HPLC vials.

HPLC Procedures. Skin anthocyanins and flavonols were analyzed using a reversed-phase HPLC (Agilent model 1260, Agilent Technologies, Santa Clara, CA, USA) which consisted of a vacuum degasser, autosampler, quaternary pump and diode array detector with a column heater. A C18 reversed-phase column (LiChrosphere 100 RP-18, 4 x 520 mm^2, 5µm particle size, Agilent Technologies, Santa Clara, CA, USA) was utilized for flavonoid analysis as well. The mobile phase flow rate was 0.5 mL min^{-1}, and two mobile phases were used, which included solvent A = 5.5% aqueous formic acid; solvent B = 5.5% formic acid in acetonitrile. The HPLC flow gradient started with 91.5% A with 8.5% B, 87% A with 13% B at 25 min, 82% A with 18% B at 35 min, 62% A with 38% B at 70 mins, 50% A with 50% B at 70.01 min, 30% A with 70% B at 75 min, 91.5% A with 8.5% B from 75.01 min to 91 min. The column temperature was

maintained at 25ºC. This elution allowed for avoiding co-elution of anthocyanins and flavonols as previously reported (Martínez-Lüscher et al., 2019). Flavonols and anthocyanins were detected by the diode array detector at 365 nm and 520 nm respectively. A computer workstation with Agilent OpenLAB (Chemstation edition, version A.02.10) was used for chromatographic analysis. Anthocyanins and flavonols were grouped into 3',4'-dihydroxylated and 3',4',5'-trihydroxylated species with regard to the B ring of the general flavonoid skeleton

Chemicals. All solvents were HPLC grade. Acetonitrile, methanol, hydrochloric acid and formic acid were purchased from Fisher Scientific (Santa Clara, CA, USA). Standards for flavonol identification (myricetin 3-*O*-glucoside, quercetin 3-*O*-glucuronide, quercetin 3-*O*-galactoside, quercetin 3-*O*-glucoside, kaempferol 3-*O*-glucoside, isorhamnetin 3-*O*-glucoside, and syringetin 3-*O*-glucoside) were purchased from Sigma-Aldrich (St. Louis, MO, USA). Oenin was purchased from Extrasynthese (Geney, France).

Statistical Analysis. Statistical analyses were conducted with R studio version 4.0.5 (RStudio: Integrated Development for R., Boston, MA, United States) for Windows. Seasonal integrals of Ψ_{stem} and gas exchange variables for each growing season and for both seasons were calculated by using the same software. All data were subjected to Shapiro–Wilk's normality test. Data were normally distributed and subsequently submitted to an analysis of variance (ANOVA) to assess the statistical differences between the overhead shade film treatments. For all data, means ± standard errors (SE) were calculated, and when the F value was significant ($p \leq 0.05$), Duncan's new multiple range *post hoc* test was executed using "agricolae" 1.2-8 R package (de Mendiburu, 2016).

Results

Meteorological Conditions during Experimental Years. The weather conditions during the 2020 and 2021 growing seasons were compared to the long-term average for the study area over the past 10 years (2009-2019) (Figure 1). Compared to the past 10 years, the 2020 growing season accumulated more growing degree days by 1 October. Conversely, 2021 was a cooler growing season with less growing degree days accumulated than the long-term average. While GDD accumulation early in the season was similar during April – June for both years, the GDD accumulation in 2020 outpaced 2021, with 1762.7°C growing degree days accumulated in 2020 compared to 1572.3°C growing degree days accumulated in 2021. The total precipitation at the experimental site from 1 March 2020 to 30 September 2020 was 84.1mm. The 2020 water year experienced 100.5 mm less precipitation than the 10-year average for the experimental site. Particularly, the 2020 growing season experienced much less precipitation during March compared to the 10-year average with 1.2mm of precipitation accumulating in March 2020. Drought conditions continued into the 2021 water year, with 66.9 mm of precipitation between 1 March 2021 and 30 September 2021. Precipitation only occurred in March and April. Precipitation in the following months of 2021 was negligible. The number of days with maximum air temperature that exceeded 34°C and 40°C in 2020 and 2021 were different (Figure S1). In 2020, there were 32 days that exceeded 34°C while in 2021 there were only 22. Likewise, in 2020 there were 6 days that exceeded 40°C while in 2021 there was only one day that exceeded 40°C.

Primary Metabolism. The integrals for gas exchange and mid-day stem water potential were calculated (Table 2). In either year, there was no effect of overhead shade films on A_{net}, g_s or

WUE_i or Ψ_{stem} integrals. Similarly, cluster number, yield per plant, and berry skin mass in both 2020 and 2021 were not affected by the shade films (Table 3). The LA:FR was not affected in either year of the trial.

Cluster Temperatures. Cluster temperatures were affected by overhead shade films during heat wave events. During heatwave events that occurred pre-veraison (11 July 2020), possible residual warming from the previous day resulted in warmer cluster temperatures in shaded treatments during the early morning hours (7:00h) (Figure 3A). Throughout the day, 2020 pre-veraison cluster temperatures in shaded and control treatments did not differ until 19:00h on 11 July, with the C0 having warmer clusters than all shaded treatments. Beginning at 9:00h on 11 July, cluster temperature in both shaded and control treatments was higher than ambient temperature for the remainder of the day. The largest warming effect (ΔT) on clusters occurred at 13:00h, with the temperature difference between C0 cluster temperature and ambient temperature being 13.3ºC. The difference in D5 cluster temperature and ambient temperature was 9.8ºC at solar noon. Cluster temperature trends were similar pre-veraison in 2021 (17 June 2021). However, differences in cluster temperature were only observed at 7:00h in 2021, again most likely residual warming effects from the previous day (Figure 3C). The largest ΔT was 11ºC between D5 and ambient temperature at 15:00h.

The cooling effect of shade films on cluster temperature was more distinct during post-veraison heatwave events (Figure 3B and D). In the afternoon hours, cluster temperatures in shaded treatments were less than the control. In 2020, cluster temperatures under overhead shade films at 17:00h were at least 4ºC cooler than clusters in C0 (Figure 3B). At 15:00h, ΔT between D3 and ambient temperature was 14ºC, the largest temperature difference observed on 18 August

2020. Similarly post-veraison C0 clusters in 2021 (28 August) consistently had higher cluster temperature compared to shaded clusters in the afternoon. Reduced cluster temperatures in shaded treatments compared to C0 were first observed midday (13:00h) and this cooling effect of the shade films continued throughout the afternoon until 17:00h (Figure 3D). During the warmest parts of the day (15:00h and 17:00h), the largest ΔT was 9^{o}C between C0 and D4. C0 was 19.8^{o}C warmer than ambient temperature at 15:00h, the hottest hour of the day. Regardless of transmission spectra, reduced solar spectra transmission significantly decreased cluster temperatures post-veraison.

Berry Weight and Juice Chemistry. In 2020, berry mass only differed between D3 and the control during post-veraison (Fig 4A). There was no significant difference in berry mass when measured pre-veraison. The differences among treatments for berry mass observed post-veraison were nonsignificant by mid-ripening and remained as such until harvest. TSS, pH and TA were also monitored throughout the growing season in both years. Overhead shade films did not affect TSS in must at any sampling point throughout the 2020 season (Fig 4B). TA was only significantly higher in D3 compared to the control, while pH was only significantly higher for the control when compared to D1. As berries developed, there was no significant effect of shade films on pH and TA (Figs 4C and 4D) compared to C0 from veraison until harvest.

Differences in berry mass occurred later in the season in 2021 compared to 2020 (Figure 5A). At mid-ripening, berry mass of D3, D4, D5 and C0 were similar and greater than that of D1. At harvest, shade films did not have any effect on berry mass. Unlike 2020, differences in TSS were observed at veraison and mid-ripening (Figure 5B). At veraison and mid-ripening, D3, D4, D5 and C0 had similar TSS. In 2021, D1 consistently differed from D5 at these sampling points

for TSS. However, it had similar TSS as D4 and C0 at mid-ripening. There were no differences in TSS in between shade film and control fruit at harvest. Early season differences in pH were observed, with C0 having similar pH to D4 and D5 (Figure 5C). When compared together, the shade films had similar pH at the green berry stage. There were no further differences in pH between treatments and control as ripening progressed. The TA only differed at mid-ripening with D1, D3 and C0 having the highest titratable acidities. D4 and D5 had similar TA, which was significantly less than D1 (Figure 5D). Titratable acidity did not differ between shaded and control fruit at harvest.

Skin Flavonoid Content. Compared to the control, grape berries grown under shade film had higher skin anthocyanins at both mid-ripening and harvest (Figure 6A) in 2020. In all treatments, total skin anthocyanin content peaked at mid-ripening and then decreased from mid-ripening to harvest, with D5 showing the smallest decrease in total skin anthocyanin content (Figure 6A). However, the shade treatment films resulted in 27% greater anthocyanin content than C0 at harvest. The proportion of tri-hydroxylated anthocyanins increased throughout berry development in all treatments (Figure 6C). However, shade films did not affect anthocyanin proportion of hydroxylation compared to the control in this year (Figure 6C).

In 2020, total skin flavonol content increased in both shaded treatments (D1, D3, D4, D5) and the unshaded control (C0) until the veraison (Figure 6B). However, C0 consistently had higher flavonol content compared to shaded treatments. Between the shaded treatments, D4 and D5 produced fruits with significantly more flavonol content per berry compared to D1 and D3 at each sampling time point, except at immediate pre-veraison, where flavonol content in D4 was not significantly different compared to D1 and D3. At mid-ripening flavonol content decreased

in both shaded and unshaded fruits. At harvest, there was no significant difference in flavonol content between C0, D4, and D5. Shade films D1 and D3 had less total skin flavonols than C0, D4 and D5, containing approximately 0.06 mg/berry. The proportion of tri– to di-hydroxylated flavonols was affected by the overhead shade films (Figure 6D). At mid-veraison, there was a greater proportion of tri-hydroxylated flavonols with D1 and D3 compared to D4, D5, and C0. The differences between treatments were pronounced at harvest in 2020 with C0 resulting with the least amount of tri-hydroxylated flavonols in 2020.

In 2021, differences in total skin anthocyanin content were evident at veraison and mid-ripening (Figure 7A). At veraison, total skin anthocyanin content was higher in D5 compared to D1. Shade films C0, D3, and D4 had similar total skin anthocyanin content to D1 and D5 at veraison. At mid-ripening, D5 has significantly higher total skin anthocyanin content to C0, with D1, D3 and D4 having similar anthocyanin content. At harvest, overhead shade films did not have an impact on total skin anthocyanin content. However, anthocyanin content increased from mid-ripening to harvest in D1, D3 and D4, while they appeared to reach a plateau in anthocyanin content in D5 and C0. The effects of overhead shade films on anthocyanin hydroxylation were only observed at mid-ripening with D1 having higher proportions of 3',4',5' to 3',4'-hydroxylated anthocyanins than D4 and D5, and C0 along with D3 did not differentiate with other treatments (Figure 7C).

In 2021, the accumulation trend of skin flavonol content differed compared to that of 2020. At the first sampling point, total skin flavonols were the highest in C0 while D1 had the lowest flavonol content (Figure 7B). The flavonol content continued to increase as ripening progressed. From mid-ripening to harvest, C0, D5 and D4 had the highest flavonol content compared to D1 and D3. In 2021, total skin flavonols did not decrease prior to harvest. The

seasonal trend of di- to tri-hydroxylated flavonols differed in 2021 compared to 2020. Early in the season, D1 and D3 had more tri-hydroxylated flavonols (Figure 7D). From veraison to harvest D1, D3 and D5 had more tri-hydroxylated flavonols compared C0. Similar to 2020, C0 consistently had the lowest ratio of tri- to di-hydroxylated flavonols at every sampling point with the difference at harvest.

In 2020, molar abundance of kaempferol peaked at mid-ripening (Figure 8A). C0 had the highest molar abundance of kaempferol. The molar abundance of kaempferol in D5 was significantly higher compared to D1 and D3. A decrease in kaempferol molar abundance was observed from mid-ripening to harvest. Nevertheless, at harvest, molar abundance of kaempferol remained the greatest in C0 compared to the other overhead shade films, and D1 had the lowest kaempferol molar abundance. In 2021, the molar abundance of kaempferol increased until mid-ripening and then appeared to either level off or decrease from mid-ripening to harvest in all treatments (Figure 8B). Differences in molar abundance of kaempferol were observed at veraison and mid-ripening but not at harvest. At veraison and mid-ripening, C0 had more kaempferol than D1 and D3. Similar molar abundance of kaempferol was observed betweenD5 and other treatments at veraison, and D4 and other treatments at mid-ripening.

Discussion

Precipitation, Heat Waves and Overhead Shade Films. The weather in 2020 and 2021 varied considerably leading to year-to-year variation in the study. In 2020, the air temperatures were higher than the long-term 20-year average for Oakville, CA. In previous studies at this experimental site, similar heat wave events were recorded. In 2017 there were 7 days above 40ºC and 64 days above 30ºC (Martínez-Lüscher et al., 2017). Conversely, 2021 was a cooler growing

season than the 20-year average and recent past years. Compared to precipitation trends of the past 20 years, 2020 and 2021 were severe drought years. The yearly variation in temperatures and precipitation in this study helps to exemplify the unpredictability of growing conditions forecasted with climate change. The application of solar radiation exclusion may become increasingly necessary for wine grape production in hot climates to maintain optimal berry and wine chemistry.

Reduction of Berry Temperature. Ponce de León and Bailey (Ponce de León and Bailey, 2021) quantified berry temperature in a VSP trellis system using thermocouples and subsequently modelled berry temperature temporally and spatially. In an uncovered VSP trellis system, black grape berries in direct sunlight can reach temperatures over 10^{o}C above ambient temperatures with the hottest hours being from 15:00h to 17:00h, while naturally shaded fruits followed ambient temperature (Ponce de León and Bailey, 2021). Similarly, Martínez-Lüscher et al. (Martínez-Lüscher et al., 2017) found that sun exposed grape berries reached temperatures approximately 15^{o}C warmer than ambient air in the afternoon. We observed a temporal shift in the efficacy of overhead shade films. Prior to veraison, overhead shade films did not reduce cluster temperatures, as green berries do not absorb as much heat as black berries after veraison. However, shaded berries were still warmer than ambient temperature which conflicted with the assumptions from the model presented by Ponce de León and Bailey(Ponce de León and Bailey, 2021). After veraison, the cooling effect of shading film was evident as black berries absorbed heat. Shade films in 2020 exceeded the performance of black shade netting with 40% shade factor used by Martínez-Lüscher et al (Martínez-Lüscher et al., 2017). Partial shading with black shade netting reduced cluster temperature of cluster temperature by 3.7^{o}C, while overhead shade films reduced cluster temperature by at least 4^{o}C compared to uncovered control vines. During a

heatwave post-veraison in 2021, berry temperatures reached a maximum temperature of 58ºC in C0, which was the highest recorded berry temperature in both years. At this temperature extreme, shade films were effective in reducing berry temperature. Even when the berry temperatures did not reach this extreme temperature, overhead shade films performed with a similar cooling effect. The cooling effect on clusters results from the shielding of grapes from NIR, which minimized the heat load on the clusters in the afternoon hours. While D4 was the most effective at reducing cluster temperature when maximum temperatures were reached, D5 optimized flavonoid development by balancing heat reduction and solar radiation exclusion. This balance was achieved with the reduction of NIR transmission by approximately 27%.

Gas Exchange, Leaf Area and Plant Water Status. Grapevine physiological responses to reduced photosynthetically active radiation (PAR) via shading in hot climates have been reported. Previous work with partial shading via colored shade nets reduced total solar radiation by 40%, without selecting specifically for PAR reduction and found no differences in net carbon assimilation, stomatal conductance, leaf water potential and most importantly, yield.(Martínez-Lüscher et al., 2017) When calculated as season-long integrals, overhead shade films had no effect on photosynthetic parameters. This may be attributed to the transmission spectra of the polyethylene shade films. Each shade film reduced PAR transmission by approximately 20% from full transmission. The photosynthetic capacity of grapevines is optimized between 800 and 1200 $\mu mol \bullet m^{-2}s^{-1}$ of solar radiation(Carvalho et al., 2016), despite 2000 $\mu mol \bullet m^{-2}s^{-1}$ of solar radiation provided under control conditions. Since leaf area was maintained across treatments and PAR was only reduced by 20%, the photosynthetic capacity of the grapevines was unaltered under the shade films. Negligible differences in canopy size and the replacement of 25% ET_c

resulted in no significant effect on Ψ_{stem} or g_s integrals between treatments within a given year. However, C0 and D4 in both years were trending towards more negative Ψ_{stem} values, which may be due to larger transmittance of NIR radiation and increased evaporative demand. Similar effects on plant water status and gas exchanges were observed by shading via shade nets when canopy size was maintained across treatments.(Martínez-Lüscher et al., 2017) By maintaining aspects such as canopy size and plant water status required for adequate ripening across the treatments(Bergqvist et al., 2001), the effects of shading on berry composition were most likely related to the fruit zone microclimate, specifically reduction of temperature.

Berry Size and Composition. Plant organ development relies on a balance of carbon and water availability(Keller, 2020) . At low doses, ultraviolet light reduces cell division and expansion(Robson et al., 2015). However, previous studies indicated that berry size is unaffected by changes in solar radiation, alterations in amounts of specific wave bands, or temperature.(Spayd et al., 2002; González et al., 2015) Rather, berry size is a function of cluster compactivity (number of berries per cluster) and the amount of irrigation (Keller et al., 2016). As our applied water amounts and cluster count were constant in both shaded and control treatments, berry size was unaffected. Consequently, yield was unaffected by overhead shade films as well.

Grapevine phenology and berry ripening are thermally regulated (Keller, 2020). In our experiment, temperature and solar radiation were coupled. However, changes to temperature caused by the overhead shade films were not enough to result in changes in berry TSS accumulation in both years. Regardless of shading, grape berries reached the commercial winemaking standard of 25 ^{o}Brix. While this desired sugar concentration is often attained in hot

vineyard climates, the decoupling of sugar and anthocyanin development driven by heat waves may cause issues with achieving commercial wine expectations, leading to higher alcoholic wines with immature flavonoid composition(Martínez-Lüscher et al., 2014a; Torres et al., 2022).

Tartaric and malic acids are present in the grape berry at all developmental stages.(Keller, 2020) As the berry ripens, malic acid accumulates until a metabolic shift at veraison. After verasion, the berry loses malic acid to cellular processes such as respiration and gluconeogenesis(Sweetman et al., 2014). Elevated temperature has been shown to reduce must acidity.(Spayd et al., 2002). Ultimately the loss of malic acid from increased temperature is demonstrated to be due to increased degradation rather than reduced pre-veraison biosynthesis. (Sweetman et al., 2014). Must acidity values as low as 4.66 $g \bullet L^{-1}$ have been reported in a hot climate region as the San Joaquin Valley, California in Merlot grapes under pre-bloom mechanical leaf removal (Cook et al., 2015). In this study, must acidity and pH at harvest were not affected by overhead shade films. Rather, titratable acidity and pH at harvest in 2020 were maintained at previously reported levels from the experimental site, despite a warmer than average growing season, where approximately 500 more GDDs accumulated in 2020 than those previously reported by Martínez-Lüscher et al. (Martínez-Lüscher et al., 2017). Despite higher recorded GDD in the present study, titratable acidity at harvest was maintained around 7 $g \bullet L^{-1}$. Ultimately the reduction in cluster temperature imparted by the shading impeded organic acid degradation therefore maintaining berry acidity.

Effects on Flavonoids. Anthocyanins are the products of the phenylpropanoid pathway. The phenylpropanoid pathway is controlled by a suite of structural genes including *chalcone synthase* (*CHS*) and *flavonoid-3-O-glucotransferase* (*UFGT*) at the beginning and end of the pathway,

respectively.(He et al., 2010) Anthocyanin biosynthesis is triggered by a sugar stimulus, resulting in a modification of *UFGT* expression.(WuDai et al., 2014) Previous work has identified a multitude of MYB-related transcription factors including VvMYBA1, VvMYBA2, VIMYBA1-2, VIMYBA1-3 AND VIMYBA2 as being temperature and light responsive in upregulating anthocyanin biosynthesis.(Kobayashi et al., 2002, 2004; Walker et al., 2007; Azuma et al., 2008) However, there was evidence to support anthocyanin downregulation with high temperatures via repression of *UFGT* by MYB4.(Mori et al., 2007) Anthocyanin compounds are also temperature sensitive and will degrade when temperatures exceed 35ºC.(Mori et al., 2007) Optimum temperature thresholds were established for anthocyanin accumulation in grape berries. It was identified that anthocyanin accumulation was maximized at 875 GDD and a daily mean light intensity of 220klm·m^{-2} after which anthocyanin content decreased in Cabernet Sauvignon.(Torres et al., 2020) Previous works that used partial shading that transmitted 60% of solar radiation had also resulted in increased anthocyanin content compared to unshaded fruit in under similar growing season and climatic conditions (Reshef et al., 2017). In 2021, shade films did not affect the anthocyanin content in berry skins at harvest, due to the cooler growing season limiting anthocyanin degradation post-veraison. The reduction in anthocyanin content observed in 2020 may result from repressed anthocyanin biosynthesis at hot temperatures via the MYB4 repressor (Mori et al., 2007). However, it is also highly likely that elevated temperatures in 2020 resulted in increased anthocyanin degradation in exposed fruit compared to shaded fruit, leading to shaded fruit having greater anthocyanin content.

Flavonols are photoprotectants and free radical scavengers in the plant kingdom (Martínez-Lüscher et al., 2014b). As such, these compounds are directly responsive to light exposure of the cluster. In the phenylpropanoid pathway, MYBF1 is a transcriptional regulator of

FLS, the key gene in flavonoid synthesis (Czemmel et al., 2009). It has been shown that MYBF1 is upregulated by UV-B light, resulting in increased flavonols in grape berry skins (Martínez-Lüscher et al., 2014b). Thresholds for optimal sunlight exposure have been elucidated in previous solar radiation exclusion experiments, where Martínez-Lüsher et al. (Martínez-Lüscher et al., 2019) tracked flavonol development over the growing season under 20% and 40% shading conditions. It was determined that net flavonol biosynthesis occurs until approximately 570 MJ m^{-2} of accumulated global radiation which corresponds with 7.6% molar abundance of kaempferol in grape skins (Martínez-Lüscher et al., 2019). Beyond these thresholds, flavonols started to be degraded in the grape berries. Our study showed a similar trend for flavonol content in hot years like 2020. The control treatments in 2020 exceeded 8.6% kaempferol abundance, while shade films were effective in maintaining kaempferol abundance below this overexposure threshold. In cooler years like 2021, flavonol degradation was not observed at the global radiation threshold as a result of the cooler growing season. Rather, biosynthesis continued to increase flavonol content until harvest in 2021. Shade films effectively lengthened the period of flavonol biosynthesis and reduced the amount of time during ripening where clusters are under flavonol degrading conditions.

Anthocyanins are comprised of two aromatic rings (the A-ring and B-ring) linked by three carbons in an oxygenated heterocycle (Bueno et al., 2012). Hydroxylation and methylation of the B- ring is responsible for color and hue of each anthocyanin molecule. Increasing free hydroxyl groups on the B-ring enhances blueness while methylation of the hydroxyl groups increases redder hues in grape skins (He et al., 2010). From a winemaking perspective, 3’4’5-OH anthocyanins are more resistant to degradation during fermentation, leading to stable wine color (Gómez-Plaza et al., 2008). In this study, overhead shade films did not affect anthocyanin

hydroxylation by harvest in either year of this study. However, shifts in anthocyanin hydroxylation have been previously documented: colored shade nets (blue and black) reducing solar radiation by 40%, showed higher anthocyanin and flavonol hydroxylation compared to unshaded treatments (Martínez-Lüscher et al., 2017). Previous studies reported increases in the ratio of di-tri hydroxylated anthocyanins in grapevines under water deficits (Castellarin et al., 2007; Cook et al., 2015; Savoi et al., 2017). The absence of this shift in anthocyanin hydroxylation under shade films was most likely due to similar grapevine water status among the shaded and control treatments, as the vines were not under water deficit conditions. However, shade films altered flavonol hydroxylation under hot growing conditions in 2020, with hydroxylation being the highest in the least exposed shade films (D1 and D3). Shade films D4 and D5 transmitted 60% and 40% of UV-B radiation respectively, resulting in less flavonol hydroxylation than D1 and D3, but more hydroxylation than the control. In cooler growing conditions in 2021, all shade films had comparable levels of flavonol hydroxylation, yet hydroxylation was still greater under shade films than the control. These results may be due to the upregulation of flavonoid 3' hydroxylase (F3'H). This enzyme is responsive under sun exposure and is responsible for the generation of 3'4' hydroxylated flavonoid precursors (Martínez-Lüscher et al., 2014a).

Conclusions

In the context of climate change, more frequent heat wave events may be deleterious on grape and wine quality. This study aimed to elucidate the optimal solar spectrum to avoid deleterious impacts on grapevine physiology and berry composition associated with increased temperatures. Overhead shade film D5 effectively reduced cluster temperature by blocking near

infrared radiation resulting in 27% greater anthocyanin content. Grapevine water status, leaf gas exchange and berry primary chemistry were maintained underneath overhead shade films. Anthocyanin content was increased under shade films in warmer than average years, ultimately due to reduced degradation from excessive cluster temperatures. Shade film D5 produced temperature and solar radiation conditions which optimized berry flavonoid content. Overhead shade films are a novel solution for grape producers in hot climate viticultural regions, as more frequent heat wave events are forecasted with climate change.

Author Contributions

SKK designed the study and acquired the funding. LEM, RY, NT, JDT executed the trial. LEM, RY, NT and JDT collected, and curated the data. LEM wrote the first draft of the manuscript. All authors contributed to the writing of the manuscript and approved the final version.

Funding

A graduate student stipend was provided to LM from University of California Davis during the execution of the trial.

Conflict of Interest

The authors declare that the research was conducted in the absence of any commercial or financial relationships that could be construed as a potential conflict of interest.

References

Adelsheim, D., Busch, C., Catena, L., Champy, B., Coetzee, J., Coia, L., et al. (2016). Climate Change: Field Reports From Leading Winemakers. J. Wine Econ. 11, 5–47. doi: 10.1017/jwe.2016.4

Azuma, A., Kobayashi, S., Mitani, N., Shiraishi, M., Yamada, M., Ueno, T., et al. (2008). Genomic and Genetic Analysis of Myb-Related Genes That Regulate Anthocyanin Biosynthesis in Grape Berry Skin. Theor. Appl. Genet. 117, 1009– 1019. doi: 10.1007/s00122-008-0840-1

Bergqvist, J., Dokoozlian, N., and Ebisuda, N. (2001). Sunlight Exposure and Temperature Effects on Berry Growth and Composition of Cabernet Sauvignon and Grenache in the Central San Joaquin Valley of California. Am. J. Enol. Vitic. 52, 1–7. doi: 10.3923/rjss.2014.31.38

Bueno, J. M., Sáez-Plaza, P., Ramos-Escudero, F., Jiménez, A. M., Fett, R., and Asuero, A. G. (2012). Analysis and Antioxidant Capacity of Anthocyanin Pigments. Part II: Chemical Structure, Color, and Intake of Anthocyanins. Crit. Rev. Anal. Chem. 42, 126–151. doi: 10.1080/10408347.2011.632314

Cartechini, A., and Palliotti, A. (1995). Effect of Shading on Vine Morphology and Productivity and Leaf Gas Exchange Characteristics in Grapevines in the Field. Am. J. Enol. Vitic. 46, 227–234.

Carvalho, L.C., Coito, J.L., Gonçalves, E.F., Chaves, M.M., and Amâncio, S. (2016). Differential Physiological Response of the Grapevine Varieties Touriga Nacional and

Trincadeira to Combined Heat, Drought and Light Stresses. Plant Biol. 18, 101–111. doi: 10.1111/plb.12410

Castellarin, S. D., Matthews, M. A., Di Gaspero, G., and Gambetta, G. A. (2007). Water Deficits Accelerate Ripening and Induce Changes in Gene Expression Regulating Flavonoid Biosynthesis in Grape Berries. Planta 227, 101–112. doi: 10.1007/s00425-007-0598-8

Cook, M. G., Zhang, Y., Nelson, C. J., Gambetta, G., Kennedy, J. A., and Kurtural, S. K. (2015). Anthocyanin Composition of Merlot is Ameliorated by Light Microclimate and Irrigation in Central California. Am. J. Enol. Vitic. 66, 266– 278. doi: 10.5344/ajev.2015.15006

Czemmel, S., Stracke, R., Weisshaar, B., Cordon, N., Harris, N. N., Walker, A. R., et al. (2009). The Grapevine R2R3-MYB Transcription Factor VvMYBF1 Regulates Flavonol Synthesis in Developing Grape Berries. Plant Physiol. 151, 1513–1530. doi: 10.1007/s00425-007-0598-8

De Bei, R., Fuentes, S., Gilliham, M., Tyerman, S., Edwards, E., Bianchini, N., et al. (2016). Viticanopy: A Free Computer App to Estimate Canopy Vigor and Porosity for Grapevine. Sensors 16, 585. doi: 10.3390/s16040585

de Mendiburu, M. (2016). “Package ‘Agricolae.’,” in Statistical Procedures for Agricultural Research. Version 1.

Gollop, R., Even, S., Colova-Tsolova, V., and Perl, A. (2002). Expression of the Grape Dihydroflavonol Reductase Gene and Analysis of its Promoter Region. J. Exp. Bot. 53, 1397–1409. doi: 10.1093/jxb/53.373.1397

Gollop, R., Farhi, S., and Perl, A. (2001). Regulation of the Leucoanthocyanidin Dioxygenase Gene Expression in Vitis Vinifera. Plant Sci. 161, 579–588. doi: 10.1016/S0168 9452(01)00445-9

Gómez-Plaza, E., Gil-Muñoz, R., Hernández-Jiménez, A., López-Roca, J. M., Ortega-Regules, A., and Martínez-Cutillas, A. (2008). Studies on the Anthocyanin Profile of Vitis Vinifera Intraspecific Hybrids (Monastrell × Cabernet Sauvignon). Eur. Food Res. Technol. 227, 479–484. doi: 10.1007/ s00217-007-0744-3

González, C. V., Fanzone, M. L., Cortés, L. E., Bottini, R., Lijavetzky, D. C., Ballaré, C. L., et al. (2015). Fruit-Localized Photoreceptors Increase Phenolic Compounds in Berry Skins of Field-Grown Vitis Vinifera L. Cv. Malbec. Phytochemistry 110, 46–57. doi: 10.1016/j.phytochem.2014.11.018

He, F., Mu, L., Yan, G. L., Liang, N. N., Pan, Q. H., Wang, J., et al. (2010). Biosynthesis of Anthocyanins and Their Regulation in Colored Grapes. Molecules 15, 9057–9091. doi: 10.3390/molecules15129057

Keller, M. (2020). Developmental Physiology. The Science of Grapevines Chapter 6: Developmental Physiology. 3rd Edition, 199–277. San Diego CA, USA, ElsevierInc.doi:10.1016/b978-0-12-816365-8.00006-3

Keller, M., Romero, P., Gohil, H., Smithyman, R. P., Riley, W. R., Casassa, L. F., et al. (2016). Deficit Irrigation Alters Grapevine Growth, Physiology, and Fruit Microclimate. Am. J. Enol. Vitic. 67, 426–435. doi: 10.5344/ajev.2016.16032

Kobayashi, S., Goto-Yamamoto, N., and Hirochika,H.(2004).Retrotransposon- Induced Mutations in Grape Skin Color. Science 304, 982. doi: 10.1126/ science.1095011

Kobayashi, S., Ishimaru, M., Hiraoka, K., and Honda, C. (2002). Myb-Related Genes of the Kyoho Grape (*Vitis Labruscana*) Regulate Anthocyanin Biosynthesis. Planta 215, 924 933. doi: 10.1007/s00425-002-0830-5

Kurtural, S. K., and Gambetta, G. A. (2021). Global Warming and Wine Quality: Are We Close to the Tipping Point? Oeno One 55, 353–361. doi: 10.20870/ oeno-one.2021.55.3.4774

Martínez-Lüscher, J., Brillante, L., and Kurtural, S.K. (2019). Flavonol Profile is a Reliable Indicator to Assess Canopy Architecture and the Exposure of Red Wine Grapes to Solar Radiation. Front. Plant Sci. 10. doi: 10.3389/ fpls.2019.00010

Martínez-Lüscher, J., Chen, C. C. L., Brillante, L., and Kurtural, S. K. (2017). Partial Solar Radiation Exclusion With Color Shade Nets Reduces the Degradation of Organic Acids and Flavonoids of Grape Berry (Vitis vinifera L.). J. Agric. Food Chem. 65, 10693 10702. doi: 10.1021/acs.jafc. 7b04163

Martínez-Lüscher, J., Sánchez-Dıáz, M., Delrot,S., Aguirreolea, J., Pascual, I., and Gomès, E. (2014a). Ultraviolet-B Radiation and Water Deficit Interact to Alter Flavonol and Anthocyanin Profile in Grapevine Berries Through Transcriptomic Regulation. Plant Cell Physiol. 55, 1925–1936. doi: 10.1093/ pcp/pcu121

Martínez-Lüscher, J., Torres, N., Hilbert, G., Richard, T., Sánchez-Dıáz, M., Delrot, S., et al. (2014b). Ultraviolet-B Radiation Modifies the Quantitative and Qualitative Profile of

Flavonoids and Amino Acids in Grape Berries. Phytochemistry 102, 106–114. doi: 10.1016/j.phytochem.2014.03.014

Matus, J. T. (2016). Transcriptomic and Metabolomic Networks in the Grape Berry Illustrate That it Takes More Than Flavonoids to Fight Against Ultraviolet Radiation. Front. Plant Sci. 7. doi: 10.3389/fpls.2016.01337

Mori, K., Goto-Yamamoto, N., Kitayama, M., and Hashizume, K. (2007). Loss of Anthocyanins in Red-Wine Grape Under High Temperature. J. Exp. Bot. 58, 1935–1945. doi: 10.1093/jxb/erm055

Movahed, N., Pastore, C., Cellini, A., Allegro, G., Valentini, G., Zenoni, S., et al. (2016). The Grapevine VviPrx31 Peroxidase as a Candidate Gene Involved in Anthocyanin Degradation in Ripening Berries Under High Temperature. J. Plant Res. 129, 513–526. doi: 10.1007/s10265-016-0786-3

Ponce de León, M. A., and Bailey, B. N. (2021). A 3D Model for Simulating Spatial and Temporal Fluctuations in Grape Berry Temperature. Agric. For. Meteorol. 306, 1–11. doi: 10.1016/j.agrformet.2021.108431

Rana, G., Katerji, N., Introna, M., and Hammami, A. (2004). Microclimate and Plant Water Relationship of the “Overhead” Table Grape Vineyard Managed With Three Different Covering Techniques. Sci. Hortic. 102, 105–120. doi: 10.1016/j.scienta.2003.12.008

Reshef, N., Walbaum, N., Agam, N., and Fait, A. (2017). Sunlight Modulates Fruit Metabolic Profile and Shapes the Spatial Pattern of Compound Accumulation Within the Grape Cluster. Front. Plant Sci. 8. doi: 10.3389/ fpls.2017.00070

Robson, T. M., Klem, K., Urban, O., and Jansen, M. A. K. (2015). Re-Interpreting Plant Morphological Responses to UV-B Radiation. Plant Cell Environ. 38, 856–866. doi: 10.1111/pce.12374

Savoi, S., Wong, D. C. J., Degu, A., Herrera, J. C., Bucchetti, B., Peterlunger, E., et al. (2017). Multi-Omics and Integrated Network Analyses Reveal New Insights Into the Systems Relationships Between Metabolites, Structural Genes, and Transcriptional Regulators in Developing Grape Berries (Vitis Vinifera L.) Exposed to Water Deficit. Front. Plant Sci. 8. doi: 10.3389/ fpls.2017.01124

Spayd, S. E., Tarara, J. M., Mee, D. L., and Ferguson, J. C. (2002). Separation of Sunlight and Temperature Effects on the Composition of Vitis Vinifera Cv. Merlot Berries. Am. J. Enol. Vitic 53:171–82. doi: 10.1021/jf970988p

Sweetman, C., Sadras, V. O., Hancock, R. D., Soole, K. L., and Ford, C. M. (2014). Metabolic Effects of Elevated Temperature on Organic Acid Degradation in Ripening Vitis Vinifera Fruit. J. Exp. Bot. 65, 5975–5988. doi: 10.1093/jxb/ eru343

Torres, N., Martínez -Lüscher, J., Porte, E., and Kurtural, S.K. (2020). Optimal Ranges and Thresholds of Grape Berry Solar Radiation for Flavonoid Biosynthesis in Warm Climates. Front. Plant Sci. 11. doi: 10.3389/ fpls.2020.00931

Torres, N., Martínez-Lüscher, J., Porte, E., Yu, R.,and Kaan Kurtural, S. (2021). Impacts of Leaf Removal and Shoot Thinning on Cumulative Daily Light Intensity and Thermal Time and Their Cascading Effects of Grapevine (*Vitis vinifera* L.) Berry and Wine Chemistry in Warm Climates. Food Chem. 343, 128447. doi: 10.1016/j.foodchem.2020.128447

Torres, N., Yu, R., Martínez -Luscher, J., Girardello, R. C., Kostaki, E., Oberholster, A., et al. (2022). Shifts in the Phenolic Composition and Aromatic Profiles of Cabernet Sauvignon (*Vitis vinifera* L.) Wines are Driven by Different Irrigation Amounts in a Hot Climate. Food Chem. 371, 10693–702. doi: 10.1016/ j.foodchem.2021.131163

Vitrac, X., Larronde, F., Krisa, S., Decendit, A., Deffieux, G., and Mérillon, J. M. (2000). Sugar Sensing and Ca2+-Calmodulin Requirement in Vitis vinifera Cells Producing Anthocyanins. Phytochemistry 53, 659–665. doi: 10.1016/ S0031-9422(99)00620-2

Walker, A. R., Lee, E., Bogs, J., McDavid, D. A. J., Thomas, M. R., and Robinson, S. P. (2007). White Grapes Arose Through the Mutation of Two Similar and Adjacent Regulatory Genes. Plant J. 49, 772–785. doi: 10.1111/j.1365- 313X.2006.02997.x

Waterhouse, A. L., Sacks, G. L., and Jeffery, D. W. (2016). Understanding Wine Chemistry The Atrium, Southern Gate, Chichester, West Sussex United Kingdom: John Wiley & Sons, Ltd. doi: 10.1002/9781118730720

Wu Dai, Z., Meddar, M., Renaud, C., Merlin, I., Hilbert, G., Delro, S., et al. (2014). Long-Term In Vitro Culture of Grape Berries and Its Application to Assess the Effects of Sugar Supply on Anthocyanin Accumulation. J. Exp. Bot. 65, 4665– 4677. doi: 10.1093/jxb/ert489

Tables and Figures

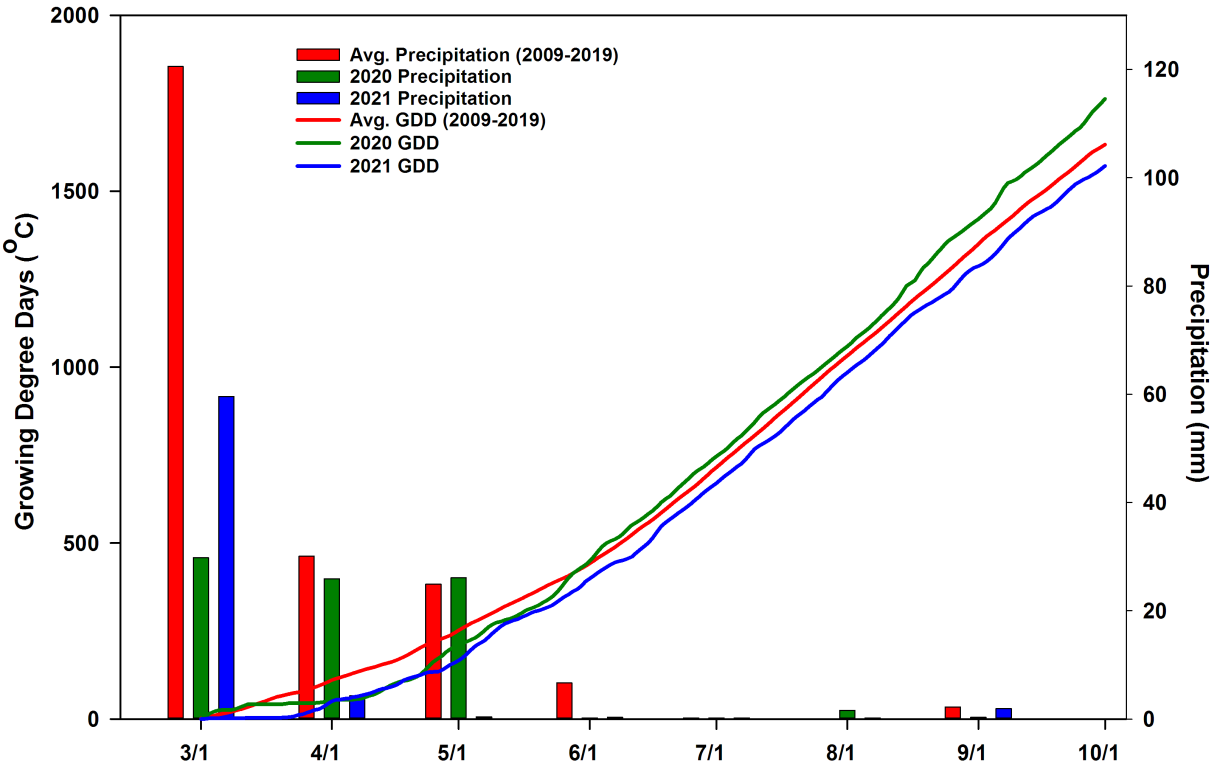

Figure 1. Average precipitation and growing degree days (2009-2019) and experimental years (2020-2021) precipitation and growing degree days at Oakville, CA, USA during the water year (March-October).

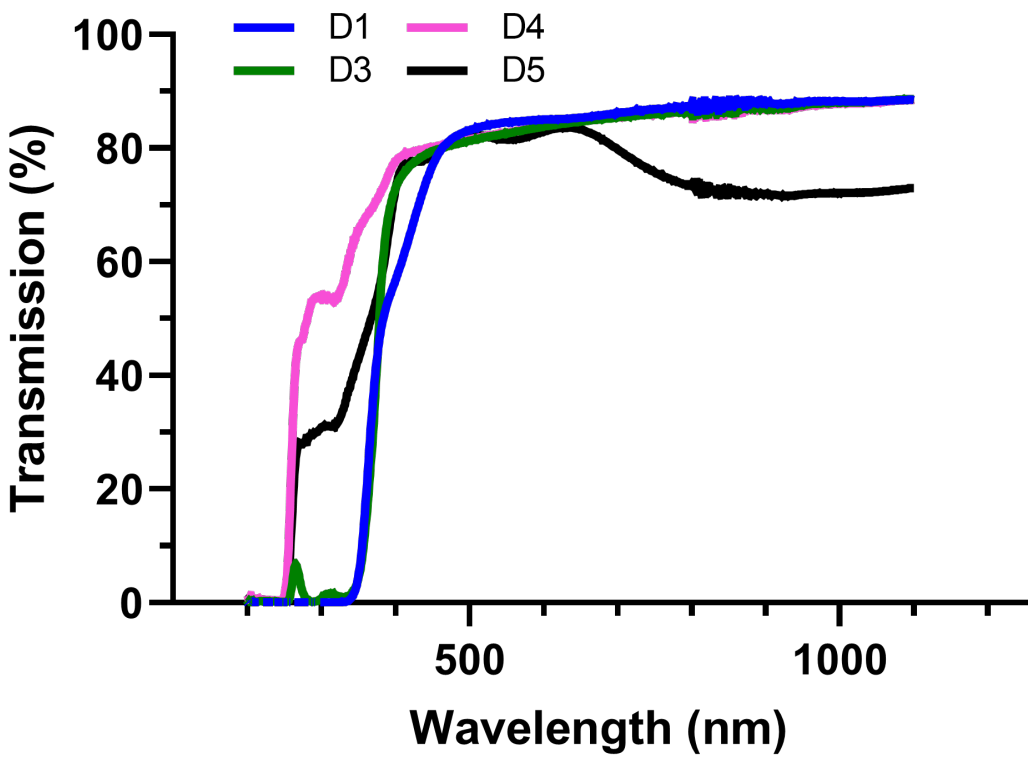

Figure 2. Spectral transmittance (%) of shade films (D1, D3, D4, D5) and percentage of specific radiation spectra compared to open air.

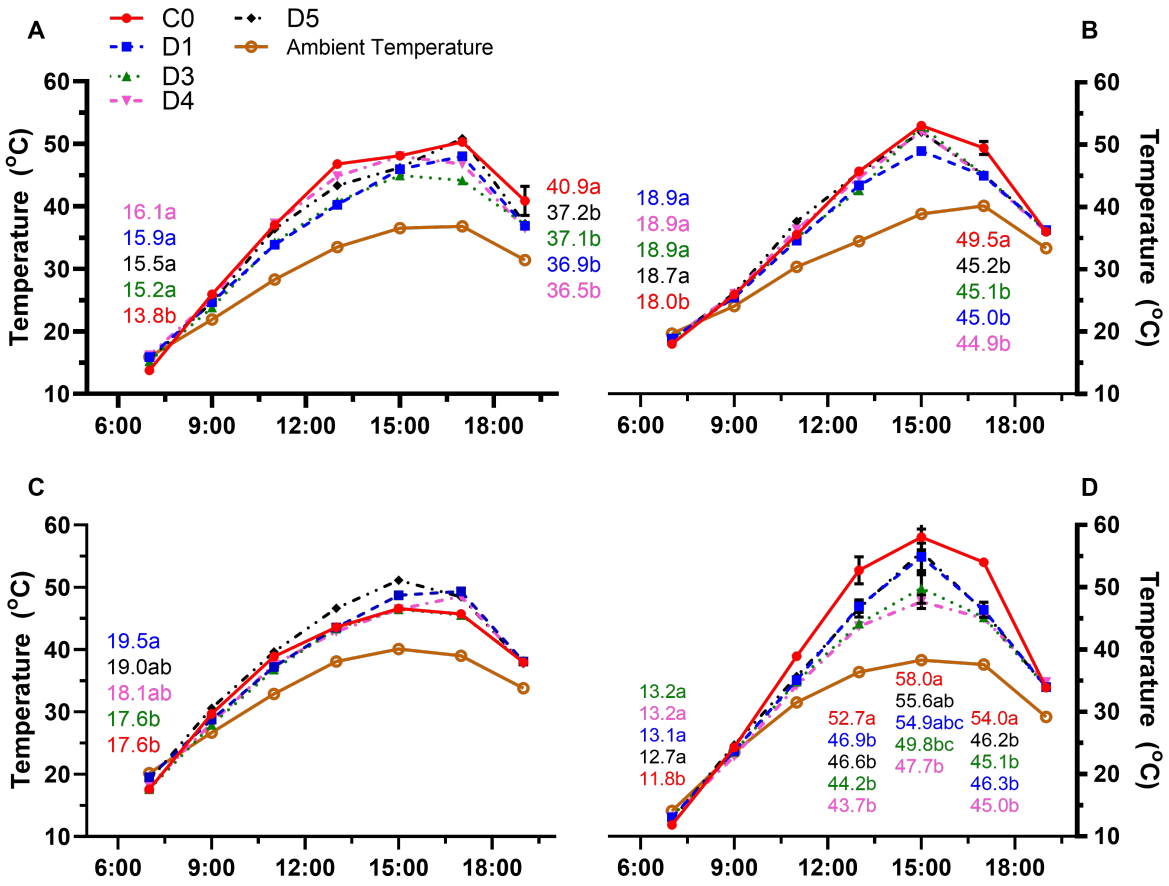

Figure 3. Air temperature and cluster temperature of control (C0) and vines under shade films (D1, D3, D4, D5) recorded during heat wave events both pre-veraison and post-veraison. Temperatures were recorded pre-veraison on (A) 11 July 2020 and (C) 17 June 2021 and post-veraison on (B) 18 August 2020 and (D) 28 August 2021. Points are means ± standard error (n = 4).

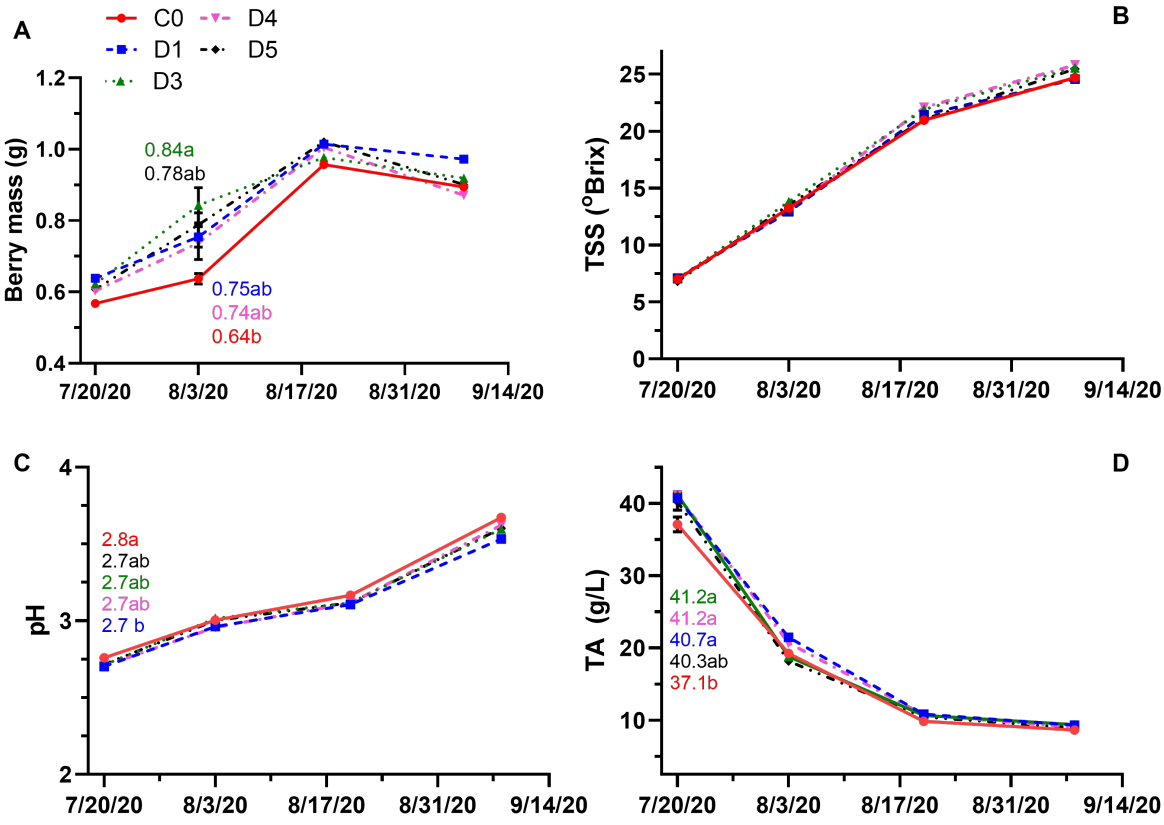

Figure 4. Berry mass (A), TSS (B), pH (C) and TA (D) throughout berry development in 2020 for untreated (C0) and shade film treatments (D1, D3, D4, D5). Points are means ± standard error (n = 4). Means with no letters in common are significantly different ($p \leq 0.05$).

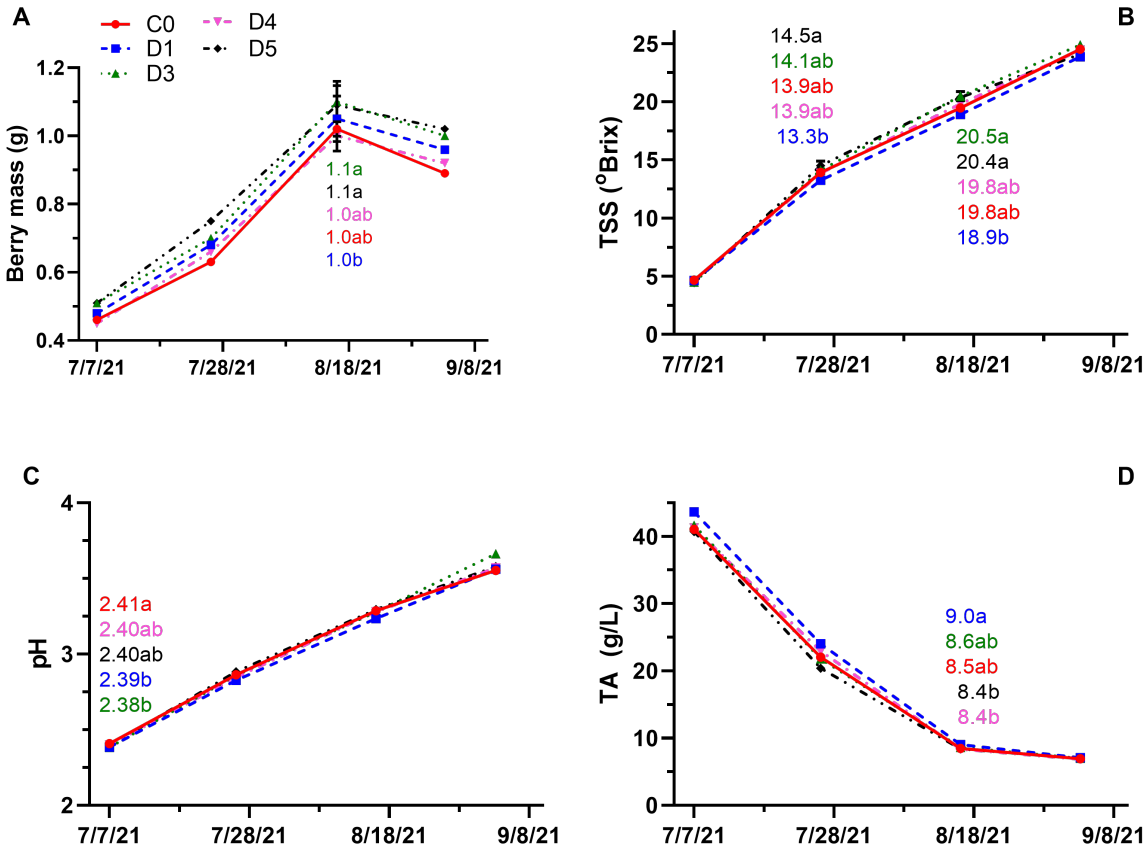

Figure 5. Berry mass (A), TSS (B), pH (C) and TA (D) throughout berry development in 2021 for untreated (C0) and shade film treatments (D1, D3, D4, D5). Points are means ± standard error (n = 4). Means with no letters in common are significantly different ($p \leq 0.05$).

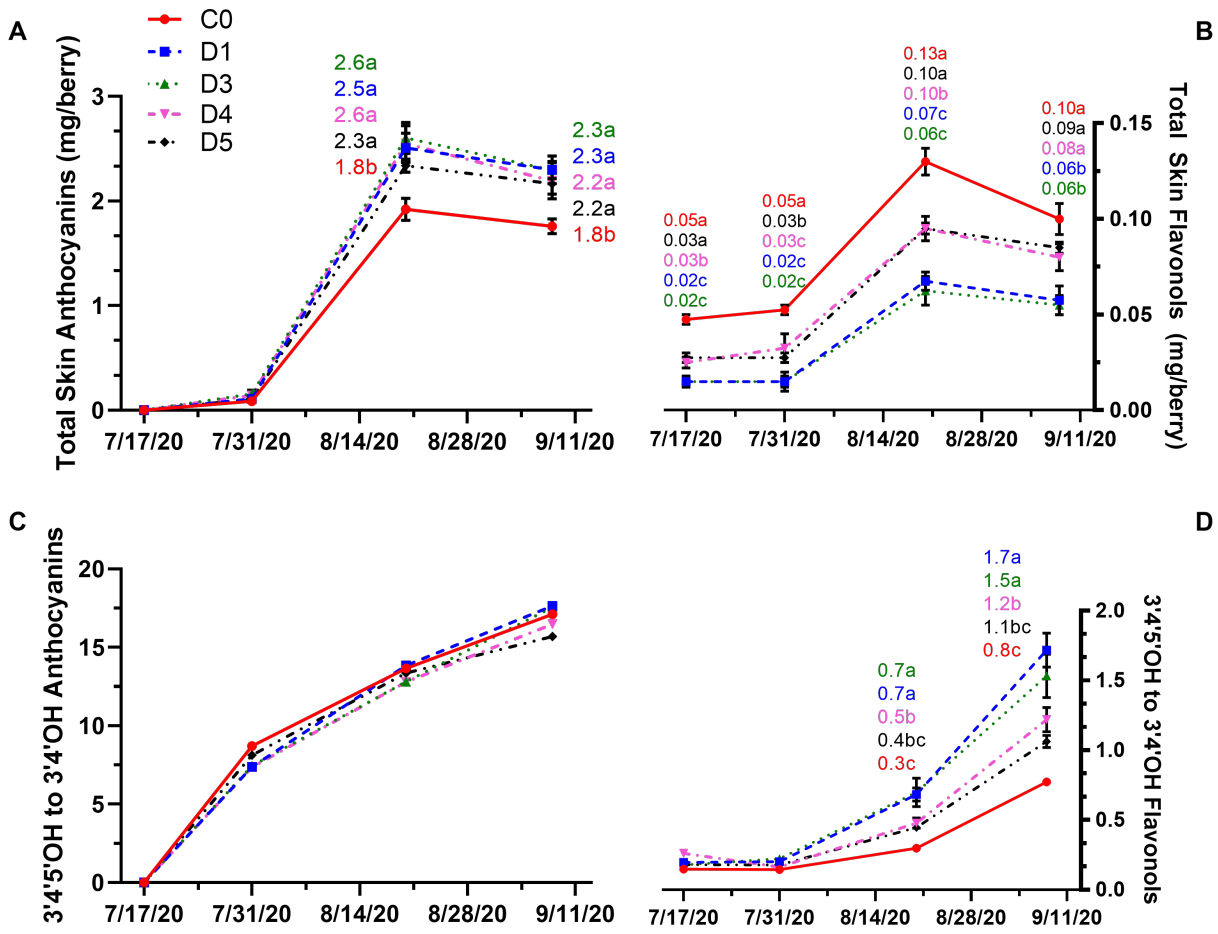

Figure 6. Total skin anthocyanin (A) and flavonol (B) content in 2020 (A, B) and 2021 (C, D) throughout berry development in untreated (C0) and shade film treatments (D1, D3, D4, D5). Points are means ± standard error (n = 4). Means with no letters in common are significantly different ($p \leq 0.05$).

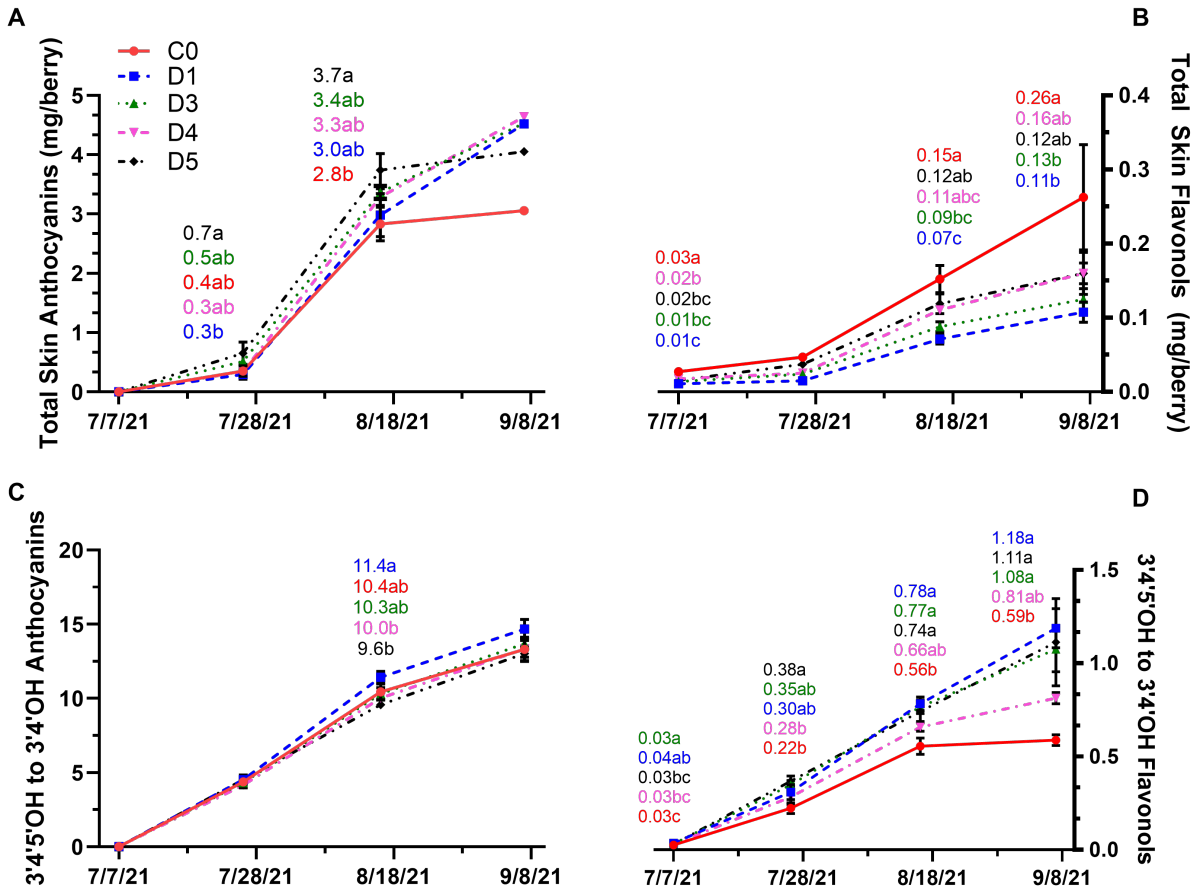

Figure 7. Total skin anthocyanin (A) and flavonol (B) content and anthocyanin (C) and flavonol (D) hydroxylation profile (ratio of 3'4'-OH and 3'4'5'-OH) throughout berry development in untreated (C0) and shade film treatments (D1, D3, D4, D5) in 2021. Points are means ± standard error (n = 4). Means with no letters in common are significantly different ($p \leq 0.05$).

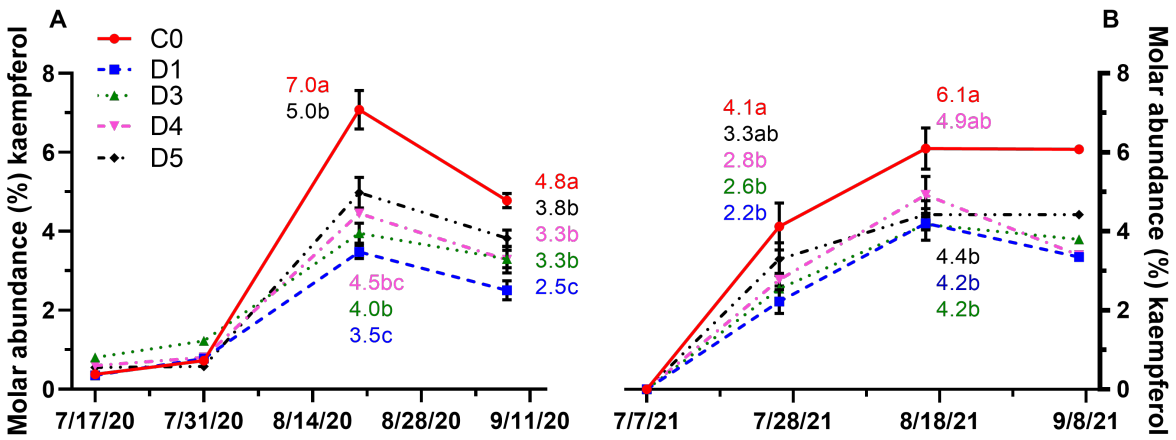

Figure 8. Molar abundance (%) of kaempferol throughout the growing season in (A) 2020 and (B) 2021 for untreated vines (C0) and vines under shade film treatments (D1, D3, D4. D5). Points are means ± standard error (n = 4). Means with no letters in common are significantly different ($p \leq 0.05$).

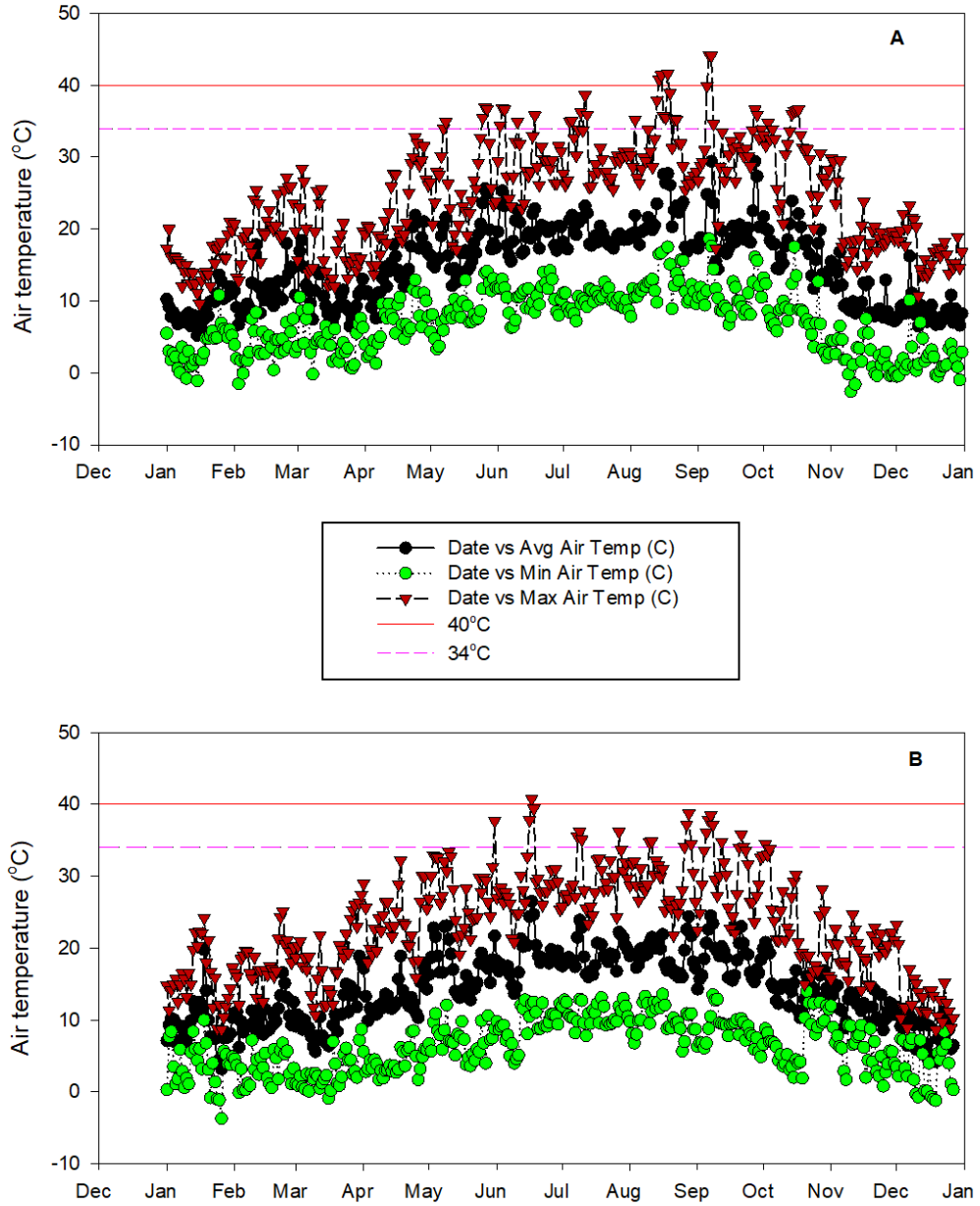

Figure S1. Daily minimum, average, and maximum air temperatures for the (A) 2020 calendar and (B) 20201 calendar years. Days with maximum temperatures above 34ºC and 40ºC are plotted.

Table 1. Percent of Solar Radiation Transmitted Through the Overhead Shade Films

Treatment	Ultraviolet A	Ultraviolet B	Ultraviolet C	Photosynthetically active radiation	Near infrared
C0	100	100	100	100	100
D1	23.3	0	0	81.2	87.8
D3	25.9	1	1	81.9	87.1
D4	66.7	53.6	16.7	82.5	86.9
D5	48.2	30.8	9.7	81.2	73.2

Table 2. Effects of Photo-selective Overhead Shade Films on Integrals of Leaf Gas Exchange and Mid-day Stem Water Potential integrals on Cabernet Sauvignon/110R in Oakville, CA USA[ab]

Treatment	A_{net} (μmol CO_2 m^{-2}•s^{-1})	g_s (mmol H_2O m^{-2}•s^{-1})	WUE_i (μmol CO_2 •mmol H_2O^{-1})	Ψ_{stem} (MPa)
2020				
Control	10.56 ± 1.44	151 ± 22	0.073 ± 0.006	-1.10 ± 0.84
D1	8.78 ± 0.71	173 ± 24	0.058 ± 0.006	-1.03 ± 0.74
D3	9.56 ±1.33	188 ± 29	0.055 ± 0.005	-1.04 ± 0.83
D4	9.28 ± 1.12	185± 36	0.058 ± 0.007	-1.11 ± 0.91
D5	9.47 ± 0.87	187 ± 36	0.061 ± 0.006	-1.05 ± 0.70
p value	n.s.	n.s.	n.s.	n.s.
2021				
Control	14.68 ± 1.37	182 ± 27	0.087 ± 0.010	-1.21 ± 0.11
D1	12.79± 0.84	187 ± 23	0.076 ± 0.009	-1.18 ± 0.11
D3	13.58 ± 1.00	196 ± 25	0.076 ± 0.010	-1.16 ± 0.10
D4	13.13 ± 1.01	185 ± 28	0.079 ± 0.010	-1.25 ± 0.11
D5	13.96 ± 0.91	202 ± 27	0.077 ± 0.010	-1.16 ± 0.09
p value	n.s.	n.s.	n.s.	n.s.

[a] Values in each column are reported as mean ± standard error of the mean
[b] n.s. indicates a *p* value ≥ 0.05

Table 3. Effects of Photo-selective Overhead Shade Films on Yield Components of 'Cabernet Sauvignon/110R' in Oakville, CA, USA[ab]

Treatment	Yield (kg•vine^{-1})	Skin weight (g)	Berry weight (g)	Leaf Area:Fruit (m^2•kg^{-1})
2020				
Control	5.10 ± 0.32	0.070 ± 0.01	0.894 ± 0.02	1.461 ± 0.222
D1	5.78 ± 0.52	0.054 ± 0.00	0.972 ± 0.05	1.612 ± 0.064
D3	5.60 ± 0.57	0.074 ± 0.01	0.919 ± 0.02	1.720 ± 0.084
D4	5.44 ± 0.41	0.065 ± 0.01	0.871 ± 0.01	1.840 ± 0.223
D5	5.34 ± 0.87	0.071 ± 0.00	0.901 ± 0.05	1.714 ± 0.306
p value	n.s	n.s.	n.s.	n.s.
2021				
Control	5.38 ± 0.67	0.067 ± 0.002	0.891 ± 0.07	0.941 ± 0.096
D1	5.86 ± 0.56	0.060 ± 0.008	0.962 ± 0.05	1.095 ± 0.072
D3	5.34 ± 0.28	0.065 ± 0.010	1.001 ± 0.01	1.587 ± 0.272
D4	5.53 ± 0.26	0.055 ± 0.007	0.925 ± 0.04	1.185 ± 0.190
D5	4.71± 0.53	0.069 ± 0.006	1.022 ± 0.10	1.499 ± 0.282
p value	n.s.	n.s.	n.s.	n.s.

[a] Values in each column are reported as mean ± standard error of the mean
[b] n.s. indicates a *p* value ≥ 0.05

Chapter 2: Overhead Photoselective Shade Films Mitigate Effects of Climate Change by Arresting Flavonoid and Aroma Composition Degradation in Wine

This chapter was previously published in Frontiers in Plant Science.

Citation:

Marigliano, L. E., Yu, R., Torres, N., Medina-Plaza, C., Oberholster, A., and Kurtural, S. K. (2023). Overhead photoselective shade films mitigate effects of climate change by arresting flavonoid and aroma composition degradation in wine. *Front Plant Sci* 14. doi: 10.3389/fpls.2023.1085939.

Keywords: **anthocyanins, climate change, flavonols, C13-norisoprenoids**

Abstract

Overhead photoselective shade films installed in vineyards improve berry composition in hot grape-growing regions. The aim of the study was to evaluate the flavonoid and aroma profiles and composition of wines from Cabernet Sauvignon grapes (*Vitis vinifera* L.) treated with partial solar radiation exclusion. Grape must from overhead shade film treatments that permitted different amounts of ultraviolet and near infra-red solar radiation spectra (D1, D3, D4, D5) and an uncovered control (C0) were vinified in triplicates. The wines from D4 treatment had greater color intensity and total phenolic index due to co-pigmentation with anthocyanins. Shade film wines D5 and D1 from the 2020 vintage demonstrated increased total anthocyanins in the hotter of the two experimental years. In 2021, reduced cluster temperatures optimized total anthocyanins in D4 wines. Reduced cluster temperatures modulated anthocyanin acylation, methylation, and hydroxylation in shade film wines. Volatile aroma composition was analyzed using gas chromatography mass spectroscopy (GCMS) and D4 wines exhibited a more fruity and pleasant aroma profile than C0 wines. Results provided evidence that partial solar radiation exclusion in the vineyard using overhead shade films directly improved flavonoid and aroma profiles of resultant wines under hot vintage conditions, providing a tool for combatting air temperatures and warmer growing conditions associated with climate change.

Introduction

It has been long recognized that the quality of wines is closely associated with the accumulation of secondary metabolites, specifically flavonoids and volatile organic compounds that have a direct effect on wine color, taste and aroma (Cortell and Kennedy, 2006)(Torres et al., 2020). Flavonoids in wine include anthocyanins, flavonols and flavan-3-ols. Wine color,

particularly its hue and intensity, are strongly determined by anthocyanin methylation, acetylation, hydroxylation of the anthocyanin B-ring, and co-pigmentation with cofactors such as flavonols (He et al., 2012a; Savoi et al., 2020).

Partial solar radiation exclusion was shown to effect anthocyanin hydroxylation. Tarara et al. (2008) demonstrated increased dihydroxylation of anthocyanins in grape berries exposed to direct solar radiation compared to shaded fruit. Likewise, Martínez-Lüscher et al. (2017) monitored anthocyanin hydroxylation under colored photoselective shade nets and found that by reducing solar radiation by 40% with black polyethylene shade nets, the ratio of tri- to di-hydroxylated anthocyanins was increased compared to uncovered control fruit. Such shifts in anthocyanin hydroxylation can impact anthocyanin hue and wine antioxidant capacity(Muñoz et al., 2009).

Wine aroma in both red and white wines is a matrix formed by a variety of volatile compounds. However, the composition of the matrix can be impacted by grape cultivar, vineyard conditions and fermentation conditions. Contribution of volatiles to wine flavor composition is related to its chemical structure (J. Zhang et al., 2021). The most abundant class of volatile compounds found in the wine matrix are higher alcohols (Zhang et al., 2021). These by-products of yeast nitrogen metabolism are usually described by unpleasant “solvent” or “fusel” aromas when present in concentrations greater than 400 mg/L (Ferreira et al., 2000; Zhang et al., 2020). The more pleasant “fruity” aromas described in wine are associated with esters. Esters are often in highest concentrations in young red wines and decrease in concentration with aging (Câmara et al., 2006). C-13 norisoprenoids and terpenes are key aromas compounds found in both red and white wines, contributing fruity and floral aromas at low olfactory concentrations (Rapp, 1998). C-13 norisopenoids are understood to be derivatives of enzymatic or photochemical degradation

of carotenoid pigments in the grape berry (Isoe et al., 1972). In plants, carotenoids have photo-protectant and antioxidant properties, making these pigments responsive to solar radiation in grape berries. Carotenoids in grape berries have been shown to increase in berries with increased in solar radiation pre-veraison (Marais et al., 1992; Gerdes et al., 2002). However, under extreme exposure to heat and solar radiation, there is a documented decrease in carotenoid concentrations during ripening (Oliveira et al., 2004). To preserve the carotenoid concentrations in the grape berry and to promote C-13 norisoprenoids in resulting wines under more frequent heat wave events and increases in air temperature, artificial shading with black polyethylene cloth has been trialed and found that shaded fruit contained more carotenoids than unshaded fruit (Lu et al., 2021). However, the effect of partial solar radiation exclusion on wine C-13 norisoprenoid content seems to be more nuanced. Wines produced from the shaded fruit contained more β-damascenone as well as esters compared to wines produced from unshaded fruit (Lu et al., 2021). Yet, there are conflicting reports showing no effect of UV exposure on β- damascenone concentrations in Shiraz wines made from clusters that underwent solar radiation exposure via varying rates of leaf removal and polycarbonate UV screens (Song et al., 2015). Like C-13 norisoprenoids, final terpene concentrations in wines depends on the net accumulation in grape clusters exposed to excessive temperatures and UV radiation (Miao et al., 2020; Song et al., 2015).

The effect of photoselective overhead shade films on whole plant physiology and temporal development of berry flavonoids of Cabernet Sauvignon development over two growing seasons was previously studied in a hot region (Marigliano et al., 2022). Grape berries growing under reduced near-infrared radiation exposure in hotter than average years, resulted in a 27% increase in anthocyanin content at harvest than the exposed control due to decreases in

anthocyanin degradation due to high berry temperatures (Marigliano et al., 2022). Moreover, flavonol degradation was similarly decreased, thus optimizing flavonol content in the grape berry under reduced near-infrared radiation exposure (Marigliano et al., 2022). The objectives of this study aimed to determine the extent to which the impact of photoselective overhead shade films on flavonoid development transfer to wine and the cascading effects of partial solar radiation exclusion had on aroma composition of resultant wines.

Materials and Methods

Chemicals. Chemicals of analytical grade included 2-undecanone. All chromatographic solvents were of high-performance liquid chromatography (HPLC) grade including acetonitrile, methanol, hydrochloric acid, and formic acid. These solvents were purchased from Thermo-Fisher Scientific (Santa Clara, CA, USA). HPLC-grade standards including quercetin 3-*O*-glucoside and malvidin chloride were purchased from Extrasynthese (Genay, France).

Plant material, experimental design, and overhead shade film treatments. The experiment was conducted in Oakville, CA, USA during two consecutive growing seasons (2020 and 2021) at the University of California Davis, Oakville Experimental Vineyard. The vineyard was planted with "Cabernet Sauvignon" (*Vitis vinifera* L.) clone FPS08 grafted onto 110 Richter rootstock. The grapevines were planted at 2.0 m × 2.4m (vine × row) and oriented NW to SE. The grapevines were trained to bilateral cordons, vertically shoot positioned, and pruned to 30-single bud spurs. Irrigation was applied uniformly from fruit set to harvest at 25% evapotranspiration (ET_c) as described elsewhere (Torres et al., 2021).

The experiment was arranged in a randomized complete block with four replications. The photoselective shade film treatments were previously described in Marigliano et al. (2022) and

their properties presented in Figure 1. Shade films were designed to target portions of the electromagnetic spectrum previously observed and measured at the experimental site (Martínez-Lüscher et al., 2017; Martínez-Lüscher et al., 2019). Briefly, four photoselective shade films (Daios S.a. Naousa, Greece) and an untreated control were installed in 3 adjacent rows on 12 September 2019. The shade films remained suspended over the vineyard until 20 October 2021. The shade films were 2 m wide and 11m long and were secured on trellising approximately 2.5 m above the vineyard floor. Each experimental unit consisted of 15 grapevines in 3 adjacent rows. Grape clusters were harvested by hand from each experimental unit when berry total soluble solids (TSS) reached 25ºBrix on 9 September 2020, and 7 September 2021, respectively.

Winemaking protocol. Vinification was conducted in 2020 and 2021 at the UC Davis Teaching and Research Winery. Upon arrival at the winery, grapes were destemmed and crushed mechanically. Must from each field experimental unit was divided into three technical fermentation replicates (200L each). $K_2S_2O_2$ was added to each treatment- replicate (50 $mg \cdot L^{-1}$ SO_2) and must was allowed to cold-soak overnight at 5ºC in jacketed stainless-steel tanks controlled by an integrated fermentation control system (TJ fermenters, Cypress Semiconductor Co., San Jose, CA, USA). The following day each treatment-replicate was inoculated with EC-1118 yeast (Lallemand Lalvin®, Montreal, Canada) to initiate fermentation. Musts were fermented at 25°C and two volumes of must were pumped over twice per day by the integrated fermentation control system. During the winemaking process, TSS was monitored daily using a densitometer (DMA 35, Anton Paar USA Inc., Ashland, VA, USA) and fermentations were considered complete once residual sugar contents were less than 3 $g \cdot L^{-1}$. Wines were then mechanically pressed using a screw-type basket press. Following pressing, wine samples were

collected for flavonoid analysis. Malolactic fermentation was initiated with the addition of Viniflora® *Oenococcus oeni* (Chr. Hansen A/S, Hørsholm, Denmark). Malolactic fermentation was carried out at 20ºC. Upon completion of MLF, free SO_2 levels were then adjusted to 35 $mg \cdot L^{-1}$ and wines were bottled.

Chemical composition of wines. A 100 mL wine sample from each technical replicate was used to determine wine pH, titratable acidity (TA) and alcohol content. The pH and TA of the wines was determined using an autotitrator (Omnis titrator, Metroohm, Switzerland). The TA was determined by neutralization with NaOH up to pH 8.2 and expressed as g/L of tartaric acid. Alcohol content in the wines was determined with an alcolyzer SP-1 m (Anton Paar, Graz, Austria) by near-infrared spectroscopy.

Wine spectrophotometric analysis. Using a spectrophotometer (Cary 100; Agilent, CA, USA), color intensity (CI), hue, total polyphenolic index (TPI) and % of polymeric anthocyanins was determined following procedures described by Ribéreau-Gayon, Glories, Maujean, and Dubourdieu (2000). Wine samples were diluted in water (1:100 v:v) and absorbance readings were taken at 280, 420, 520, and 620nm. The absorbance at 740 nm was subtracted from all absorbance readings to eliminate turbidity. CI was calculated as the sum of absorbance at 420, 520 and 620nm. Hue was calculated as the ratio between the absorbance at 420 and 520nm. The percentage of polymeric anthocyanins was determined via absorbance measurements at 520nm after anthocyanin bleaching with a sodium bisulfite solution (10mg/mL). TPI was determined by diluting wines with water (1:100) and recording absorbance at 280nm.

Wine flavonoid concentration and composition. Wine flavonoid composition was determined following procedures previously described (Torres et al., 2022). Briefly, wine samples collected after pressing were centrifuged at 5,000 rpm for 10 mins, filtered with PTFE membrane filters (diameter 13mm, pore size: 45 µm, Thermo Fisher Scientific, San Jose, CA) and transferred to high performance liquid chromatography (HPLC) vials prior to injection. An Agilent 1260 series HPLC system with a reversed-phase C18 column (LiChrosphere 100 RP-18, 4 x 520 mm^2, 5µm particle size, Agilent Technologies, Santa Clara, CA, USA) was used to simultaneously determine the anthocyanin and flavonol concentrations. The mobile phase flow rate was 0.5 mL min^{-1}, and two mobile phases were used, which included solvent A = 5.5% aqueous formic acid; solvent B = 5.5% formic acid in acetonitrile. The HPLC flow gradient started with 91.5% A with 8.5% B, 87% A with 13% B at 25 min, 82% A with 18% B at 35 min, 62% A with 38% B at 70 mins, 50% A with 50% B at 70.01 min, 30% A with 70% B at 75 min, 91.5% A with 8.5% B from 75.01 min to 91 min. The column temperature was maintained at 25ºC. This elution allowed for avoiding co-elution of anthocyanins and flavonols as previously reported (Martínez-Lüscher et al., 2019). Flavonols and anthocyanins were quantified by determining the peak absorbance at 365nm and 520nm, respectively. Quercetin 3-*O*-glucoside and malvidin chloride (Extrasynthese, Genay, France) were used as quantitative standards.

Wine aromatic profile. Volatile compounds in wine samples were analyzed following procedures described previously (Torres et al., 2022). Briefly, 10-mL of each wine sample was transferred to a 20-mL amber glass vial (Agilent Technologies, Santa Clara, CA, USA). Each vial also contained 3 g of NaCl (Sigma Aldrich, St. Louis, MO) and 50µg of an internal standard solution of 2-undecanone (10µg/L prepared in 100% ethanol). After agitating at 500 rpm for 5 mins at 30ºC, samples were exposed to 1 cm polydimethylsiloxane/divinylbenzene/Carboxen

(PDMS/DVB/CAR) (Supelco Analytical, Bellefonte, PA), 23-gauge SPME fiber for 45 mins. Helium was used as a carrier gas at a flow rate of 0.8636 mL/min in a DB-Wax 231 ETR capillary column (30m, 0.25mm, 0.25µm film thickness) (J&W Scientific, Folsom, CA, USA) with constant pressure and temperature at 5.5311 psi and 40°C, respectively. The oven temperature was kept at 40°C for 5 mins and then incrementally increased by 3°C/min until reaching 180°C. Oven temperature was then increased by 30°C/min until reaching 260°C, at which temperature was maintained for 7.67min. The SPME fiber was desorbed split mode with a 10:1 split for wine samples and held in the inlet for 10min to prevent carryover effects. The method was retention time-locked to the 2-undecanone internal standard. The total run time per sample was 61.67min. Electron ionization was performed with a source temperature of 230°C and the quadrupole at 150°C. The wine samples were measured using synchronous scan and selected ion monitoring (SIM mode). The mass spectrometer scanned from *m/z* 40 to 300. Compounds were detected using between two and six selected ions.

Data was analyzed using MassHunter Qualitative Analysis software (version B.07.00) (Agilent Technologies, Santa Clara, CA, USA). After normalization with 2-undecanone internal standard, results were expressed as peak areas. Compounds were tentatively identified in the mass spectrometry spectrum of the peaks and confirmed by comparison to the National Institute of Standards and Technology database (NIST) (https://www.nist.gov). The ions used SIM for each compound and retention times were reported previously by (Girardello et al., 2019). The odor activity value thresholds (OAV) were obtained from a selected review of published literature of young red wines (Francis and Newton, 2005)and were used in comparing the monitored compounds (Table S1).

Statistical analysis. Statistical analyses were conducted with R Studio version 4.0.5 (RStudio: Integrated Development for R., Boston, MA, USA) for Windows. All data were subjected to the Shapiro-Wilk's normality test. Data was subjected to two-way analysis of variance (ANOVA) to assess the statistical differences between the applied shade film vineyard treatments and the vintage and their combination. Means ± standard errors (SE) were calculated and when the *F*-value was significant ($p \leq 0.10$), a Duncan's new multiple range *post-hoc* test was executed using "agricolae" 1.2-8 R package (de Mendiburu, 2016). Principal component analysis (PCA) was conducted and visualized with the same software, using the "factoextra" package(Kassambara, 2016). Pearson correlation analyses were performed with using the same software with the "corrplot" package (Wei et al., 2017).

Results

Experimental weather conditions. Meteorological data collection and climactic conditions at the experimental site for the 2020 and 2021 growing seasons are described in detail by Marigliano et al. (2022). Briefly, there were 1762.7°C growing degree days (GDDs) accumulated in 2020 compared to 1572.3°C GDDs accumulated in 2021, with similar GDD accumulation from April to June in both years. Compared to the 10-year average (2009-2019), the 2020 growing season accumulated more growing degree days by 1 October. The 2021 growing season was a cooler year with less accumulated GDD than the 10-year average. The total precipitation at the experimental site from 1 March 2020 to 30 September 2020 was 84.1mm, a notable 100.5mm less precipitation than the 10-year average for the experimental site. Drought conditions continued into the 2021 water year, with 66.9 mm of precipitation between 1 March 2021 and 30 September 2021. Precipitation only occurred in March and April 2021 and was negligible in the

following months. Given the severe drought conditions in both experimental years, precipitation had a negligible effect on plant water status in control and shaded treatments with 25% ET_c replacement, as demonstrated by no significant effects on stem water potential integrals between control and shaded treatments in either experimental year (Marigliano et al., 2022).

Color parameters and chemical characteristics. Grapes resulting from field treatments were vinified under the same conditions in both years. In 2020 alcohol content was the highest in D1 and D4 wines (Table 1), while alcohol content and residual sugar concentration was lowest in C0 in 2020. All shade film wines contained more alcohol and residual sugar than C0. In 2021, alcohol content and residual sugar concentration was unaffected across all wines. In 2020, pH was only decreased in D3 wines. In 2021, C0 wines had the lowest pH compared wines from shaded grapes. Among the shaded treatments, D4 and D5 wines had higher pH compared to D1 and D3 wines. In 2020, titratable acidity only increased in D3 wines compared to C0, D1 and D5 wines. C0, D1, D4 and D5 wines were indistinguishable in titratable acidity. While C0 had one of the lowest values for TA in 2020, C0 wines in 2021 had one of the highest TA values, along with D3 and D5 wines. The lowest TA value was observed in D4 wines from 2021.

Color intensity (CI) within the 2020 wines varied considerably, with the D4 having the greatest value for CI (Table 1). In 2021, D4 again had the highest values for CI, while the remaining wines were statistically not different from each other. Hue decreased only in D3 wines during the 2020 vintage, while there was no effect of shade films of wine hue during the 2021 vintage (Table 1). The trend for the percentage of polymeric anthocyanins was consistent in both vintages. D1 and D4 had the highest percentage of polymeric anthocyanins, while D5, D3

and C0 wines had less (Table 1). In 2020, D1 and D4 wines had higher TPI values compared to C0 and D3 wines. In 2021, TPI of wines was not affected by shade films except for D4.

3.3 Wine flavonoid content and profile

Wine anthocyanin profiles were separated into glucosides, 3-acetylated and coumarylated anthocyanins (Table 2). The total free anthocyanin concentration was the lowest in C0 wines compared to shade film treatments in 2020. Concentrations of 3-glucosides and 3-acteylated glucosides increased for all anthocyanins under shading treatments compared to C0, except for peonidin 3-acetyl-glucoside and cyanidin 3-glucoside in which shading treatments had no effect. The composition of coumarylated 3'4'5'-hydroxylated anthocyanin modifications was largely impacted by shading, with the largest concentrations detected in C0, D1 and D5 wines. Overall, the ratio of di- to tri-hydroxylated anthocyanins was the largest in C0 wines and the lowest in D5. Conversely in 2021, total free anthocyanin concentrations were the highest in D4, C0, and D1 wines. Anthocyanin modifications due to shading treatments were more varied in 2021 compared to 2020. Overall, wines from D4 had the most 3-glucosides and 3-acetylated glucosides, while C0 and D5 consistently had less. Coumarylated anthocyanin concentrations were reduced in D3 and D5 wines compared to C0 wines. This was not consistent with the concentrations observed in 2020. Likewise, there was no statistically significant effect on the anthocyanin hydroxylation ratio in 2021 wines, while shading had an impact on anthocyanin hydroxylation in wines in 2020.

Nine flavonol compounds were monitored in wines using HPLC (Table 2). For all monitored flavonol compounds except myricetin-3-glucuronide, C0 wines consistently had the highest concentrations in 2020 compared to shaded wines, with D4 and D5 wines following in flavonol concentration. Subsequently, C0 also had the highest wine flavonol concentration when

calculated as total flavonols in 2020. A similar trend occurred in 2021. C0 wines from 2021 also contained greater concentrations of each flavonol compared to shaded treatments, as well as total flavonol concentration.

Wine aroma content and profile. The wine aroma profiles from the 2020 and 2021 vintages were analyzed with (GCMS) and 29 volatile compounds were identified and categorized into their respective compound classes (Table 3). The aromas profiles of wines depended highly on vintage, resulting in distinct aroma profiles. Generally, in 2020, total higher alcohols were unaffected by shade treatments, except for isoamyl alcohol and benzyl alcohol. Wines produced from shaded fruit had similar concentrations of isoamyl alcohol while the C0 had the lowest isoamyl alcohol concentration. Benzyl alcohol concentrations were reduced in D3 and D5 wines compared to C0, D1 and D4 wines. In 2021, shading treatments did not impact the concentration of higher alcohols in the resulting wines except for benzyl alcohol, which increased in 2021 D3 wines compared to all other treatments.

Acetate esters and fatty acid ethyl esters showed varied effects in wines due to shading in 2020. C0 and D5 had the lowest ethyl acetate concentrations compared to the other shade treatments. Likewise, isoamyl acetate was reduced in C0, D4 and D5 wines compared to D1 and D3 wines. Among the shade film treatments (D1, D3, D4 and D5), ethyl hexanoate and ethyl octanoate concentrations were comparable between D1 and D5 wines and were greater than concentrations found in D3 wines. C0 and D5 wines were indistinguishable in ethyl butyrate, ethyl-2-methylbutyrate and ethyl valerate in 2020, with D1 and D3 wines having the highest concentrations of each these ester compounds. Isobutyric acid increased in D4 in 2020. In 2021,

there were no significant impacts of shading on acetate esters, fatty acid ethyl esters, ethyl butyrate, ethyl-2-methylbutyrate or ethyl valerate.

The effect of shade films on various terpenes and norisoprenoids was highly dependent on vintage conditions. Alpha-terpinene was highest in D5 wines but was significantly reduced in D1 and D3 wines in 2020. The D4 wines had the most cis-rose-oxide while C0 wines had the least. Linalool concentrations were reduced in C0, D4 and D5 wines. Among the shaded treatments, nerol concentrations were enhanced in D5 wines in 2020, while there was no effect of shading on nerol concentration in 2021. D5 did not differ from the C0 in nerol concentration in 2020. Farnesol in D3 was reduced in 2020 whereas farnesol concentrations were not affected in 2021 wines. Conversely, nerolidol was unaffected by shade films in 2020, whereas significant decreases in nerolidol concentrations were observed in D4 and D5 wines in 2021. It was observed that β-damascenone were elevated in 2020 in C0 wines, yet differences in β-damascenone concentrations were nonsignificant between shade film treatments. In 2021, only significant differences in β-damascenone concentrations were observed in wines, with C0 wines containing the most β-damascenone and D5 wines containing the least. β-ionone concentrations were not statistically significant between all treatments in 2020 and 2021.

Relationships between chemical parameters, flavonoid composition, and aromatic profiles. To determine the effects of partial solar shading on wine chemistry, flavonoid composition, and aromatic profiles of wines we conducted a principal components analysis for both vintages (Figure 2). In 2020, PCA indicated that PC1 accounted for 30.8%, and PC2 accounted for 22.1% of the total variance. The C0 treatments clustered together, separately from the partial solar shading treatments. The separation along PC1 was explained by the ratio of di- to tri-

hydroxylated anthocyanins in wines, norisoprenoids and flavonols, as well as lower CI, alcohol content and TPI. The separation along PC2 was explained by TA, pH, terpenes and the percentage of polymeric anthocyanins in wine samples. In 2021, PCA indicated PC1 accounted for 29.9%, and PC2 accounted for 22.2% of the total variance. The C0 treatments again separated from shade film treatments, but less so than in 2020. The separation in PC1 was again explained by the ratio of di- to tri-hydroxylated anthocyanins, along with the total glucosides, total methylated anthocyanins, and total anthocyanins. The separation of C0 was along PC2 and thus was associated with higher concentrations of flavonols, terpenes, norisoprenoids, and polymeric anthocyanins in wine.

We analyzed the relationships further between the variables monitored with a correlation analysis in wines (Figure S1). In 2020, CI in wines had the strongest positive correlation with TPI and acids (Figure S1). Alcohol percentage and ketones were also positively correlated to TPI and acids, although less so than CI. Ketones also were very strongly positively correlated with higher alcohols, while higher alcohols were less strongly correlated to acids. Conversely, flavonols were strongly negatively correlated with acetate esters and other esters in wines. Norisporenoids and pH were less negatively correlated to acetate esters. Fatty acid ethyl esters particularly showed to be negatively correlated with TA.

In 2021, the strongest positive correlations in wines were between total anthocyanins and total glucosides and total methylated anthocyanins (Figure S2). Total coumarylated anthocyanins were significantly and positively correlated to total anthocyanins, methylated anthocyanins, and total glucosides. Strong negative correlations were found between hue and ester compounds including fatty acid ethyl esters and acetate esters. Alcohol percentage and norisoprenoids were also negatively correlated with each other. A strong negative correlation existed between the

ration of di- to tri-hydroxylated anthocyanins and total acetylated anthocyanins. Lastly, total higher alcohols and pH were strongly negatively correlated with each other.

Discussion

Partial solar radiation effects on wine color and chemical properties were driven partial solar radiation exclusion. In hot viticulture regions, there is a desire to reduce excessive alcohol content in wines due to marketability and taxation concerns(Varela et al., 2017). Numerous studies have demonstrated that partial solar radiation exclusion is an effective method for reducing the amount of ethanol in wines by reducing TSS in shaded clusters (Joscelyne et al., 2007; Caravia et al., 2016; Lu et al., 2021). However, in the present study, C0 wines consistently had the lowest alcohol content and the lowest concentration of residual sugars in 2020 compared to shaded fruit, despite grapes at harvest having similar TSS values across the treatments (Marigliano et al., 2022). This may be due to the composition of sugars in the grape berry being affected by excessive cluster temperatures in C0 fruit. Sepúlveda and Kliewer (1986) showed that heat stress at 40°C post-veraison decreases glucose and fructose in the grape berry. During heat wave events post-veraison, cluster temperatures in C0 reached a maximum temperature of 58°C, exceeding the point at which glucose and fructose content is altered (Marigliano et al., 2022). Additionally, the production of non-fermentable sugars such as arabinose, raffinose and xylose are known to be present in the grape berry (Kliewer, 1965b). Genes involved in the production of these sugars have been shown to be upregulated under heat stress conditions in grapevine (Pillet et al., 2012). While the grape berry is 95-99% glucose and fructose at harvest, these non-fermentable sugars are included in the metric of total soluble solids (Kliewer, 1965a). As a result, while TSS was unaffected by shade films (Marigliano et al., 2022), the proportion of

fermentable to nonfermentable sugars may be impacted, thus leading to 2020 C0 wines with reduced alcohol content. This difference in alcohol content between 2021 wines was not observed most likely due to the 2021 growing season being cooler with less GDDs (1572.3°C GDD) than 2020 (1762.7 GDD°C) (Marigliano et al., 2022). While C0 wines in this study demonstrated lower alcohol content than shaded wines, previous literature corroborates cluster temperature reduction by partial solar radiation exclusion as an effective method to lessen sugar content in the grape berry and thus reduce alcohol content of wines (Joscelyne et al., 2007; Caravia et al., 2016; Lu et al., 2021).

The effect of partial solar radiation exclusion in semi-arid climates on berry pH and TA is mixed. Previous work demonstrates partial solar radiation exclusion to reduce pH and increase TA in grape berries by reducing the thermal degradation of organic acids (Martínez-Lüscher et al., 2017; Lu et al., 2021). However, in the present study, berry pH and TA at harvest were unaffected in either year by shade films (Marigliano et al., 2022). Nonetheless, there were apparent effects on wine pH and TA that were vintage dependent. In the present study, D3 wines had the lowest pH and highest TA, while C0 wines did not differ from the shade films D1, D4 or D5 in pH or TA in 2020. Differences observed in pH between the wines ultimately affect the colorimetric properties of these wines. In 2021, D4 and D5 wines showed the highest pH values. It is understood that the pH of the wines can shift the anthocyanin equilibrium in wine solution between the flavylium and quinoidal (colorless) base forms (He et al., 2012a). In the present study, D4 wines had the highest pH and the highest CI. In many cases, when pH rises, CI will decline as anthocyanin equilibrium shifts away from the flavylium form towards the colorless quinoidal forms (He et al., 2012a). However, this was not the case in the present study. Rather,

improved color intensity at elevated wine pH could be attributed to co-pigmentation in the wine matrix.

Co-pigmentation refers to non-covalent interactions between anthocyanins and cofactors such as flavonols, flavan-3-ols and proanthocyaninidins, that results in greater absorbance of the wine than color what would be indicated by anthocyanin content and pH conditions (Waterhouse et al., 2016a). Copigmentation in young wines was shown to increase color intensity in young red wines (Jensen et al., 2008). In the hotter 2020 vintage, the total flavonols in grape berries were increased in D4 fruit compared to other treatments (Marigliano et al., 2022). This increased berry flavonol content was transmissible during winemaking, as D4 wines also showed the highest total flavonols with similar concentrations as C0 wines in 2020. TPI was also enhanced in D4 wines. As such, this increased the abundance of cofactors in the wine matrix. Thus, improved color intensity documented in D4 wines in both vintages could be due to the enhancement of absorbance from increased flavonol content by reducing thermal degradation in the vineyard (Marigliano et al., 2022). In the cooler 2021 growing season, shade films produced wines with less flavonols than C0, but greater anthocyanin content, thus leading to improved color intensity in D4 wines.

The increase of phenolic cofactors in D4 wines not only enhanced color and hue, but also led to a higher percentage of polymeric anthocyanins when compared to other shade treatments. Phenolic and polyphenolic compounds from grape skins and seeds can form polymeric pigments in wine with anthocyanins(He et al., 2012b). These polymeric anthocyanins are more stable than monomeric anthocyanins and help to stabilize wine color. This occurs as the proportion of monomeric anthocyanins decreases, leaving color to be maintained by polymeric anthocyanins (He et al., 2012b). Across both vintages, the percentage of polymeric anthocyanins was

maximized in D4 wines, indicating that these wines may have greater aging potential than wines from C0 and other shading treatments.

Anthocyanin and flavonol profiles of wine. In the present study, partial solar radiation exclusion modified the composition of anthocyanins in wine. Partial solar radiation exclusion resulted in increased anthocyanin glycosides in wine from shade film treatments except for D4 wines in 2020. In 2021, D4 consistently showed the lowest cluster temperatures post-veraison and as a result, demonstrated the highest concentration of glucosides in resultant wines. Excessive berry temperatures post-veraison in both vintages (>55°C) led to C0 fruit with reduced total anthocyanin content at harvest and this carried over into resultant wines (Marigliano et al., 2022). The reduction of near-infrared radiation by at least 15% produced a cluster temperature conducive to anthocyanin accumulation, as these compounds are susceptible to thermal degradation above 35°C (Spayd et al., 2002). When comparing total anthocyanin and flavonol concentrations between 2020 and 2021, regardless of treatment, 2020 wines had anthocyanin and flavonol concentrations six to seven times less than those in 2021 wines. As flavonoids are susceptible to thermal degradation, this drastic difference in total flavonoid concentrations may be attributed to hotter vintage air temperatures in 2020 compared to 2021.

Previous works show berry sunlight exposure to alter the composition of anthocyanins, such as the proportion of acetylated and coumarylated forms (Haselgrove et al., 2000; Spayd et al., 2002; Downey et al., 2008; Chorti et al., 2010). Modulation of acylated, methylated, and hydroxylated forms of anthocyanins result from the synergistic effect of solar radiation exposure and the coupled increases in berry temperature (Tarara et al., 2008). Generally, high berry temperatures resulting from increased solar exposure results in increased acylated anthocyanins

in the grape berry, particularly coumarylated forms (Downey et al., 2008; Tarara et al., 2008). Also, high temperatures result in accumulation of highly methylated anthocyanins such as malvidin derivatives, as these compounds are less likely to degrade than their counterparts (Mori et al., 2007). In 2020, D1 and D5 wines demonstrated highest concentrations of acetylates, coumarylates, and methylated anthocyanins compared to C0 wines. While D1 and D5 treatments demonstrated cluster temperatures less than those from C0 treatments (Marigliano et al., 2022), the concomitant thermal degradation of total anthocyanins in C0 treatments proved to negate any modulation towards acylated or methylated forms in resultant wines. Similarly in 2021, C0, D1 and D5 wines exhibited reduced acylation compared to D4 wines. Again, while D4 consistently exhibited less intense cluster temperatures, the thermal degradation in more exposed treatments eclipsed any identifiable acylation modulation from hot growing conditions. Acylated anthocyanins are more stable compounds and provide color stability and increase blueness in wine (de Rosas et al., 2017; Alappat and Alappat, 2020). However, an increase in methylated anthocyanins will lead to redder hues in wine (Alappat and Alappat, 2020). Therefore, the improvement in acylated and methylated anthocyanin content due to partial solar radiation exclusion may enhance color perception in young red wines through color stabilization and alteration of wine hue.

Likewise, anthocyanin hydroxylation is also directly influenced by temperature and solar radiation exposure. Previous studies on berry exposure utilizing UV selective shade nets as well as leaf removal, demonstrated anthocyanin tri-hydroxylation increases with increasing berry temperature (Chorti et al., 2010). Increases in tri-hydroxylation are driven by accumulation of malvidin derivatives and the temperature sensitivity of F3’H, the catalyzing enzyme for 3’-hydroxylated anthocyanin biosynthesis (Tarara et al., 2008; Chorti et al., 2010). The highest ratio

of tri- to di-hydroxylated anthocyanins in 2020 C0 wines were driven by higher concentrations of 3-p-coumaroyl-glucoside derivatives of delphinidin, petunidin and malvidin, despite the ratio of tri- to di-hydroxylated anthocyanins being unaffected at harvest in the grape berry in 2020 (Marigliano et al., 2022). Among shade film treatments in 2020, the reduction of UV light exposure, was the determining factor in anthocyanin hydroxylation patterns rather than berry temperature. Previous shade net studies at the experimental site showed a reduction in UV radiation with black-40% and blue-40% shade nets led to higher anthocyanin tri-hydroxylation in the grape berry compared to control vines at harvest (Martínez-Lüscher et al., 2017). With the reduction of UVB and UVC radiation in D4 and D5 vines, anthocyanin tri-hydroxylation was reduced, regardless of temperature. Ultimately, the upregulation of F3'H from sun exposure could be negated by the reduced catalytic activity of this enzyme under high temperatures experienced in 2020. In the cooler 2021 vintage, the ratio of tri- to di-hydroxylated anthocyanins was unaffected, due to non-significant effect of shade films on acetylated anthocyanins. Ultimately, increased tri-hydroxylation in young red wines will also impact wine hue, resulting in more purple wines (Savoi et al., 2017).

Flavonols in the grape berry skin act as photoprotectants and are strongly induced by ultraviolet radiation (Agati and Tattini, 2010). Flavonol composition in the grape berry can be used to determine overexposure, specifically by quantifying the molar abundance of kaempferol. C0 berries in this study were shown to be overexposed by surpassing the previously described threshold of approximately 7% molar abundance of kaempferol (Martínez-Lüscher et al., 2019). In both years of the study, flavonol composition in grape berries was maximized in C0 fruit, but D4 and D5 fruit contained the most flavonols across the shade films with minimal thermal degradation of the compounds on the vine(Marigliano et al., 2022). Likewise in both wine

vintages, flavonol concentration was modulated by UV radiation exposure, proportional to the amount of UV radiation transmitted to the grapevine. Of the wines produced from shade films treatments, D4 allowed for the most UV transmission while subsequently reducing near infrared transmission by approximately 15%. These light conditions ultimately optimized flavonol content in D4 wines compared to the other shade treatments from both wine vintages. As such, this demonstrated the transmissibility of berry composition under shade treatments to directly improve wine flavonoid profiles. For hot viticulture regions, photoselective solar radiation exclusion provides a strategy to improve not only flavonoid profile but also wine color intensity through copigmentation with anthocyanins.

Wine aroma profiles. C6-alcohols such as 1-hexanol and (*E)*-2-hexen-1-ol are often found in wines as fermentation products. These compounds are derived from microbial mediated cleavage of the C-C double bonds in linoleic and linolenic acids, by lipoxygenase and alcohol dehydrogenate enzymes in yeast (Vilanova et al., 2012; Waterhouse et al., 2016b). Compounds such as 1-hexanol and (*E)*-2-hexen-1-ol are associated with aromas such as cut grass, green, fat, and herbaceous aromas and their OAV thresholds are 8000 and 400 ug/L, respectively (Francis and Newton, 2005). The effect of shade films on C6-alcohols was evident in both years; however, there was a yearly effect on which alcohol was altered by the treatment. In 2020, (*E)*-2-hexen-1-ol was the lowest in D4. In 2021, (*E)*-2-hexen-1-ol was unaffected by shade films, while 1-hexanol was highest in C0, D4 and D5. Although there was a statistical difference in C6 alcohols, the differences were not large enough between C0 and treatments to cross the OAV thresholds (Francis and Newton, 2005) for these compounds. Increases of C6-alcohols in C0, D4, and D5 wines may be explained by solar radiation overexposure in the treated clusters. L. He et

al. (2020) reported higher linoleic and linolenic acid biosynthesis with leaf removal at veraison. Subsequently, fruit exposed to increased solar radiation had elevated precursors for C6-alcohol production during yeast metabolism. Additionally, L. He et. al. (2020) showed higher initial concentration of C6-alcohols in grape berries from leaf removal treatments due to modulation of the volatile compound metabolome and transcriptome in grape berries exposed to sunlight under dry-hot conditions. Therefore, in our experiment which has similar climatic conditions to L. He et. al. (2020), fruit from shade films with higher percentages of UV radiation may have both an increase in linoleic and linolenic acids to act as C6-alcohols aromas precursors and increased C6-alcohols in the exposed grape berries. Ultimately, overexposure of the grape berry led to more green and grassy aromas in wine, which may lead to an unripe perception of these wines.

Higher alcohols are also produced during fermentation from yeast metabolism of amino acids. These compounds are generally pleasant aromas including mushroom, roses, honey, candy, and fruity notes. Of these compounds, shade treatments increased isoamyl alcohol concentration in 2020 and benzyl alcohol concentration in wines from both vintages. Isoamyl alcohol is associated with solvent and cheese aromas and, while benzyl alcohol is characterized as being citrusy and sweet (Yue et al., 2015). The odor active thresholds for these compounds are 30000 μg/L and 10000 μg/L, respectively (Table 1S). In 2020, C0 had the lowest concentration of isoamyl alcohol in wines. The effect of shading on the concentration of isoamyl alcohol in wines varies in literature (Lu et al., 2021; Li et al., 2022). In hot growing regions, 75% of total solar radiation exclusion with black polyethylene canopy side shade nets resulted in wines with reduced isoamyl alcohol compared to the uncovered control vines (Lu et al., 2021). However, this experimental site was in a region that received approximately 704.5°C less growing degree days than the present experimental site in the hotter 2020 season, and 514.1°C growing degree

days less than the cooler 2021 season. In the study by Lu et al. 2021, reduced solar radiation exposure in a cooler growing region may have resulted in reduced isoamyl alcohol in shaded fruit. When cluster temperatures exceed 42°C in exposed vines, there is a reduction in isoamyl alcohol in resultant wines compared to wines produced from fruit under red and black shade nets (Li et al., 2022). With cluster temperatures of C0 fruit exceeding 42°C, excessive cluster temperatures may be prompting the reduction in isoamyl alcohol and overall wine fruitiness from those produced from overexposed clusters. However, while there was a statistical difference in isoamyl alcohol concentrations between C0 and treatment wines, the effect was not large enough to exceed the OAV threshold for this compound (Table 1S).

Shade films affected the ester composition predominantly in 2020 wines. Pleasant esters in red wines include ethyl acetate which has a OAV threshold of 12264 $\mu g \bullet L^{-1}$ and is described as fruity and balsamic (Jiang and Zhang, 2010; Arcari et al., 2017), as well as isoamyl acetate, described as banana aroma with a OAV threshold of 30 $\mu g \bullet L^{-1}$ (Francis and Newton, 2005). In 2020, ethyl acetate was reduced in C0 and D5 wines, shading and reduced cluster temperatures preserved isoamyl acetate aromas in D1, D3 and D5 wines. When compared to wines from 2021, cooler vintage conditions did not result in ester compositional changes in exposed and shaded wines. Similarly, fatty acid esters were preserved in shaded wines, while 2020 C0 wines consistently had the lowest concentration of all measured fatty acid ethyl esters and various esters, all of which are associated with fruity and candy-like aromas(Jiang and Zhang, 2010). Concentrations of ethyl octanoate and ethyl decanoate remained beneath the reported perception threshold, thus observed shifts in composition with shading may be undetectable in Cabernet Sauvignon wines. However, ethyl hexanoate and ethyl isovalerate have remarkably low OAV thresholds of 5 $\mu g \bullet L^{-1}$ and 1 $\mu g \bullet L^{-1}$, respectively (Table 1S). In the present study, all wines were

above these thresholds, indicating that reductions in fruitiness may be perceived. This overall decrease in fruity aromas with cluster exposure and excess temperatures may negatively impact the marketability of Cabernet Sauvignon wines from hot viticulture regions with increasingly more frequent heat wave events associated with climate change.

Unpleasant and rancid aromas include isobutyric acid which imparts a cheese aroma and benzaldehyde which is associated with almond aroma in red wines (Jiang and Zhang, 2010). In this study, isobutyric acid concentrations were only affected in 2020, with D4 having the highest isobutyric acid concentration. The detection threshold for this aroma compound is 2300µg•L^{-1} (Table 1S). Concentrations detected in the experimental wines were substantially below this threshold, indicating that this slight increase in rancid aromas in D4 wines may not negatively impact overall wine perception. Given that D4 wines also exhibited enhanced fruitiness in with improved ester composition, the trade-off of slight increases in rancid aromas may be offset by the net benefit from increased fruity aromas in the wine aroma profile.

While terpenes are often critical in white wines, these compounds when present in red wines have a large effect on wine aromas as their OAV thresholds are relatively low (Yang et al., 2019). The OAV threshold for a-terpinene, cis-rose-oxide and linalool are 250 µg•L^{-1}, 0.2 µg•L^{-1} and 25.2 µg•L^{-1}, respectively (Table 1S). The In 2020, α-terpinene, cis-rose-oxide and linalool were all reduced in C0 wines compared D4 and D5 wines, however concentrations of these compounds did not exceed the OAV threshold. These compounds produce odors such as peach, citrus, rose, and floral aromas in red wines (Jiang and Zhang, 2010; Yue et al., 2015). Previous work indicated an increase in terpenoids, particularly linalool in wines produced from fruit under black and red shade nets (Li et al., 2022). It was demonstrated that heat treatment will down-regulate genes encoding key enzymes in terpenoid metabolism in Cabernet Sauvignon

grapevines (Lecourieux et al., 2017). Thus, increases in terpenoid content in shade film wines in 2020 may be due to reduced cluster temperature in a growing season with frequent heat wave events. In 2021, C0 wines exhibited the highest concentration α-terpinene, while cis-rose-oxide concentrations remained low in C0, and linalool was unaffected. In 2021, a cooler growing season with fewer days above 38°C may have resulted in less variation in terpenoid composition and net accumulation of terpenoids in exposed fruit (Marigliano et al., 2022). Ultimately, climatic shifts towards more frequent heat wave events will reduce floral and citrus aromas in wines produced from overexposed clusters. However, the year-to-year weather variation will enhance the unpredictability of the development of these compounds, leading to challenges for wine producers looking to produce a consistent product.

As carotenoid breakdown products, C-13 norisoprenoids like β-damascenone often described by sweet and floral aromas (Yue et al., 2015) and has an OAV threshold of 0.05 $\mu g \cdot L^{-1}$ (Table 1S). C-13 norisoprenoids have been shown to have a positive linear relationship with sunlight exposure to the grape cluster (Marais et al., 1992; Gerdes et al., 2002; Lee et al., 2007). Under extreme light intensity and temperature conditions, there are decreases in carotenoid concentration in the berry, thus reducing C-13 norisoprenoid precursors. In the present study, β-damascenone was highest in C0, D4 and D5 wines in 2020, while β-damascenone was highest in C0 and D1 wines in 2021, contrary to previous findings in hot viticultural areas. Lee et al. (2007) reported that grape clusters without leaf removal and inner canopy clusters contained more β-damascenone than south-facing clusters exposed to solar radiation by leaf removal. Likewise, black cloth and red shade net enhanced β-damascenone concentration compared to uncovered control (Lu et al., 2021; Li et al., 2022). Despite varied reports, Lee et al. (2007) also demonstrated a linear positive relationship between norisoprenoids in the grape berry and

concentrations in wine, with the berry concentration was always greater than that of the resultant wines. It may be possible that carotenoid degradation due to excessive temperatures in C0 treatments was negligible or less than the biosynthesis of C-13 norisoprenoids, resulting in similar concentrations as D4 and D5 shade film treatments. Therefore, the results of this study demonstrated that partial solar radiation exclusion with reductions in UVA, UVB and NIR radiation does not hinder norisoprenoid content in wines. Additionally, the concentrations of β-damascenone across all treatments in both years exceeded the odor active threshold for this compound, indicating that significant differences in β-damascenone concentrations between C0 and treatments may be perceivable in resultant wines.

Conclusion

Traditional viticulture management practices encouraged solar radiation exposure in wine grape fruit zone to promote flavonoid and aroma development. However, increasingly frequent heat wave events in hot grape growing regions are threating wine quality due to degradation of these desirable compounds in the grape berry (Gambetta and Kurtural, 2021). Thus, to maintain desirable chemical and aromatic properties in red wines, heat mitigation strategies need to be implemented in the vineyard. We determined the cascading effects of partial solar radiation exclusion in the vineyard on resultant wine flavonoid and aroma composition. Overhead shade film D4 produced wines with improved color intensity, TPI, anthocyanin and flavonol profiles compared to C0 wines. Likewise, D4 wines were fruitier and with pleasant aroma profile compared to C0 wines. Ultimately, overhead shade film D4 positively enhanced wine composition in the hotter of the two experimental years, thus demonstrating partial solar

radiation exclusion with overhead shade films to be a viable option for maintaining wine quality with forecasted climate change conditions in hot viticulture regions.

Author Contributions

SK designed the trial. LM, RY, NT, and SK conducted the experiments. AO and CM assisted with volatome analysis, LM curated the data and wrote the first version of the manuscript. All authors contributed to the article and approved the submitted version.

Funding

Part of the publishing fees for this paper has been defrayed by University of California Davis library. A graduate student stipend was provided to LEM from University of California Davis during the execution of the trial.

Conflict of Interest

The authors declare that the research was conducted in the absence of any commercial or financial relationships that could be construed as a potential conflict of interest.

References

Agati, G., and Tattini, M. (2010). Multiple functional roles of flavonoids in photoprotection. New Phytol. 186, 786–793. doi: 10.1111/j.1469-8137.2010.03269.x

Alappat, B., and Alappat, J. (2020). Anthocyanin pigments: Beyond aesthetics. Molecules 25, 5500. doi: 10.3390/molecules25235500

Arcari, S. G., Caliari, V., Sganzerla, M., and Godoy, H. T. (2017). Volatile composition of merlot red wine and its contribution to the aroma: optimization and validation of analytical method. Talanta 174, 752–766. doi: 10.1016/j.talanta.2017.06.074

Câmara, J. S., Alves, M. A., and Marques, J. C. (2006). Changes in volatile composition of Madeira wines during their oxidative ageing. Analytica Chimica Acta 563, 188–197. doi: 10.1016/j.aca.2005.10.031

Caravia, L., Collins, C., Petrie, P. R., and Tyerman, S. D. (2016). Application of shade treatments during Shiraz berry ripening to reduce the impact of high temperature. Aust. J. Grape Wine Res. 22, 422–437. doi: 10.1111/ajgw.12248

Chorti, E., Guidoni, S., Ferrandino, A., and Novello, V. (2010). Effect of different cluster sunlight exposure levels on ripening and anthocyanin accumulation in nebbiolo grapes. Am. J. Enol Vitic 61, 23–30. doi: 10.5344/ajev.2010.61.1.23

Cortell, J. M., and Kennedy, J. A. (2006). Effect of shading on accumulation of flavonoid compounds in (Vitis vinifera l.) pinot noir fruit and extraction in a model system. J. Agric. Food Chem. 54, 8510–8520. doi: 10.1021/jf0616560

de Mendiburu, M. (2020). Agricolae: Statistical procedures for agricultural research. https: //CRAN.R-project.org/package=agricolae

de Rosas, I., Ponce, M. T., Malovini, E., Deis, L., Cavagnaro, B., and Cavagnaro, P. (2017). Loss of anthocyanins and modification of the anthocyanin profiles in grape berries of Malbec

and Bonarda grown under high temperature conditions. Plant Sci. 258, 137– 145. doi: 10.1016/j.plantsci.2017.01.015

Downey, M. O., Harvey, J. S., and Robinson, S. P. (2008). The effect of bunch shading on berry development and flavonoid accumulation in Shiraz grapes. Aust. J. Grape Wine Res. 10, 55–73. doi: 10.1111/j.1755-0238.2004.tb00008.x

Ferreira, V., López, R., and Cacho, J. F. (2000). Quantitative determination of the odorants of young red wines from different grape varieties. J. Sci. Food Agric. 80, 1659– 1667. doi: 10.1002/1097-0010(20000901)80:11<1659

Francis, I. L., and Newton, J. L. (2005). Determining wine aroma from compositional data. Aust. J. Grape Wine Res. 11, 114–126. doi: 10.1111/j.1755-0238.2005.tb00283.x

Gambetta, G., and Kurtural, S. K. (2021). Global warming and wine quality: are we close to the tipping point? OENO One 55, 353–361. doi: 10.20870/oeno- one.2021.55.3.4774

Gerdes, S. M., Winterhalter, P., and Ebeler, S. E. (2002). Effect of sunlight exposure on norisoprenoid formation in white Riesling grapes. ACS Symposium Ser. 802, 262–272. doi: 10.1021/bk-2002-0802.ch019

Girardello, R. C., Rich, V., Smith, R. J., Brenneman, C., Heymann, H., and Oberholster, A. (2019). The impact of grapevine red blotch disease on vitis vinifera l. Chardonnay grape and wine composition and sensory attributes over three seasons. J. Sci. Food Agric. 100, 1436–1447. doi: 10.1002/jsfa.10147

Haselgrove, L., Botting, D., van Heeswijck, R., Hoj, P. B., Dry, P. R., Ford, C., et al. (2000). Canopy microclimate and berry composition: The effect of bunch exposure on the phenolic composition of vitis vinifera l. cv. Shiraz grape berries. Aust. J. Grape Wine Res. 6, 141–149. doi: 10.1111/j.1755-0238.2000.tb00173.x

He, F., Liang, N. N., Mu, L., Pan, Q. H., Wang, J., Reeves, M. J., et al. (2012a). Anthocyanins and their variation in red wines i. monomeric anthocyanins and their color expression. Molecules 17, 1571–1601. doi: 10.3390/molecules17021571

He, F., Liang, N. N., Mu, L., Pan, Q. H., Wang, J., Reeves, M. J., et al. (2012b). Anthocyanins and their variation in red wines II. anthocyanin derived pigments and their color evolution. Molecules 17, 1483–1519. doi: 10.3390/molecules17021483

He, L., Xu, X. Q., Wang, Y., Chen, W. K., Sun, R. Z., Cheng, G., et al. (2020). Modulation of volatile compound metabolome and transcriptome in grape berries exposed to sunlight under dry-hot climate. BMC Plant Biol. 20, 59. doi: 10.1186/ s12870-020-2268-y

Isoe, S., Hyeon, S. B., Katsumura, S., and Sakan, T. (1972). Photo-oxygenation of carotenoids. II. the absolute configuration of loliolide and dihydroactinidiolide. Tetrahedron Lett. 13, 2517–2520. doi: 10.1016/S0040-4039(01)84863-2

Jensen, J. S., Demiray, S., Egebo, M., and Meyer, A. S. (2008). Prediction of wine color attributes from the phenolic profiles of red grapes (Vitis vinifera). J. Agric. Food Chem. 56, 1105–1115. doi: 10.1021/jf072541e

Jiang, B., and Zhang, Z. (2010). Volatile compounds of young wines from Cabernet Sauvignon, Cabernet Gernischet and Chardonnay varieties grown in the loess plateau region of China. Molecules 15, 9184–9196. doi: 10.3390/molecules15129184

Joscelyne, V. L., Downey, M. O., Mazza, M., and Bastian, S. E. P. (2007). Partial shading of Cabernet Sauvignon and Shiraz vines altered wine color and mouthfeel attributes, but increased exposure had little impact. J. Agric. Food Chem. 55, 10889–10896. doi: 10.1021/ jf0721621

Kassambara, A., and Mundt, F. (2020). Package 'factoextra'. Extract and visualize the results of Multivariate data Analyses. Version, 1.0.7.

Kliewer, W. M. (1965a). Changes in concentration of glucose, fructose and total soluble solids in flowers and berries of *Vitis vinifera*. Am. J. Enol Vitic 16, 101–110.

Kliewer, W. M. (1965b). The sugars of grapevines. II. identification and seasonal changes in the concentration of several trace sugars in *Vitis vinifera*. Am. J. Enol Vitic 16, 168–178.

Lecourieux, F., Kappel, C., Pieri, P., Charon, J., Pillet, J., Hilbert, G., et al. (2017). Dissecting the biochemical and transcriptomic effects of a locally applied heat treatment on developing Cabernet Sauvignon grape berries. Front. Plant Sci. 8. doi: 10.3389/ fpls.2017.00053

Lee, S.-H., Seo, M.-J., Riu, M., Cotta, J. P., Block, D. E., Dokoozlian, N. K., et al. (2007). Vine microclimate and norisoprenoid concentration in Cabernet Sauvignon grapes and wine. Am. J. Enol Vitic 58, 291–300. doi: 10.5344/ajev.2007.58.3.291

Li, W., Liu, M., Chen, K., Zhang, J., Xue, T., Cheng, Z., et al. (2022). The roles of different photoselective nets in the targeted regulation of metabolite accumulation, wine aroma and sensory profiles in warm viticulture regions. Food Chem. 396, 133629. doi: 10.1016/j.foodchem.2022.133629

Loscos, N., Hernandez-Orte, P., Cacho, J., and Ferreira, V. (2007). Release and formation of varietal aroma compounds during alcoholic fermentation from nonfloral grape odorless flavor precursors fractions. J. Agric. Food Chem. 55, 6674–6684. doi: 10.1021/jf0702343

Lu, H. C., Wei, W., Wang, Y., Duan, C. Q., Chen, W., Li, S., et al. (2021). Effects of sunlight exclusion on leaf gas exchange, berry composition, and wine flavour profile of Cabernet Sauvignon from the foot of the north side of Mount Tianshan and a semi-arid continental climate. Oeno One 55, 267–283. doi: 10.20870/OENO-ONE.2021.55.2.4545

Marais, J., van Wyk, C. J., and Rapp, A. (1992). Effect of sunlight and shade on norisoprenoid levels in maturing Weisser Riesling and Chenin blanc grapes and Weisser Riesling wines. South Afr. J. Enology Viticulture 13, 23–32.

Marigliano, L. E., Yu, R., Torres, N., Tanner, J. D., Battany, M., and Kurtural, S. K. (2022). Photoselective shade films mitigate heat wave damage by reducing anthocyanin and flavonol degradation in grapevine (*Vitis vinifera* L.) berries. Front. Agron. 4. doi: 10.3389/fagro.2022.898870

Martínez-Lüscher, J., Brillante, L., and Kurtural, S.K. (2019). Flavonol profile is a reliable indicator to assess canopy architecture and the exposure of red wine grapes to solar radiation. Front. Plant Sci. 10. doi: 10.3389/fpls.2019.00010

Martínez-Lüscher, J., Chen, C.C.L., Brillante, L., and Kurtural, S.K. (2017). Partial solar radiation exclusion with color shade nets reduces the degradation of organic acids and flavonoids of grape berry (*Vitis vinifera* L.). J. Agric. Food Chem. 65, 10693–10702. doi: 10.1021/acs.jafc.7b04163

Miao, W., Luo, J., Liu, J., Howell, K., and Zhang, P. (2020). The influence of UV on the production of free terpenes in *Vitis vinifera* cv. Shiraz. Agronomy 10, 1431. doi: 10.3390/ agronomy10091431

Mori, K., Goto-Yamamoto, N., Kitayama, M., and Hashizume, K. (2007). Loss of anthocyanins in red-wine grape under high temperature. J. Exp. Bot. 58, 1935–1945. doi: 10.1093/jxb/erm055

Muñoz, N. C., González, M. F., Alonso, S. G., Romero, E. G., and Gutiérrez, I. H. (2009). Red color related phenolic composition of Garnacha tintorera (*Vitis vinifera* L.) grapes and red wines. J. Agric. Food Chem. 57, 7883–7891. doi: 10.1021/jf9002736

Oliveira, C., Ferreira, A. C., Costa, P., Guerra, J., and de Pinho, P. G. (2004). Effect of some viticultural parameters on the grape carotenoid profile. J. Agric. Food Chem. 52, 4178 4184. doi: 10.1021/jf0498766

Pillet, J., Egert, A., Pieri, P., Lecourieux, F., Kappel, C., Charon, J., et al. (2012). VvGOLS1 and VvHsfA2 are involved in the heat stress responses in grapevine berries. Plant Cell Physiol. 53, 1776–1792. doi: 10.1093/pcp/pcs121

Rapp, A. (1998). Volatile flavour of wine: Correlation between instrumental analysis and sensory perception. Nahrung - Food 42, 351–363. doi: 10.1002/(sici)1521 3803(199812)42:06<351

Savoi, S., Herrera, J. C., Carlin, S., Lotti, C., Bucchetti, B., Peterlunger, E., et al. (2020). From grape berries to wines: Drought impacts on key secondary metabolites. Oeno One 54, 569–582. doi: 10.20870/OENO-ONE.2020.54.3.3093

Savoi, S., Wong, D. C. J., Degu, A., Herrera, J. C., Bucchetti, B., Peterlunger, E., et al. (2017). Multi-omics and integrated network analyses reveal new insights into the systems relationships between metabolites, structural genes, and transcriptional regulators in developing grape berries (*Vitis vinifera* L.) exposed to water deficit. Front. Plant Sci. 8. doi: 10.3389/fpls.2017.01124

Sepulveda, G., and Kliewer, W. M. (1986). Effect of high temperature on grapevines (*Vitis vinifera* L.). II. Distribution of soluble sugars. Am. J. Enol Vitic 37, 20–25.

Slegers, A., Angers, P., Ouellet, É., Truchon, T., and Pedneault, K. (2015). Volatile compounds from grape skin, juice and wine from five interspecific hybrid grape cultivars grown in Québec (Canada) for wine production. Molecules 20, 10980–11016. doi: 10.3390/ molecules200610980

Song, J., Smart, R., Wang, H., Dambergs, B., Sparrow, A., and Qian, M. C. (2015). Effect of grape bunch sunlight exposure and UV radiation on phenolics and volatile composition of *Vitis vinifera* L. cv. Pinot noir wine. Food Chem. 173, 424–431. doi: 10.1016/j.foodchem.2014.09.150

Spayd, S. E., Tarara, J. M., Mee, D. L., and Ferguson, J. C. (2002). Separation of light and temp on Merlot. Am. J. Enol. Vitic. 3, 171–182.

Tarara, J., Lee, J., Spayd, S. E., and Scagel, C. F. (2008). Berry temperature and solar radiation alter acylation, proportion, and concentration of anthocyanin in Merlot grapes. Am. J. Enol Vitic 59, 235–247. doi: 10.5344/ajev.2008.59.3.235

Torres, N., Martínez-Lüscher, J., Porte, E., Yu, R., and Kaan Kurtural, S. (2020). Impacts of leaf removal and shoot thinning on cumulative daily light intensity and thermal time and their cascading effects of grapevine (*Vitis vinifera* L.) berry and wine chemistry in warm climates. Food Chem. 343, 128447. doi: 10.1016/j.foodchem.2020.128447

Torres, N., Yu, R., and Kurtural, S. K. (2021). Arbuscular mycrorrhizal fungi inoculation and applied water amounts modulate the response of young grapevines to mild water stress in a hyper-arid season. Front. Plant Sci. 11, 622209. doi: 10.3389/fpls.2020.622209

Torres, N., Yu, R., Martínez - Lüscher, J., Girardello, R. C., Kostaki, E., Oberholster, A., et al. (2022). Shifts in the phenolic composition and aromatic profiles of Cabernet Sauvignon (*Vitis vinifera* L.) wines are driven by different irrigation amounts in a hot climate. Food Chem. 371, 131163. doi: 10.1016/j.foodchem.2021.131163

Varela, C., Barker, A., Tran, T., Borneman, A., and Curtin, C. (2017). Sensory profile and volatile aroma composition of reduced alcohol Merlot wines fermented with *Metschnikowia pulcherrima* and *Saccharomyces uvarum*. Int. J. Food Microbiol. 252, 1-9. doi: 10.1016/j.ijfoodmicro.2017.04.002

Vilanova, M., Genisheva, Z., Bescansa, L., Masa, A., and Oliveira, J. M. (2012). Changes in free and bound fractions of aroma compounds of four *Vitis vinifera* cultivars at the last ripening stages. Phytochemistry 74, 196–205. doi: 10.1016/j.phytochem.2011.10.004

Waterhouse, A. L., Sacks, G. L., and Jeffery, D. W. (2016a). "Anthocyanins," in Understanding wine chemistry (Chichester, West Sussex, UK: John Wiley and Sons, Ltd), 131–139.

Waterhouse, A.L., Sacks, G.L., and Jeffery, D.W. (2016b). "Conversion of variety specific components, other," in Understanding wine chemistry. (Chichester, West Sussex, UK: John Wiley and Sons, Ltd), 265– 277.

Wei, T., Simko, V., Levy, M., Xie, Y., Jin, Y., and Zemla, J. (2017). R package "corrplot": Visualization of a correlation matrix. Statistician 56, 316–324.

Yang, Y., Jin, G. J., Wang, X. J., Kong, C. L., Liu, J., and Tao, Y. S. (2019). Chemical profiles and aroma contribution of terpene compounds in Meili (*Vitis vinifera* L.) grape and wine. Food Chem. 284, 155–161. doi: 10.1016/j.foodchem. 2019.01.106

Yue, T. X., Chi, M., Song, C. Z., Liu, M. Y., Meng, J. F., Zhang, Z. W., et al. (2015). Aroma characterization of Cabernet Sauvignon wine from the plateau of Yunnan (China) with different altitudes using SPME-GC/MS. Int. J. Food Prop 18, 1584–1596. doi: 10.1080/10942912.2014.923442

Zhang, J., Wang, T., Zhao, N., Xu, J., Qi, Y., Wei, X., et al. (2021). Performance of a novel b glucosidase BGL0224 for aroma enhancement of Cabernet Sauvignon wines. LWT 144, 111244. doi: 10.1016/j.lwt.2021.111244

Zhang, Q. A., Xu, B. W., Chen, B. Y., Zhao, W. Q., and Xue, C. H. (2020). Ultrasound as an effective technique to reduce higher alcohols of wines and its influencing mechanism investigation by employing a model wine. Ultrason Sonochem 61, 104813. doi: 10.1016/j.ultsonch.2019.104813

Tables and Figures

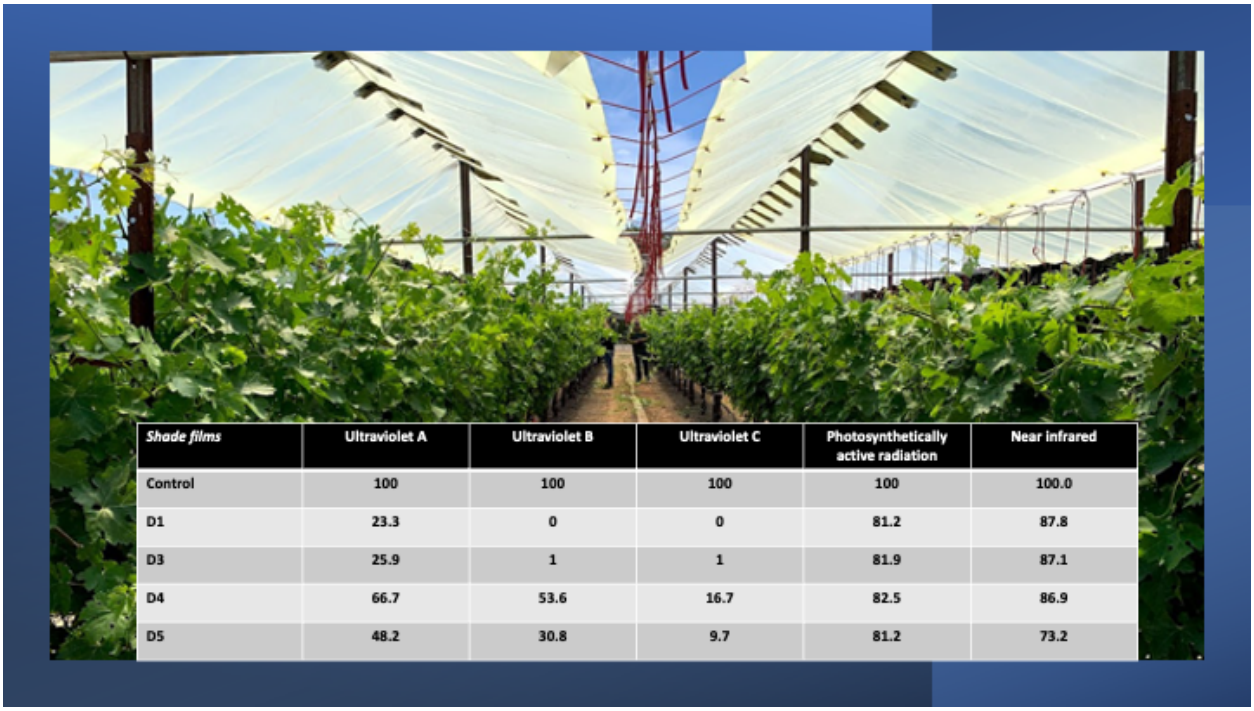

Shade films	Ultraviolet A	Ultraviolet B	Ultraviolet C	Photosynthetically active radiation	Near infrared
Control	100	100	100	100	100.0
D1	23.3	0	0	81.2	87.8
D3	25.9	1	1	81.9	87.1
D4	66.7	53.6	16.7	82.5	86.9
D5	48.2	30.8	9.7	81.2	73.2

Figure 1. Overhead shade films installed above the experimental vineyard and the percentage of solar radiation spectra transmitted through them at solar noon. Portion of this figure previously appeared in Marigliano et al. (2022)

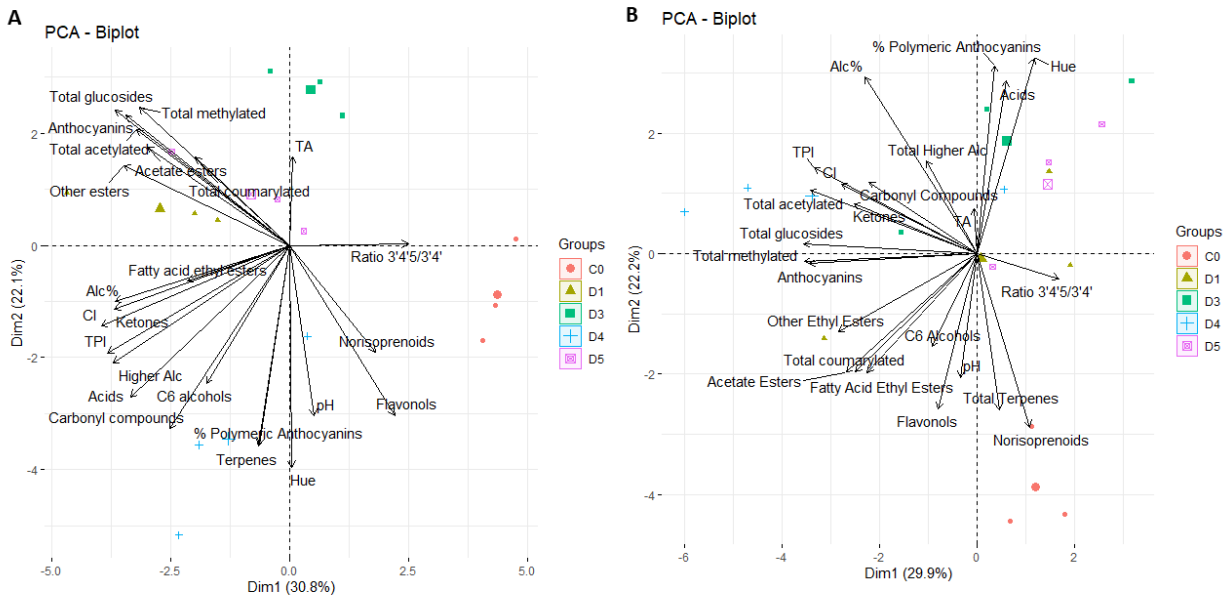

Figure 2. Principal component analysis (PCA) score and loadings plot obtained from the statistical analysis of wine characteristics, flavonoid and aroma profiles of 15 wines from Cabernet Sauvignon grapevines subjected to partial solar radiation exclusion using 4 overhead shade film treatments (D1, D3, D4, D5) and an uncovered control (C0) during the 2020 (A) and 2021 (B) growing seasons.

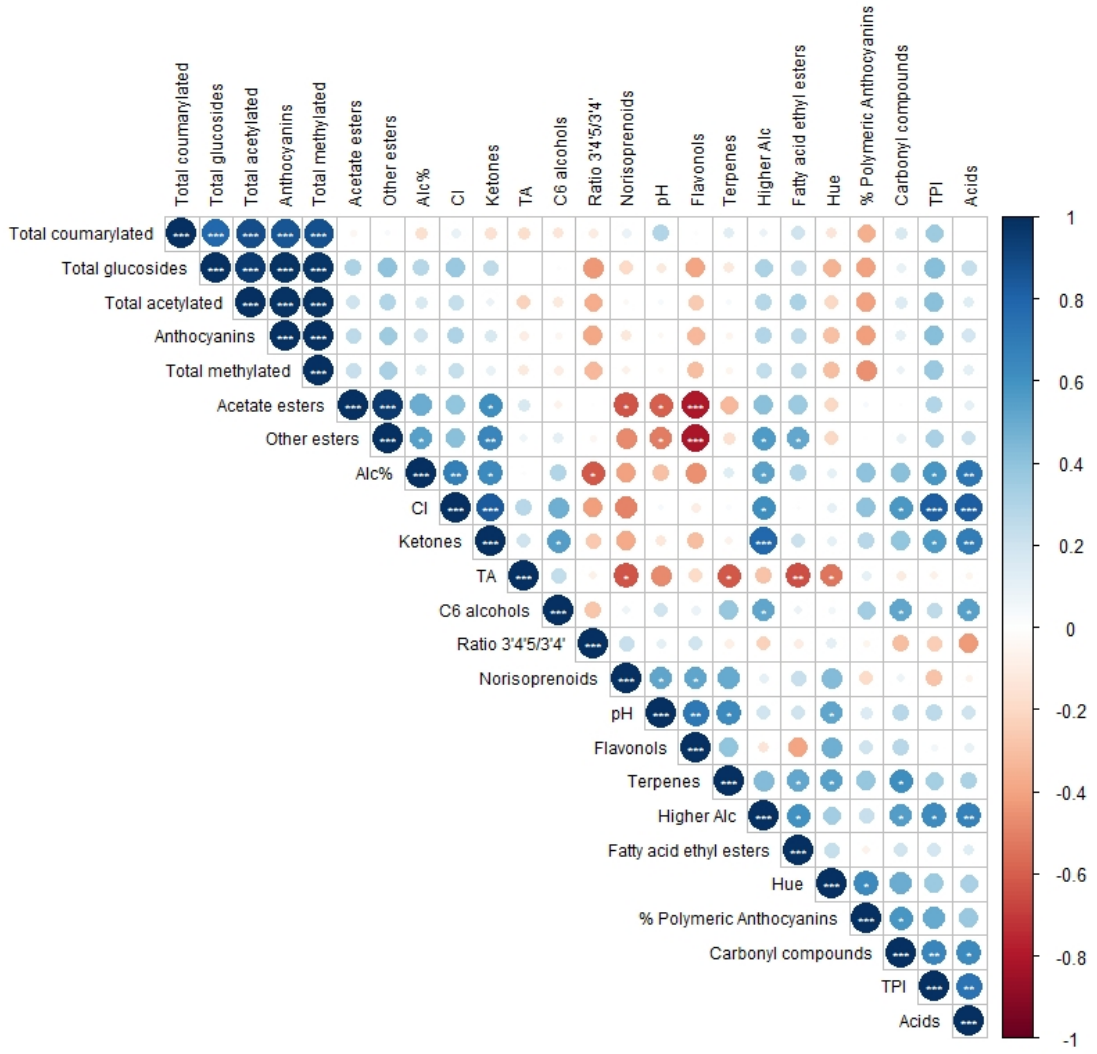

Figure S1. Correlation matrix among wine characteristics, flavonoid and aroma profiles of 15 wines from Cabernet Sauvignon grapevines subjected to partial solar radiation exclusion using 4 overhead shade film treatments (D1, D3, D4, D5) and an uncovered control (C0) during the 2020 growing season. Circle size and color represent *R* values for Pearson's correlation analysis. *, **, and *** indicate significance at 5%, 1% and 0.1%, respectively. CI: color intensity; TA: titratable acidity; TPI: total polyphenolic index.

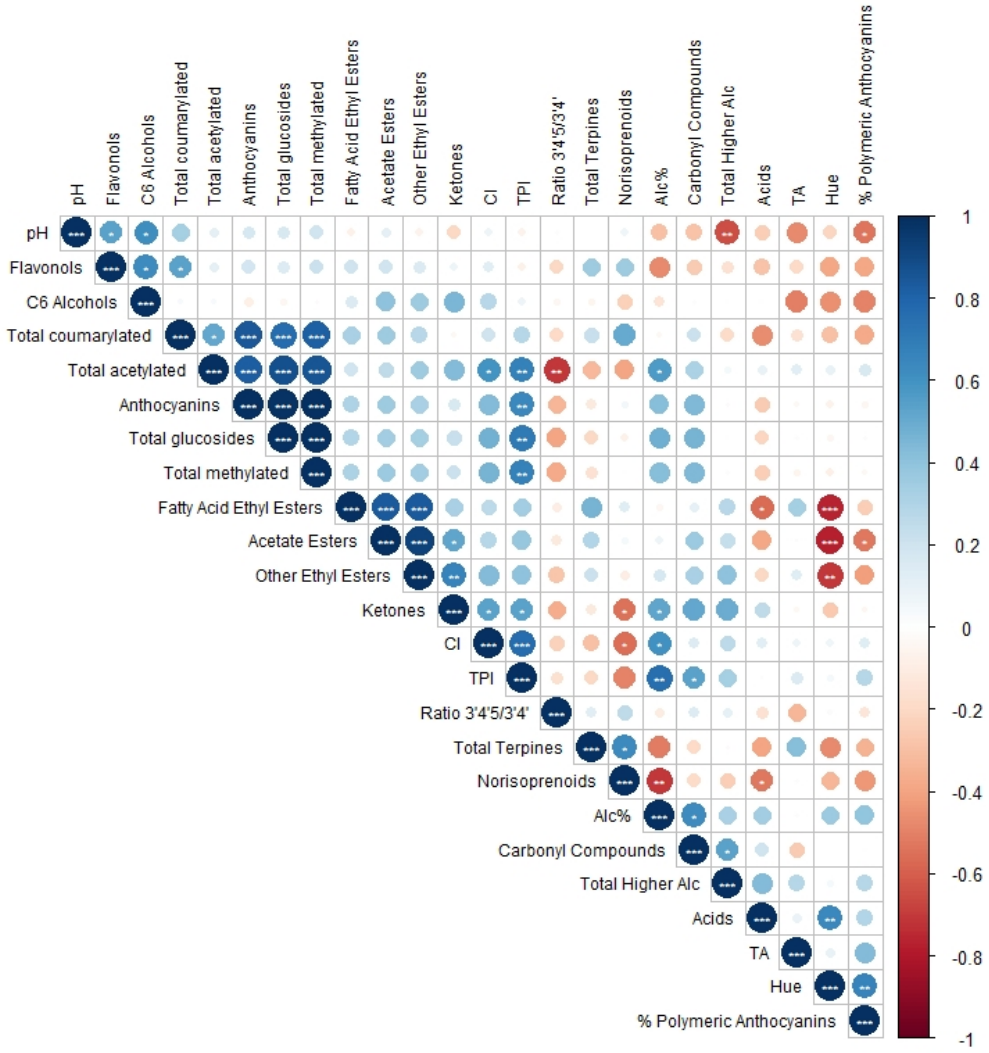

Figure S2. Correlation matrix among wine characteristics, flavonoid and aroma profiles of 15 wines from Cabernet Sauvignon grapevines subjected to partial solar radiation exclusion using 4 overhead shade film treatments (D1, D3, D4, D5) and an uncovered control (C0) during the 2021 growing season. Circle size and color represent *R* values for Pearson's correlation analysis. *, **, and *** indicate significance at 5%, 1% and 0.1%, respectively. CI: color intensity; TA: titratable acidity; TPI: total polyphenolic index.

Table 1. Chemical and colorimetric properties of wine samples from 'Cabernet Sauvignon' grapevines subjected to different photoselective shade film treatments in a vineyard in Oakville, CA, USA in two growing seasons (2020 and 2021)

	2020						2021						Y	Y x S
Wine color parameters	**C0**	**D1**	**D3**	**D4**	**D5**	**Sig.**	**C0**	**D1**	**D3**	**D4**	**D5**	**Sig.**		
CI	12.8[a] ±0.2c	15.1±0.9 ab	14.4±0.2b c	16.2±0.3 a	14.1±0.7bc	*	15.3±0.2 b	15.4±0.1 b	15.7±0.0 b	16.6±0.5a	15.7±0.1 b	*	***	.
hue	0.62±0.00 a	0.61±0.00a	0.59±0.00 b	0.63±0.01 a	0.61±0.01a	*	0.61±0.01	0.62±0.01	0.63±0.01	0.63±0.01	0.63±0.01	ns	**	*
% Polymeric anthocyanins	37.5±0.8b	38.2±0.6ab	37.0±0.6 b	41.5±1.0 a	36.2±2.0 b	.	27.9±0.4 b	28.8±0.7 ab	30.2± 0.6b	29.3± 0.3 a	29.4±0.3 b	.	***	*
TPI (AU)	47.1±1.2b	54.8± 2.9a	48.2± 0.9 b	55.1± 2.0 a	50.9±0.3ab	*	55.8± 2.6 b	64.2±1.3 ab	64.9±5.1 ab	74.4± 3.9 a	63.7±3.2 ab	*	***	ns
Chemical characteristics														
Alcohol content (%)	14.7±0.09 c	15.2±0.05a b	15.2±0.03 b	15.4±0.10 a	15.1±0.05b	***	15.3± 0.01	15.2 ± 0.07	15.3 ± 0.13	15.5 ± 0.17	15.3 ± 0.17	ns	**	.
Residual Sugar (g/L)	0.19±0.02 b	0.30±0.02a	0.26±0.01 a	0.27±0.02a	0.26±0.00a	*	0.07±0.02	0.05±0.00	0.05±0.01	0.06±0.01	0.05±0.01	ns	***	**
pH	3.66±0.01 a	3.64± 0.01a	3.61±0.01 b	3.66±0.00a	3.66±0.00a	***	3.65±0.02c	3.69±0.01b	3.72±0.01b	3.76±0.01 a	3.75±0.00 a	***	***	***
Titratable acidity (g/L)	5.45±0.04 b	5.43±0.08b	5.65±0.07 a	5.49±0.03a b	5.41±0.01b	.	6.12±0.01a	5.97±0.01b c	6.06±0.05a b	5.85±0.06 c	6.08±0.06a b	**	***	*

[a] Values represent means ± (n = 3) separated by Duncan's new multiple range post-hoc text at ($\alpha = 0.05$). Means separated by different letters are significantly different within each year. AU : absorbance units, CI: Color intensity, TPI: total polyphenol index. Significance or non-significance for shade treatment, year (Y) and interactions between year and shade treatment (Y*S) are indicated by: 'ns'= not significant; '.' $p \leq 0.1$; '*' $p \leq 0.05$; '**' $p \leq 0.01$; '***' $p \leq 0.001$.

Table 2. HPLC separations of flavonoids in wines from Cabernet Sauvignon grapevines subjected to different photoselective shade film treatments in Oakville, CA, USA in 2020 and 2021 growing seasons[a]

		2020						2021						Y	Y x S
		C0	D1	D3	D4	D5	*p*-value	C0	D1	D3	D4	D5	*p*-value		
Anthocyanin 3-glucoside (mg/L)	Delphinidin	2.6 ±0.1b	4.2±0.4a	3.8±0.1a	4.2±0.1a	4.1±0.1a	***	31.8±1.1bc	33.5±0.7b	31.4±1.1bc	37.2±0.4a	30.6±0.6 c	**	***	***
	Cyanidin	0.20±0.06	0.16±0.02	0.16±0.02	0.24±0.06	0.23±0.03	ns	1.1±0.0 b	1.2±0.1 b	1.3± 0.1 ab	1.5±0.2 a	1.2±0.2ab	.	***	ns
	Petunidin	3.3±0.1b	4.6 ± 0.3a	4.3 ± 0.1 a	4.5 ± 0.1 a	4.6±0.1a	**	34.4±1.7b	36.5±0.8b	34.4±1.0b	42.3±1.6a	34.1±0.4b	**	***	***
	Peonidin	1.3±0.1c	1.8±0.2b	1.7±0.04b	1.7±0.1b	2.2±0.04 a	**	10.5±0.5	9.8±0.2	11.5±1.6	14.9±4.3	9.2±0.2	ns	***	ns
	Malvidin	46.5±1.3b	53.6 ± 2.5 a	50.1 ± 1.2 ab	46.5 ± 1.2 b	53.7 ± 1.7 a	*	342.0±15.6	369.0±13.8	345.0±10.1	384.7±17.1	334.8±7.2	ns	***	ns
	Total glucosides	53.9±1.4b	64.4±3.4a	60.2±1.5ab	57.2±1.5b	64.7±2.0a	*	419.9±18.8b	450.1±15.5ab	423.6±12.2b	480.7±23.1a	409.9 ± 8.0b	.	***	*
3-Acetyl-glucoside (mg/L)	Delphinidin	0.84±0.05 b	1.41± 0.16 a	1.28±0.07a	1.46± 0.05 a	1.47 ± 0.11 a	**	11.5 ± 0.6 b	14.0 ± 0.3 ab	13.2 ± 0.5 b	17.2 ± 2.4 a	13.1 ± 0.5 b	.	***	ns
	Cyanidin	0.74± 0.05 c	0.88±0.02bc	0.94±0.03ab	0.99±0.03ab	1.08 ± 0.07 a	**	5.8 ± 0.6	6.2 ± 0.7	9.5 ± 3.0	9.7 ± 2.2	5.6 ± 1.4	ns	***	ns
	Petunidin	1.2 ± 0.1 b	2.4 ± 0.5 a	1.7 ± 0.1 ab	2.2 ± 0.3 a	2.1 ± 0.2 ab	.	13.8 ± 0.9 b	16.0 ± 0.6 ab	14.8 ± 0.6 b	18.5 ± 1.4 a	14.3 ± 0.6 b	*	***	*
	Peonidin	0.27 ± 0.03	0.20 ± 0.11	0.28 ± 0.02	0.26 ± 0.04	0.34 ± 0.03	ns	10.7 ± 0.4 ab	9.7 ± 0.3 bc	9.0 ± 0.2 c	11.6 ± 0.8 a	10.2 ± 0.5 abc	*	***	*
	Malvidin	28.5± 0.8 b	31.7 ± 1.0 a	28.7 ± 0.8 b	27.0 ± 0.6 b	31.6 ± 1.0 a	*	2.1 ± 0.2	1.9 ± 0.2	2.0 ± 0.1	2.3 ± 0.4	2.1 ± 0.2	ns	***	**
	Total acetylates	31.6± 0.9 b	36.6 ± 1.7 a	32.9 ± 0.9 b	31.9 ± 0.5 b	36.7 ± 0.8 a	*	43.9 ± 2.1 b	47.7 ± 1.9 ab	48.5 ± 3.4 ab	59.3 ± 6.3 a	45.2 ± 2.1 b	.	***	*
3-p-Coumaroyl-glucoside (mg/L)	Delphinidin	1.1± 0.1 ab	1.3 ± 0.05 a	1.1 ± 0.1 ab	0.94 ± 0.1 b	1.2 ± 0.1 a	*	194.4±11.0ab	212.0 ± 8.9a	189.2±6.5 ab	210.3±5.6 a	175.7 ± 4.5 b	*	***	*
	Cyanidin	0.45 ± 0.03	0.42 ± 0.1	0.37 ± 0.08	0.50 ± 0.0	0.40 ± 0.04	ns	2.7 ± 0.2 ab	2.3 ± 0.1 bc	2.1 ± 0.1 bc	3.1 ± 0.3 a	1.9 ± 0.2 c	*	***	*
	Petunidin	0.28 ± 0.01	0.39 ± 0.14	0.35 ± 0.06	0.34 ± 0.03	0.32 ± 0.03	ns	1.8 ± 0.2 a	1.0 ± 0.0 c	1.0 ± 0.2 bc	1.5 ± 0.1 ab	1.1 ± 0.1 bc	**	***	**
	Peonidin	0.28±0.01bc	0.36±0.01ab	0.27±0.05c	0.31±0.01bc	0.42±0.02a	*	3.24±0.1a	2.6±0.1b	2.6±0.2b	2.8±0.2ab	2.5±0.0b	*	***	**

	Malvidin	5.2±0.2ab	5.8±0.4a	4.8±0.05b	4.5±0.1b	5.7±0.3a	**	44.0±3.1a	43.8±2.3a	38.3±1.5ab	44.6±2.0a	35.1±1.3b	*	***	*
	Total coumarylated	6.2±0.2ab	7.0±0.5a	5.8±0.2b	5.7±0.1b	6.9±0.2a	*	51.7±3.5a	49.7±2.5a	44.0±1.7ab	52.0±2.3a	40.6±1.6b	*	***	**
	Total methylated anthocyanins (mg/L)	86.9±2.4b	100.8±5.0a	92.3±2.3ab	87.4±1.9b	100.9±2.8a	*	462.6±22.1ab	490.3±18.2ab	458.7±13.4b	523.3±26.2a	443.4±9.1b	.	***	*
	Total free anthocyanins (mg/L)	92.8±2.5b	109.1±5.6a	100.0±2.4ab	95.7±2.0b	109.4±3.0a	*	709.8±35.4ab	759.5±28.6ab	705.4±20.7b	802.3±35.9a	671.3±15.5b	.	***	*
	Ratio 3'4'5'/3'4'	36.2±3.5a	32.4±1.2ab	30.5±0.5abc	28.0±1.5bc	26.0±1.1c	*	35.3±0.1	40.0±0.4	33.0±3.8	31.3±5.8	38.2±0.7	ns	**	ns
Flavonols (mg/L)	Myricetin-3-glucoside	0.59±0.03ab	0.53±0.05b	0.51±0.01b	0.66±0.02a	0.55±0.01b	*	3.7±0.1a	2.8±0.2b	2.9±0.1b	3.4±0.1b	3.0 ±0.1b	**	***	***
	Myricetin-3-glucuronide	3.2±0.1	3.4±0.2	3.2±0.1	3.4±0.1	3.5±0.1	ns	21.4±0.5ab	18.8±0.6c	18.6±1.1c	22.4±1.1a	19.5±0.4bc	*	***	*
	Quercetin-3-galactoside	0.39±0.04ab	0.24±0.03c	0.26±0.0c	0.41±0.03a	0.31±0.03bc	**	2.0±0.1a	1.0±0.0c	1.1±0.1c	1.6±0.1b	1.2±0.2c	**	***	***
	Quercetin-3-glucoside	2.1±0.05a	1.2±0.11c	1.2±0.03c	1.6±0.03b	1.5±0.01b	***	9.8 ± 0.6a	5.8±0.1c	6.1±0.2c	7.4±0.3b	6.6±0.4bc	***	***	***
	Quercetin-3-glucuronide	2.3±0.04a	1.4± .05d	1.4±0.08d	2.0±0.08b	1.7±0.07c	***	12.0±0.8a	5.6±0.1d	6.7±0.2cd	8.4±0.0b	7.8±0.5bc	***	***	***
	Laricitrin-3-glucoside	0.98±0.03a	0.81±0.05bc	0.78±0.03c	0.91±0.03ab	0.88±0.02abc	*	3.9±0.4	3.1±0.2	3.4±0.2	4.0±0.1	3.6±0.1	ns	***	ns
	Kaempferol-3-glucoside	0.42±0.02a	0.23±0.02c	0.23±0.02c	0.31±0.01b	0.27±0.02bc	***	1.8±0.2a	0.7±0.0c	1.0±0.1bc	1.2±0.0b	1.1±0.1b	***	***	***
	Isorhamnetin-3-glucoside	0.73±0.04a	0.44±0.06b	0.38±0.01b	0.46±0.01b	0.45±0.05b	***	2.9±0.4a	1.5±0.1c	1.9±0.1bc	2.3±0.1ab	2.0±0.1bc	**	***	*
	Syringetin-3-glucoside	1.3±0.03a	1.0±0.06c	1.0±0.05c	1.2±0.02ab	1.1±0.02bc	**	4.6±0.3a	3.1±0.1c	3.5±0.0bc	4.0±0.1b	3.6± .2b	***	***	***
	Total flavonols	11.9±0.2 a	9.3±0.6 cd	9.0±0.3d	11.0±0.2ab	10.2±0.1bc	***	62.0±2.4a	42.3±0.7d	45.1±1.7cd	54.7±1.5b	48.4±1.4c	***	***	***

[a]Values represent means ± SE (n=3) separated by Duncan's new multiple range *post hoc* test (α=0.05). Means separated by different letters are significantly different within each year. Significance or non-significance for shade treatment, year (Y) and interactions between year and shade treatment (YxS) are indicated by: 'ns'= not significant; '.' $p \leq 0.1$; '*' $p \leq 0.05$; '**' $p \leq 0.01$; '***' $p \leq 0.001$.

Table 3. Aromatic composition of Cabernet Sauvignon wines from grapevines subjected to different photoselective shade film treatments in Oakville, CA, USA in 2020 and 2021 growing seasons[a]

	2020						2021						Y	Y x S
Total C6 alcohols	C0	D1	D3	D4	D5	*p*-value	C0	D1	D3	D4	D5	*p*-value		
1-Hexanol (µg/L)	18.8 ± 1.1	19.5 ± 0.9	19.2 ± 0.2	22.8 ± 2.8	18.7 ± 0.4	ns	14.1 ± 0.4 a	11.9 ± 0.5 b	11.6 ± 0.3 b	13.8 ± 0.4 a	14.4±0.4 a	**	***	ns
(*E*)-2-Hexen-1-ol (µg/L)	0.28±0.001ab	0.35±0.028a	0.27±0.017ab	0.21±0.055b	0.36±0.022a	*	0.21 ± 0.04	0.17 ± 0.05	0.17 ± 0.02	0.22 ± 0.03	0.21± 0.01	ns	***	ns
Total higher alcohols														
Isoamyl alcohol (mg/L)	0.84±0.04b	0.97±0.01 a	0.90±0.02ab	0.99±0.04 a	0.90±0.03ab	*	0.94±0.03	0.94 ±0.05	0.99 ±0.04	1.00 ±0.04	0.96 ±0.02	ns	*	ns
1-Octen-3-ol (µg/L)	0.75±0.03	0.66±0.3	0.67±0.2	0.96±0.2	0.83±0.09	ns	0.58±0.04	0.58±0.05	0.54±0.13	0.56±0.14	0.58±0.02	ns	*	ns
2-Phenyl-1-ethanol (mg/L)	2.1±0.1	2.3±0.1	2.1±0.1	2.3±0.1	2.2±0.1	ns	2.4±0.1d	2.4 ±0.1 c	2.8±0.2a	2.5±0.1bc	2.6±0.1ab	ns	***	ns
Isobutanol (µg/L)	0.72±0.57	1.94±0.84	0.21±0.04	1.39±0.62	1.69±0.77	ns	1.38±0.65	0.11±0.02	0.81±0.70	0.53 ±0.42	0.12±0.02	ns	ns	ns
Benzyl alcohol (µg/L)	3.1±0.08a	3.2±0.1a	2.7±0.05b	3.1±0.1a	2.9±0.1ab	*	2.9±0.1d	3.5±0.1c	4.2±0.1a	3.7±0.1bc	3.9±0.1ab	***	***	***
Total acetate esters														
Ethyl acetate (mg/L)	0.39±0.02c	0.47±0.00a	0.45±0.00ab	0.48±0.01a	0.42±0.02bc	**	0.36±0.01	0.35±0.02	0.37±0.02	0.38±0.02	0.36±0.03	ns	***	ns
Isoamyl acetate (mg/L)	0.31±0.02b	0.45±0.03a	0.44±0.03a	0.32±0.04b	0.37±0.01ab	*	0.49±0.01	0.47±0.07	0.43±0.04	0.46±0.03	0.44±0.04	ns	**	ns
Total fatty acid ethyl esters														
Ethyl hexanoate (mg/L)	1.18±0.06b	1.40±0.05a	1.25±0.06b	1.24±0.01b	1.31±0.03ab	.	0.89±0.05	0.82±0.07	0.82±0.07	0.81±0.05	0.77±0.04	ns	***	ns
Ethyl octanoate (mg/L)	9.09±0.3ab	10.5±0.6a	8.76±0.5b	9.43±0.3ab	10.2±0.2a	.	7.98±0.6	7.47±0.8	7.73±1.1	7.78±0.7	6.84±0.6	ns	***	ns
Ethyl decanoate (µg/L)	0.06±0.01bc	0.08± 0.01a	0.08± 0.00ab	0.06 ± 0.01c	0.06±0.00c	*	0.12±0.00	0.12±0.01	0.12±0.01	0.12 ±0.00	0.11±0.01	ns	***	ns

Ketones														
Ethyl isodiacetyl (mg/L)	2.1±0.08c	2.4±0.02ab	2.3±0.03ab	2.5± 0.00a	2.2±0.1 bc	*	2.1±0.08	2.1±0.08	2.2±0.07	2.3±0.09	2.2±0.07	ns	*	ns
Total other esters														
Ethyl butyrate (µg/L)	41.7±2.4c	55.0±2.6a	49.9±2.6ab	47.0±0.7bc	47.0±1.1bc	*	41.2±2.1	40.3±4.1	41.9±3.0	43.5 ± 3.3	39.3 ± 2.8	ns	***	ns
Ethyl-2-methylbutyrate (µg/L)	5.8±0.1b	6.9±0.05ab	7.6±0.7a	6.8±0.2ab	6.2±0.3b	*	4.0±0.7	3.3±0.1	3.4±0.2	3.3±0.1	3.4±0.1	ns	***	*
Ethyl isovalerate (µg/L)	7.2±0.1c	9.1±0.2a	9.0±0.2a	8.5±0.1ab	7.9 ± 0.4bc	***	3.7±0.3	3.5±0.2	3.5±0.2	3.6 ±0.1	3.6±0.1	ns	***	***
Total acids														
Isobutyric acid (µg/L)	1.4±0.07 b	1.6±0.05b	1.5±0.04b	1.8±0.10a	1.5±0.09b	*	2.1±0.12	2.2±0.06	2.8±0.37	2.7±0.21	2.9±0.34	ns	***	ns
Total carbonyl compounds														
Benzaldehyde (µg/L)	0.90 ± 0.2	1.34 ± 0.3	0.60±0.0	1.60±0.5	0.91±0.1	ns	1.06±0.05	1.20±0.08	1.14±0.05	1.17±0.02	1.14±0.02	ns	ns	ns
Total Terpenes														
β-Myrcene (µg/L)	0.06±0.01	0.07±0.01	0.06±0.00	0.06±0.02	0.07±0.00	ns	0.08±0.00	0.08±0.01	0.08±0.00	0.09±0.01	0.09±0.00	ns	**	ns
α-Terpinene (µg/L)	0.24±0.01bc	0.21±0.01c	0.21±0.01c	0.27±0.01ab	0.31±0.01a	**	0.14±0.01a	0.11±0.01b	0.11±0.01b	0.12±0.01ab	0.12±0.01ab	.	***	**
cis-Rose-oxide (µg/L)	0.11±0.01c	0.12±0.01abc	0.12±0.02bc	0.12±0.01a	0.15±0.01ab	.	0.07±0.01b	0.08±0.01ab	0.07±0.01ab	0.09±0.01ab	0.09±0.01 a	.	***	ns
Linalool (µg/L)	2.0±0.07b	2.2±0.02a	2.0±0.06b	2.2±0.07a	2.0±0.03b	*	1.8±0.07	1.8±0.01	1.8±0.09	1.8±0.09	1.7±0.02	ns	***	ns
Nerol (µg/L)	0.12±0.01a	0.11±0.01ab	0.09±0.01b	0.09±0.01b	0.12±0.01a	*	0.17±0.01	0.16±0.01	0.16±0.01	0.16±0.01	0.15±0.01	ns	***	*
Nerolidol (µg/L)	2.4±0.05	2.8±0.07	2.4±0.07	2.9±0.23	2.8±0.21	ns	1.63±0.03a	1.48±0.08ab	1.50±0.16ab	1.27±0.02b	1.25±0.03 b	*	***	*
Farnesol (µg/L)	0.81±0.02a	0.73±0.07a	0.47±0.04b	0.68±0.08ab	0.67±0.08ab	*	0.81±0.03	0.60±0.08	0.65±0.11	0.56±0.01	0.57±0.04	ns	ns	ns
Total norisoprenoids														

β-Damascenone (µg/L)	3.3±0.01a	3.0±0.17ab	2.8±0.04b	3.0±0.14ab	3.1±0.09ab	.	3.6±0.14a	3.3±0.05ab	3.1±0.08bc	2.9±0.09cd	2.8±0.07d	**	ns	**
β-Ionone (µg/L)	0.070±0.001	0.065±0.001	0.064±0.001	0.067±0.003	0.068±0.002	ns	0.043±0.001	0.040±0.002	0.040±0.002	0.039±0.002	0.041±0.001	ns	***	ns

[a]Values represent means ± SE (n=3) separated by Duncan's new multiple range *post hoc* test (p=0.05). Means separated by different letters are significantly different within each year. Significance or non-significance for shade treatment, year (Y) and interactions between year and shade treatment (Y*S) are indicated by: 'ns'= not significant; '.' $p \leq 0.1$; '*' $p \leq 0.05$; '**' $p \leq 0.01$; '***' $p \leq 0.001$.

Table S1. Thresholds of odor active chemicals in young red wines complied by Frank and Newton (2005) from selected recent studies, unless otherwise specified.

Compound	Odor Activity Threshold (µg/L)
Total C6 alcohols	
1-Hexanol (µg/L)	8000
(*E*)-2-Hexen-1-ol (µg/L)	400
Total higher alcohols	
Isoamyl alcohol (mg/L)	30000
1-Octen-3-ol (µg/L)	1[a]
2-Phenyl-1-ethanol (mg/L)	10000-14000
Isobutanol (µg/L)	40000
Benzyl alcohol (µg/L)	10000[a]
Total acetate esters	
Ethyl acetate (mg/L)	12264
Isoamyl acetate (mg/L)	30
Total fatty acid ethyl esters	
Ethyl hexanoate (mg/L)	5-14
Ethyl octanoate (mg/L)	2-5
Ethyl decanoate (µg/L)	200
Ketones	
Ethyl isodiacetyl (mg/L)	100
Total other esters	
Ethyl butyrate (µg/L)	20
Ethyl-2-methylbutyrate (µg/L)	1-18
Ethyl isovalerate (µg/L)	1[b]
Total acids	
Isobutyric acid (µg/L)	2300
Total carbonyl compounds	
Benzaldehyde (µg/L)	2000[c]
Total Terpenes	
β-Myrcene (µg/L)	14[d]
α-Terpinene (µg/L)	250[a]
cis-Rose-oxide (µg/L)	0.2
Linalool (µg/L)	25.2

Nerol (μg/L)	400[d]
Nerolidol (μg/L)	700[e]
Farnesol (μg/L)	200[f]
Total norisoprenoids	
β-Damascenone (μg/L)	0.05
β-Ionone (μg/L)	0.09

[a] Yue et al., 2015
[b] Arcari et al., 2017
[c] Jiang and Zhang, 2010
[d] Slegers et al., 2015
[e] Yang et al., 2019
[f] Loscos et al., 2007

Chapter 3: Trellis Systems Can Reduce Water Footprint and Increase Water Use Efficiency of Microirrigated Grapevine Grown in Hot Climates

A scientific article drawn from Chapter 3 is currently being prepared for internal review and submission to the refereed journal Frontiers in Plant Science.

Keywords: grapevine training system, water requirements, semi-arid growing environment climate change, deficit irrigation

Abstract

Global increases in air temperature and increasing drought frequency and severity challenge grape and wine production. Grape and wine quality are responsive to solar radiation interception and applied water amounts. Previous works have highlighted improvements to grape flavonoid composition under sprawling trellis systems compared to traditional VSP. Recommendations to utilize sprawling canopies for reducing cluster temperature are followed by a lack of information regarding the amounts of applied water necessary to sustain larger vine canopies. With water supply restrictions due to environmental regulations and recurring droughts, the viability of grape wine production with larger vine canopies is unsubstantiated. In this study, we examined six trellis systems under three regimes of applied water (corresponding to 25%, 50% and 100% ET_c) and determined their water use efficiency in a hot viticultural region. The six trellises included a traditional VSP, two modified VSP systems which slightly open the canopy respectively to ~60^o and ~80^o (VSP60 and VSP80), VSP with Guyot pruning, single high wire (SH) and high quadrilateral (HQ). Under prolonged drought conditions that occurred over the experimental years, SH vines had the highest WUE_c due to increased fruit yields under a given amount of applied water. Additionally, WUE_c decreased linearly with increasing amounts of applied water. SH vines outperformed other trellis systems in terms of fruit yield per meter of vine row, while reductions in the amounts of applied water decreased the yield. The total vine's water footprint decreased in SH vines under irrigation at 50-100% ET_c, indicating improved vineyard sustainability. Our study indicated that despite water scarcity brought on by anthropogenic climate change, SH trellis system under irrigation at 50-100% ET_c maintain carbohydrate allocation and fruit yields, while reducing cluster temperatures and reducing vineyard water footprint. Our results provide relevant information to wine grape

growers seeking to mitigate climate change and ensure future vineyard sustainability in an uncertain, highly variable, and changing climate.

Introduction

Although grapevine is one of the most resilient crops globally, the changing climate is one of the many challenges to its cultivation and ultimately wine production. According to the Intergovernmental Panel on Climate Change (IPCC), global air temperatures are likely to increase 1.5-4.5ºC between 2030 and 2052 (IPCC et al., 2018). Historical records of growing degree day (GDD) accumulation demonstrate that air temperatures in the world's most notable grape growing regions have increased steadily within the last 70 years (Kurtural and Gambetta, 2021). Such increases in GDD accumulation disrupt the natural coupling and balance of primary and secondary metabolites during ripening, corresponding with a plateau in wine quality ratings (Kurtural and Gambetta, 2021). Subsequently, excessive air temperatures reduce pleasant and desirable wine aroma compounds, but also contribute to reductions in wine quality (Marigliano et al., 2022). Moreover, predicted changes in precipitation patterns and increased drought frequency threaten grapevine water status conducive to market-desired fruit yield and composition and long-term vineyard sustainability.

With increasingly frequent and prolonged drought periods and less predictable rainfall, vineyards will need to adapt to changes in water availability. Adaptations to water shortages have been investigated at both the plant and field scales. The evaluation and performance of drought tolerant rootstock and scion cultivars has also been investigated (Tomás et al., 2014; Vaz et al., 2016); however, their adoption may be limited due to historical and cultural connections to popular grape cultivars. Additionally, the effect of rootstock-scion interactions on water use efficiency is poorly understood and only recently became an area of research (Medrano et al.,

2015; Duchêne, 2016). At the field scale, wider row spacing to decrease vine density can decrease overall vineyard evapotranspiration by reducing the competition for water between vertically shoot-positioned vines (Naulleau et al., 2021). Pieri et al. (2012) examined the water balance of two planting densities (3,000 and 9,000 vines/ha) in five viticultural regions of France and concluded that lower planting densities utilizing constrained canopies can maintain vine water status within moderate stress levels in forecasted climate change conditions. However, decreased plant density may result in lower yields at the field-scale, requiring an economic cost/benefit analysis to determine its viability as a water conserving solution. Reducing applied water through sustained (SDI) and regulated deficit irrigation (RDI) strategies is already commonly used to improve flavonoid composition in the grape skins (Castellarin et al., 2007; Ollé et al., 2011; Munitz et al., 2017). Furthermore, varied amounts of applied water have been trialed in a hot growing region such as California and demonstrated that irrigating at 50% of potential grapevine evapotranspiration (ET_c) was sufficient to mitigate water shortages when dormant season precipitation was limited (Torres et al., 2021). More deliberate interventions to adapt to heat and water shortages in the vineyard include the use of shade cloths and films to reduce canopy temperatures and vine evapotranspiration (Caravia et al., 2016; Marigliano et al., 2022). Again however, the implementation of these shade structures is under question as they present barriers to vineyard mechanization and may be a costly and unfeasible long-term solution.

Adapting trellis systems may be another method for mitigation of climate change impacts in production vineyards. Choosing an appropriate trellis system is an important pre-planting decision during vineyard establishment. An appropriate trellis system optimizes the vine's capacity to intercept solar radiation and produce a canopy microclimate that results in optimal

berry ripening without excessive direct solar radiation overexposure to the fruit zone. A traditional and commonly used trellis system in various grapevine production areas worldwide is the vertically shoot positioned (VSP) trellis. While VSP trellises were traditionally thought to improve berry ripening, the VSP trellis system maximizes light penetration and canopy porosity, producing a canopy microclimate which increases cluster vulnerability to overexposure in hot viticulture regions (Dry, 2009). More recent work has investigated the resiliency of red wine grapes in hot viticulture regions when training systems are varied from the traditional VSP trellis. In a study conducted in Napa Valley CA, USA, trellis systems with free and sprawling canopies such as a single-high wire (SH) and high-quadrilateral (HQ) systems increased yield and produced berries with improved flavonoid profiles that are attributed to reduction in chemical degradation compared to traditional VSP trellis systems regardless of applied water amounts (Yu et al., 2022). Additionally, the interactive effect of varied applied water amounts and trellis systems has been minimally investigated. Williams and Heymann (2017) applied various fractions of estimated potential grapevine evapotranspiration to VSP and Scott-Henry trellis systems to elucidate the effect of applied water on vine productivity and fruit composition in Livermore, CA. In their study, irrigation amounts had a larger effect on vine productivity and berry quality than trellis systems due to VSP and Scott-Henry trellis systems having similar levels of overexposure to the fruit zone (Williams and Heymann, 2017). Free and sprawling trellis systems which can shade the fruit zone and protect it from overexposure conditions can provide a long-term feasible heat avoidance strategy for hot viticulture regions due to promoting larger canopies.

While there are demonstrated improvements to grape chemical composition with the adoption of these sprawling trellis systems, it is understood that trellis systems promoting larger

leaf area indices (LAIs) will have a higher water demands (Williams and Ayars, 2005; Williams, 2014). In regions where irrigation is required to supplement seasonal precipitation, maintaining these larger canopies may prove difficult, especially with increasingly stringent environmental regulations such as the Sustainable Groundwater Management Act (SGMA) in the state of California. SGMA limits groundwater extraction for agricultural irrigation (Kiparsky, 2016). Compliance with SGMA will result in allotted water use restrictions in California's Napa Valley, limiting growers to 120 mm of applied water each season. Therefore, there is uncertainty surrounding how growers will respond to such water restrictions in tandem with adapting to increasing temperatures in a climate change scenario. Ultimately, there is a lack of information on the water footprint of resilient trellis systems hindering their adoption in microirrigated wine grape production vineyard.

Our previous works conducted with VSP trellis indicated that irrigating at different percent of potential grapevine ET affected grapevine physiology leading to different carbon allocation, water footprint, and water use efficiency in hot climates (Torres et al., 2021). Likewise, our previous work provided evidence that trellis systems other than VSPs provide better adaptation of wine grapes to climate change by ameliorating physiological performance and berry chemistry due their canopy architecture (Yu et al., 2022). Therefore, the objective of this experiment was to determine the water use efficiency of grapevine with trellis and pruning types that are commonly used in production regions characterized by hot climates. We hypothesized that the new trellises that were indicated to be more resilient to climate change would have different water needs than traditional VSP. Therefore, we applied fractions of the potential grapevine evapotranspiration estimated for VSP to different trellis systems to compare their water productivity relative to VSP under a climate change scenario.

Material and Methods

Vineyard site, plant material and experimental design

The experiment was conducted in Oakville, CA, USA during three consecutive growing seasons (2020, 2021 and 2022) at the University of California Davis, Oakville Experimental Vineyard in Oakville, CA, USA (38.428° N, 122.409° W). The vineyard was planted with "Cabernet Sauvignon" (*Vitis vinifera* L.) clone FPS08 grafted on 3309C rootstock (*Vitis riparia* × *Vitis rupestris*) in 2015. The grapevines were planted at 1.52 m × 2.13 m (vine × row) and oriented NW to SE. Data collection commenced in October 2019. The weather data at this vineyard was obtained from the California Irrigation Management Information System (CIMIS) (station #77, Oakville, CA). The weather station was located 160 m from the experimental vineyard block.

The study was conducted in a split-plot factorial design that utilized two factors and was described previously by Yu et al (2022). Briefly, six trellis systems randomly combined with three different applied water amounts applied at random to each row with four replications in each treatment, which consisted of seven vines. There were 72 experimental units in total. The main treatment (trellis systems) was applied to every row, and the sub-plot (applied water amounts) was applied at random to seven consecutive vines within each row so that three separate irrigation sub-plot factors were contained in every row within the vineyard block. The five middle vines were used for on-site measurements.

Trellis systems

Six trellis systems were used in this experiment and were previously described by Yu et al. (2022) (Figure 1). Briefly, the six trellis systems included a vertical-shoot positioned trellis

(VSP), two additional VSP trellises that were modified to further open the canopies ("relaxed VSPs" with ~60° and ~80° shoot orientations: VSP60 and VSP80, respectively), a VSP trellis pruned with the Guyot method (GY), a single high wire trellis (SH) and a high-quadrilateral trellis (HQ). The cordon height for VSP, VSP60, VSP80 and HQ was 0.96 m above the vineyard floor. The cordon height for SH was 1.54 m above the vineyard floor. The cordon height for GY was 1.70 m about the vineyard floor. The canopy management conducted for this experiment was previously described (Yu et al., 2022) and followed common local practices.

Irrigation treatments

The irrigation treatments consisted of the application of different fractions of the estimated potential grapevine evapotranspiration (ET_c). Vineyard ET_c was calculated using the following equation:

$$\text{Eq.1. } ET_c = ET_o \times K_c$$

where ET_o is the reference evapotranspiration obtained with a weekly time-step throughout all seasons from the onsite CIMIS weather station, and K_c is the crop coefficient calculated using the shade cast method as described by Williams (2014) specific for a VSP trellis adjusted for row spacing. Briefly, three neighboring rows of VSP trellis in the same vineyard were irrigated at 100% of ET_o. The shade cast by the grapevine canopy was measured weekly starting in mid-April of each experimental year and Kc was calculated (Figure 2).

Irrigation treatments in this study aimed to apply water amounts corresponding to 100% ET_c, 50% ET_c and 25% ET_c. Irrigation treatments were implemented using varying emitter numbers per vine, with irrigation duration calculated with respect to the treatment at 100% ET_c. NETAFIM™ pressure compensating on-line button drippers were installed to apply different

irrigation rates: 2 drippers per vine with an emission rate of 4 L h^{-1} to irrigate at 100% ET_c , 2 drippers with emission rate of 2 L h^{-1} per vine to irrigate at 50% ET_c , and 2 drippers with emission rate of 1 L h^{-1} to irrigate at 25% ET_c. The amount of water applied was calculated by multiplying the number of operating hours of the irrigation pump by the measured output of drip emitters installed for the different treatments. These values were then checked against the flow meters installed at the 50% ETc treatment irrigation lines.

Canopy architecture and components of yield

Canopy architecture was assessed using digital photography as previously reported by Martínez-Lüscher et al.(2019). The leaf area index (LAI) was assessed with the smartphone application VitiCanopy on an iOS operating system (Apple Inc., Cupertino CA, USA) (De Bei et al., 2016). The settings used for this vineyard site are briefly described by Yu et al. (2021). The total leaf area was calculated based on the measured LAI values multiplied by the unit ground area for each vine (3.15 m^2) that result from the planting spacing.

Clusters were harvested by hand at approximately 23 - 25° Brix, and all clusters in each treatment-replicate were harvested, counted, and weighed on a single harvest day each season. Yield components were assessed or calculated for cluster weight, yield per meter of row, leaf area to fruit ratio and crop water use efficiency (WUE_c). The WUE_c was calculated as the ratio between yields expressed as kg·ha^{-1} and the amount of water applied to each plot ($m^3 \cdot ha^{-1}$) according to (Medrano et al., 2015).

Water footprint assessment

Water footprint (WF) was calculated following the methods described in Zotou and Tsihrintzis (2017) with minor modifications (Torres et al., 2021). The vineyard received 20.2

kg·ha^{-1} of nitrogen, 20.2 kg·ha^{-1} of phosphorous and 41 kg·ha^{-1} of potassium injected and applied through the irrigation system in each year through a separate irrigation hose that delivered 4 L·h^{-1} per grapevine when shoots were approximately 40 cm long.

Briefly, WF was derived as the sum of the green, blue and grey WFs and expressed in m^3 of water consumed per tonne of fruit harvested. Green, blue, and grey components were calculated using the following equations:

$$\text{Eq. 2.} \qquad WF_{green} = \frac{\sum Pm}{Y}$$

where P_m is the monthly effective precipitation expressed in m^3·ha^{-1} after applying a conversion factor of 10 to the measure rainfall (mm) and Y is the yield of grapevines expressed in tonne·ha^{-1}.

$$\text{Eq. 3.} \qquad WF_{blue} = \frac{\sum WUm}{Y}$$

where WU_m is the total amount of irrigation water received monthly by the grapevines expressed in m^3·ha^{-1}and Y is the yield of grapevines expressed in tonne·ha^{-1}

$$\text{Eq. 4.} \qquad WF_{grey} = \frac{\alpha AR}{(cmax - cnat)\, Y}$$

where α is the percentage of fertilizer that leaches to the surrounding vineyard aquatic system; AR is the amount of fertilizer applied to the grapevines expressed in kg · ha^{-1}; c_{max} is the maximum acceptable concentration of fertilizer in the aquatic system (mg · L $^{-1}$); and c_{nat} is the natural concentration of the pollutant in the aquatic system (mg · L^{-1}). P_m values were obtained from the CIMIS weather station placed in the vineyard. For the calculation of grey component, only nitrogen fertilization was considered given the environmental problems derived from its use in agriculture (Kerlin, 2016). The percentage of nitrogen entering the surrounding water system of the area was assumed 10% according to Mekonnen and Hoekstra (2011). The maximum acceptable concentration of nitrogen (45 mg · L^{-1}) was obtained from CDFA (2020). According to Hoekstra

et al. (2011), the natural concentration of pollutants was taken equal to zero, as proposed when data was missing.

Cluster temperatures

Cluster temperatures were measured for each trellis system, irrigated at 50% ET_c. One cluster on the NW and SE sides of the vine canopy was marked for repeated measurements. Using an infrared thermometer, three temperature readings were taken from berries located at the top, middle and bottom of the clusters. The temperature measurements were conducted every two hours from 8:00h to 16:00h.

Statistical analysis

The statistical analysis for this experiment was performed using R Studio version 4.2.2 (RStudio: Integrated Development for R., Boston, MA, USA) for macOS. All data were subjected to the Shapiro-Wilk's normality test. Data was subjected to two-way analysis of variance (ANOVA) to assess the statistical differences between the trellis systems and irrigation treatments and their combination. Means ± standard errors (SE) were calculated and when the *F*-value was significant ($p \leq 0.05$), a Duncan's new multiple range *post-hoc* test was executed using "agricolae" 1.2-8 R package (de Mendiburu, 2016). Figures were created using GraphPad Prism version 9.5.1 (GraphPad Software, Boston, MA, USA).

Results

Weather conditions at the experimental site

Mean precipitation and monthly air temperatures were obtained from data measured at the CIMIS station (Figure 3). Precipitation measurements were recorded starting in October of

the previous year to account for dormant season precipitation. The severe drought in 2019-2020 and 2020-2021 growing seasons resulted in negligible precipitation in October of each year, while the research site received 230mm of precipitation in October 2021, thus in the fall preceding the 2022 growing season. Despite the wet winter months (October-January), the spring of 2022 was particularly dry compared to the spring of 2020 and 2021. Negligible precipitation was recorded between June and August in all growing seasons of the study. Data from the CIMIS weather station revealed that the 2021 growing season was characterized by the coolest mean air temperature in all months, except for that of October 2020. The 2020 and 2022 growing seasons showed similar temperature trends; however, the 2021-2022 season had the coolest December and the warmest March of the three years.

Irrigation treatments and trellis types affected grapevine WUE_c

During the course of the study years, WUE_c was significantly higher for the irrigation treatments at 25% and 50% ET_c compared to the 100% ET_c treatment (Figure 4A). The trellis systems did not affect WUE_c in 2020, but their effects were observed in 2021 and 2022 (Figure 4B). In 2021, SH had the greatest WUE_c followed by HQ and VSP60. Significantly lower WUE_c was observed in VSP, VSP80 and GY vines compared to SH. In 2022, SH vines had significantly higher WUE_c compared to all other trellis systems.

Yield and vegetative growth are impacted by trellis types and irrigation treatments

Yield per meter of grapevine row was significantly affected by trellis systems in each experimental year (Table 1). In 2020, SH, VSP, VSP60 and GY had similar fruit yields, while it was lower with the VSP80 and HQ. Likewise, SH in 2021 had greater yield compared to all

vertically shoot positioned trellises (VSP, VSP60, VSP80 and GY). HQ vines produced similar yield to SH vines in 2021. In the 2022 growing season, SH outperformed all VSP-type trellis systems again. Irrigation treatments produced a consistent pattern in yield per meter of vine row across all experimental years. Yield was consistently reduced in vines irrigated at 25% ET_c. compared to other irrigation treatments. In 2020, yield was similar between 50% and 100% ET_c treatments, while yield under 50% ET_c irrigation treatments was lower compared to vines irrigated at 100% ET_c in 2021. In 2022, vines irrigated at 50% ET_c and 100% ET_c yielded similarly at harvest.

In 2020, cluster mass was larger in vertically-shoot positioned trellis designs (VSP, VSP60, VSP80 and GY). Conversely, the smallest cluster mass was observed in SH vines. In 2021, cluster mass was largest in GY vines, followed by VSP, VSP60 and VSP80 treatments. Again, SH had the smallest cluster mass. In 2022, all vertically shoot positioned trellises (VSP, VSP60, VSP80 and GY) had comparable cluster mass and produced heavier clusters than SH and HQ vines. In this year, mass of SH and HQ clusters was similar and not statistically different from each other as in 2020 and 2021. Irrigation treatments in all years resulted in statistically significant effects on cluster mass. In 2020, cluster mass was lower in the 25% ET_c treatments compared to 50% and 100% ET_c treatments. In 2021, 50% ET_c treatments produced the largest cluster mass, with lower cluster mass again in the 25% ET_c treatments. In 2022, cluster mass was lower in both 25% and 50% ET_c irrigation treatments compared to the treatment at 100% ET_c.

Trellis systems effected LAI only in 2022. The VSP60, VSP80 and GY had the largest LAI, followed by SH and VSP vines. The HQ had the lowest LAI overall. Irrigation treatments consistently resulted in a statistically significant reduction of LAI with the 25% ET_c treatments compared to 50% and 100% ET_c treatments. In 2022, the effects of irrigation treatments were

negligible. Neither trellis types nor irrigation treatments affected leaf area to fruit ratio in any of the experimental years.

Total water footprint and its components are altered by irrigation treatments and trellis systems

The total water footprint and its components were calculated for each experimental year (Figure 5A-F). The 25% ET_c irrigation treatment had higher WF_{green} in the first two experimental years, but not in the third. Furthermore, the irrigation treatment at 25% ET_c had lower WF_{blue} in all three years. The effects of irrigation treatments on WF_{grey} and WF_{total} were only observed in 2020 and 2021, with the 25% ET_c treatments resulting in greater WF_{grey} and WF_{total} compared to those resulting with the 50% and 100% ET_c treatments. Irrigation treatments did not affect WF_{grey} and WF_{total} in 2022 (Figure 5C).

Trellis systems effected WF_{total} and its components. In 2020, WF_{blue} was the largest in HQ trellis and the lowest in SH trellis (Figure 5D). Trellis systems did not affect WF_{green}, WF_{grey} and WF_{total} in 2020 (Figure 5D). In 2021, WF_{green}, WF_{blue}, WF_{grey} and WF_{total} were lower in the SH and HQ trellis systems compared to all the vertically shoot positioned trellises (VSP, VSP60, VSP80 and GY) (Figure 5E). Contrary to the first two experimental years, there was no significant effect of trellis on WF_{total} and its components in 2022 (Figure 5F).

Discussion

Unpredictable variations of the mean air temperature and precipitation were observed over three experimental years

Climate change in hot viticultural regions brings two prominent challenges: higher air temperatures with unpredictable heat wave events and increased drought frequency (Marigliano

et al., 2022, 2023). At the experimental site in Oakville, CA, the 2021 growing season (April-October) was cooler than both the preceding and following growing seasons. Hot air temperatures may create untoward growing conditions that affect whole grapevine physiology (Martínez-Lüscher et al., 2017).

In hot viticultural regions like California, prolonged drought conditions are becoming more common and increasingly severe. In the current study, extreme and exceptional drought conditions were recorded across the three experimental years. Total precipitation at the experimental site during the water year (October 1st through September 30th) within the last decade was previously reported as approximately 768mm (CIMIS) (Torres et al., 2021; Marigliano et al., 2022). The total precipitation recorded during the 2019-2020 and 2020-2021 growing seasons was 234.2mm and 278.3mm, respectively and was substantially less than the long-term average. Precipitation recorded in the 2021-2022 season was 635.4mm, and while this was the wettest among the study years, precipitation remained below the long-term average precipitation for the region. The hyper-arid conditions across the three study years highlighted the necessity of irrigation water in production regions that were historically dry-farmed and are now affected by substantial changes in precipitation patterns.

Canopy architecture and yield components were responsive to trellis system and irrigation treatments

In the present study, LAI was affected by trellis system and irrigation water amount separately in each year. In the drier study years (2020 and 2021), trellis systems had negligible effects on LAI while irrigation treatments had statistically significant effects. In the 2020 and 2021 seasons, the 25% ET_c treatment exhibited smaller LAI than the 50 and 100% ET_c

treatments. This aligns with previous work which found that irrigating at 25% ET_c produces less leaves and smaller LAI than irrigation at 50 and 100% ET_c at the study vineyard with similar vintage climactic conditions (Torres et al., 2021).

In 2022, the wettest study year, effects due to trellis system effects were observed while effects due to applied irrigation water were negligible. In 2022, when trellis systems demonstrated greater effect on LAI, the VSP60, VSP80, GY and SH trellises had increased LAI values compared to the HQ and VSP trellises. Similar work comparing head-trained caned pruning, California Sprawl and single high wire training systems found that single high wire vines to had greater leaf area per vine than head-trained cane pruned vines (Kurtural et al., 2019). Additionally, HQ vines at the study vineyard previously demonstrated smaller leaf area than vertically shoot positioned trellis systems (Yu et al., 2022). Based on results obtained from that study, the authors concluded that HQ resulted in less leaf area and higher crown porosity due to HQ vines continuing to fill up spaces with new growth compared to relatively more established vertically shoot positioned trellis types. Given that the leaf area is a major component of LAI, this continuation of canopy growth could also explain differences observed in LAI values in 2022.

Selecting a trellis system is an important decision when establishing a vineyard to ensure proper solar radiation interception and penetration into the canopy to optimize fruit yields and ripening. It has been widely documented that divided trellis systems will produce more yield due to both increased leaf area to support photosynthesis as well as more buds retained per meter of vine row (Reynolds and Vanden Heuvel, 2009). In the present study, SH vines consistently produced the highest fruit yields per meter of vine row; however, there was a trade-off with cluster mass, as SH vines consistently had the smallest cluster mass in all years. Previous work

has demonstrated that trellis systems alter the allocation of carbohydrate resources in the vine (Reynolds, 1988). While there was no statistical difference in leaf area to fruit ratio among trellis systems, SH vines often had lower leaf area to fruit ratios (not statistically significant). As such, the retention of more buds for vines with sprawling canopies may require the vine to divide limited resources amongst a greater number of fruiting positions, thus resulting in smaller cluster mass.

Yield per meter of vine row and cluster mass responded as expected to various applied water amounts. In this present study, yield in all years increased when the applied irrigation water was increased from 25% to 50% ET_c. However, yields plateaued when irrigation was increased from 50% to 100% ET_c. Similar yield response to applied irrigation water amounts was observed in Thompson Seedless or Cabernet Sauvignon (*Vitis vinifera*. L) grapevines in hot climates (Williams et al., 2010; Torres et al., 2021).

Improving WUE_c through optimizing the amounts of applied irrigation water and trellis types

Crop water use efficiency (WUE_c) for grapevine is defined as the ratio between fruit yield and the amount of water consumptively used to produce that yield. Reducing the amounts of applied irrigation water through regulated deficit irrigation (RDI) is common in vineyard systems seeking to improve grape quality with minimal reductions in yield. In the present study, WUE_c decreased linearly with increasing amount of applied irrigation water. Improvements to WUE_c have been observed in hot viticultural regions when the applied irrigation water was reduced from full irrigation (100% ET_c) to irrigation aiming partial ET_c replacement, whether it be through RDI or partial root zone drying (Chaves et al., 2007; Edwards and Clingeleffer, 2013;

Torres et al., 2021). Regarding the trellis systems, in the present study the variations in fruit yield drove changes in WUE_c in 2021 and 2022. Improvements in water use efficiency were evident for SH trellises, as these vines produced higher yield with similar irrigation amounts compared to all other trellis systems.

Sprawling trellis systems and reduced irrigation amounts improved vine water footprint

Irrigation may be more necessary in the near future, especially in areas that were previously characterized by cool climates and that were historically dry farmed. With natural and legislative restrictions on available water supply for irrigation, wine grape growers will need to implement improved irrigation schedules that maximize WF_{green} and minimize WF_{blue} to reduce WF_{total}. The WF_{total} for vineyards outpaces that of other crops suitable for similar hot and dry environments such as olives and other fruit trees (Zotou and Tsihrintzis, 2017). Previous reports estimate vineyard water footprint as 2400 $m^3 \cdot tonne^{-1}$ (Mekonnen and Hoekstra, 2011). The total water footprints in the present study ranged from 1016.8 $m^3 \cdot tonne^{-1}$ to 3528.35 $m^3 \cdot tonne^{-1}$, which are in accordance with vineyard water footprint estimates (Mekonnen and Hoekstra, 2011). Variations in WF_{total} were due to seasonal precipitation (determining WF_{green}), amounts of applied irrigation water (determining WF_{blue}), and trellis system, and were driven primarily by the fruit yield achieved with different trellis systems.

Previous work in the Napa Valley quantified the total water footprint and its components on Cabernet Sauvignon on a VSP trellis under varied applied water amounts (Torres et al., 2021). Under the 25 % ET_c irrigation treatment, the authors reported a trade-off between WF_{blue} and WF_{grey}, with higher WF_{grey} compared to the irrigation treatments at 50% and 100% ET_c (Torres et al., 2021). In the present study, this trade-off was observed between the amounts of applied

irrigation applied water in the study years experiencing severe drought (2020 and 2021). While decreasing WF_{blue} is an objective for improving vineyard sustainability, D'Ambrosio et al. (2020) report the current vineyards' WF_{grey} to be unsustainable, as the actual runoff of surface water is unable dilute the pollutant load associated with the diffuse and point sources to values below the maximum acceptable concentration. Subsequently, increases in WF_{grey} were the contributing component resulting in higher WF_{total} among vines irrigated at 25% ET_c compared to irrigation treatmenrs at 50% and 100% ET_c. Under drought conditions, the WF_{total} of the 50% and 100% ET_c treatments were comparable. Thus, reducing the amounts of applied irrigation water from 100% to 50% ET_c would allow for water conservation in wine grape production vineyards. Previous work reported that irrigating at 50% ET_c was sufficient to maintain fruit yields, grape quality, and carbohydrate balance in seasons with scarce precipitation (Torres et al., 2021). While previous irrigation recommendations applied to VSP trellis systems, our study provides further evidence to support vineyard irrigation at 50% ET_c despite trellis system under drought conditions.

The effect of trellis system on water footprint varied depending on vintage, most likely due to variations in seasonal precipitation. In 2020, trellis system differences in WF_{blue} were significant; however not large enough to produce quantifiable improvements to WF_{total}. Unlike the trend observed with applied water amounts, there was no observable trade-off between WF_{blue} and WF_{grey} when comparing water footprints due to trellis systems. In fact, in 2021 when drought was more severe, free sprawling trellis systems like SH and HQ which reduced WF_{green} and WF_{blue} also reduced WF_{grey} and WF_{total}. Previous work on Chardonnay in California across multiple vintages reported differences in annual fruit yield as a driver of variation in vine water footprint (Williams, 2014). Likewise, increased yields in SH and HQ vines drove improvements

in WF_{blue} compared to VSP-type trellises, as higher fruit yields can be produced for a certain amount of applied irrigation water. Additionally, shifting from traditional VSP trellises to SH and HQ trellises provides a solution for improving WF_{grey} to more sustainable levels, thus reducing the potential for pollution of water bodies due to surface runoff from vineyards (D'Ambrosio et al., 2020). Overall, a reduction in WF_{total}, especially in drought conditions, will improve long-term vineyard sustainability.

It is important to mention that vine canopies in the SH and HQ trellises not only improve water footprint in drought years, but also provide a method for heat wave mitigation. Cluster temperatures were recorded on the morning and afternoon sides of grapevine canopies irrigated at 50% ET_c between 8:00 h and 16:00 h (Figure S1). Compared to VSP and GY trellis systems, VSP60, SH and HQ trellises reduced cluster temperature at 10:00 h on the east side of the canopy (Figure S1A). The ΔT between VSP and SH was 5.1° C. Reductions in cluster temperature were not observed on the west side of the canopy until 16:00 h (Figure S1B). SH vines produced clusters will the lowest temperature, while GY vines had clusters with the highest temperature. The ΔT between GY and SH clusters was 5.2° C.

Conclusion

The changing climate in the world's dominant wine grape production regions brings increased air temperatures and droughts. Additionally, social factors such as increasingly stringent environmental regulations on water supplies and usage, along with labor shortages challenge the future sustainability wine grape production systems. This study examined the water use efficiency and water footprints of six commonly used trellis systems under three irrigation regimes. Under drought experimental conditions, the SH trellis system provided the highest yield

per meter of grapevine row compared to all other trialed trellis systems while also providing a natural reduction in cluster temperatures. Subsequently, amounts of applied irrigation water corresponding to 50% of grapevine ET_c were able to maintain carbohydrate allocation in SH vines, also allowing for irrigation water conservation. Reductions in applied irrigation water to 50% ET_c improved vine water footprint and WUE_c. Such improvements are on target for reaching sustainable vineyard water footprints based on previous research works and estimates. In the prospects of a changing climate and reduction of available and trainable labor, our study provided information and evidence that SH irrigated toat least 50% of ET_c achieved adequate yield, while reducing the WF_{total} and improving WUE_c. As such, this study provides crucial information to wine grape growers and vineyard managers for planning replants or developing new wine grape production vineyards in the new climatic reality.

Author Contributions

SK designed the trial. LEM, RY, NT, and SK conducted the experiments. LEM curated the data and wrote the first version of the manuscript. All authors contributed to the article and approved the submitted version.

Funding

A graduate student stipend was provided to LEM from University of California Davis during the execution of the trial.

Conflict of Interest

The authors declare that the research was conducted in the absence of any commercial or financial relationships that could be construed as a potential conflict of interest.

References

Caravia, L., Collins, C., Petrie, P. R., and Tyerman, S. D. (2016). Application of shade treatments during Shiraz berry ripening to reduce the impact of high temperature. *Aust J Grape Wine Res* 22, 422–437. doi: 10.1111/ajgw.12248.

Castellarin, S. D., Matthews, M. A., Di Gaspero, G., and Gambetta, G. A. (2007). Water deficits accelerate ripening and induce changes in gene expression regulating flavonoid biosynthesis in grape berries. *Planta* 227, 101–112. doi: 10.1007/s00425-007-0598-8.

CDFA California Department of Food and Agriculture (2020). About Fertilizer. *CA.gov*. Available at: https://www.cdfa.ca.gov/is/ffldrs/about_fertilizer.html [Accessed March 23, 2023].

Chaves, M. M., Santos, T. P., Souza, C. R., Ortuño, M. F., Rodrigues, M. L., Lopes, C. M., et al. (2007). Deficit irrigation in grapevine improves water-use efficiency while controlling vigour and production quality. *Annals of Applied Biology* 150, 237–252. doi: 10.1111/j.1744-7348.2006.00123.x.

D'Ambrosio, E., Gentile, F., and De Girolamo, A. M. (2020). Assessing the sustainability in water use at the basin scale through water footprint indicators. *J Clean Prod* 244. doi: 10.1016/j.jclepro.2019.118847.

De Bei, R., Fuentes, S., Gilliham, M., Tyerman, S., Edwards, E., Bianchini, N., et al. (2016). Viticanopy: A free computer app to estimate canopy vigor and porosity for grapevine. *Sensors (Switzerland)* 16. doi: 10.3390/s16040585.

de Mendiburu, M. (2016). Package 'Agricolae.' Statistical Procedures for Agricultural Research. Version 1.

Dry, P. (2009). Bunch exposure management. *Australian Wine Research Institute*, 1–12.

Duchêne, E. (2016). How can grapevine genetics contribute to the adaptation to climate change? *Oeno One* 50, 113–124. doi: 10.20870/oeno-one.2016.50.3.98ï.

Edwards, E. J., and Clingeleffer, P. R. (2013). Interseasonal effects of regulated deficit irrigation on growth, yield, water use, berry composition and wine attributes of Cabernet Sauvignon grapevines. *Aust J Grape Wine Res* 19, 261–276. doi: 10.1111/ajgw.12027.

Hoekstra, A. Y., Chapagain A.K., Aldaya, M. M., and Mekonnen, M. M. (2011). *The Water Footprint Assessment: Setting the Global Standard*. , ed. Earthscan London: WATER Footprint Network.

IPCC, Hoegh-Guldberg, O., Jacob, D., Bindi, M., Brown, S., Camilloni, I., et al. (2018). "Impacts of 1.5°C Global Warming on Natural and Human Systems," in *Global Warming of 1.5C: An IPCC Special Report*, eds. V. Masson-Delmotte, P. Zhai, H. O. Portner, D. Roberts, J. Skea, P. R. Shukla, et al. (Helsinki: IPCC Secretariat), 175–311. Available at: http://hdl.handle.net/10138/311749.

Kerlin, K. (2016). California Nitrogen Assessment Shows the State of the Science on Nitrogen Use and Pollution. *UC Davis*. Available at: https://climatechange.ucdavis.edu/news/first state-level-nitrogen-assessment-shows-state-science-nitrogen-use-and pollution#:~:text=Much%20excess%20nitrogen%20from%20crops,is%20lost%20as%2 air%20pollution [Accessed March 23, 2023].

Kiparsky, M. (2016). Unanswered questions for implementation of the sustainable groundwater management act. *Calif Agric (Berkeley)* 70, 165–168. doi: 10.3733/ca.2016a0014.

Kurtural, S. K., Beebe, A. E., Martínez-Lüscher, J., Zhuang, S., Lund, K. T., McGourty, G., et al. (2019). Conversion to mechanical pruning in vineyards maintains fruit composition while

reducing labor costs in ‘merlot’ grape production. *Horttechnology* 29, 129–139. doi: 10.21273/HORTTECH04204-18.

Kurtural, S. K., and Gambetta, G. A. (2021). Global warming and wine quality: Are we close to the tipping point? *Oeno One* 55, 353–361. doi: 10.20870/oeno-one.2021.55.3.4774.

Marigliano, L. E., Yu, R., Torres, N., Medina-Plaza, C., Oberholster, A., and Kurtural, S. K. (2023). Overhead photoselective shade films mitigate effects of climate change by arresting flavonoid and aroma composition degradation in wine. *Front Plant Sci* 14. doi: 10.3389/fpls.2023.1085939.

Marigliano, L. E., Yu, R., Torres, N., Tanner, J. D., Battany, M., and Kurtural, S. K. (2022). Photoselective Shade Films Mitigate Heat Wave Damage by Reducing Anthocyanin and Flavonol Degradation in Grapevine (Vitis vinifera L.) Berries. *Frontiers in Agronomy* 4. doi: 10.3389/fagro.2022.898870.

Martínez-Lüscher, J., Brillante, L., and Kurtural, S. K. (2019). Flavonol profile is a reliable indicator to assess canopy architecture and the exposure of red wine grapes to solar radiation. *Front Plant Sci* 10, 1–15. doi: 10.3389/fpls.2019.00010.

Martínez-Lüscher, J., Chen, C. C. L., Brillante, L., and Kurtural, S. K. (2017). Partial Solar Radiation Exclusion with Color Shade Nets Reduces the Degradation of Organic Acids and Flavonoids of Grape Berry (Vitis vinifera L.). *J Agric Food Chem* 65, 10693–10702. doi: 10.1021/acs.jafc.7b04163.

Medrano, H., Tomás, M., Martorell, S., Escalona, J. M., Pou, A., Fuentes, S., et al. (2015). Improving water use efficiency of vineyards in semi-arid regions. A review. *Agron Sustain Dev* 35, 499–517. doi: 10.1007/s13593-014-0280-z.

Mekonnen, M., and Hoekstra, A. Y. (2011). National Water Footprint Accounts: The green, blue and grey water footprint of production and consumption. Volume 1: Main Report. Lincoln Available at: https://digitalcommons.unl.edu/wffdocs.

Munitz, S., Netzer, Y., and Schwartz, A. (2017). Sustained and regulated deficit irrigation of field-grown Merlot grapevines. *Aust J Grape Wine Res* 23, 87–94. doi: 10.1111/ajgw.12241.

Naulleau, A., Gary, C., Prévot, L., and Hossard, L. (2021). Evaluating Strategies for Adaptation to Climate Change in Grapevine Production–A Systematic Review. *Front Plant Sci* 11. doi: 10.3389/fpls.2020.607859.

Ollé, D., Guiraud, J. L., Souquet, J. M., Terrier, N., AgeorgeS, A., Cheynier, V., et al. (2011). Effect of pre- and post-veraison water deficit on proanthocyanidin and anthocyanin accumulation during Shiraz berry development. *Aust J Grape Wine Res* 17, 90–100. doi: 10.1111/j.1755-0238.2010.00121.x.

Pieri, P., Lebon, E., and Brisson, N. (2012). Climate Change Impact on French Vineyards as Predicted by Models. *Acta Hortic* 931, 29–37. doi: 10.17660/ActaHortic.2012.931.2.

Reynolds, A. G. (1988). Response of Okanagan Riesling Vines to Training System and Simulated Mechanical Pruning. *Am J Enol Vitic* 39, 205–212. doi: 10.5344/ajev.1988.39.3.205.

Reynolds, A. G., and Vanden Heuvel, J. E. (2009). Influence of grapevine training system on vine growth and fruit composition: A review. *Am J Enol Vitic* 60, 251–268. doi: 10.5344/ajev.2009.60.3.251.

Tomás, M., Medrano, H., Escalona, J. M., Martorell, S., Pou, A., Ribas-Carbó, M., et al. (2014). Variability of water use efficiency in grapevines. *Environ Exp Bot* 103, 148–157. doi: 10.1016/j.envexpbot.2013.09.003.

Torres, N., Yu, R., Martínez-Lüscher, J., Kostaki, E., and Kurtural, S. K. (2021). Effects of Irrigation at Different Fractions of Crop Evapotranspiration on Water Productivity and Flavonoid Composition of Cabernet Sauvignon Grapevine. *Front Plant Sci*. doi: 10.3389/fpls.2021.712622.

Vaz, M., Coelho, R., Rato, A., Samara-Lima, R., Silva, L. L., Campostrini, E., et al. (2016). Adaptive strategies of two Mediterranean grapevines varieties (Aragonez syn. Tempranillo and Trincadeira) face drought: physiological and structural responses. *Theor Exp Plant Physiol* 28, 205–220. doi: 10.1007/s40626-016-0074-6.

Williams, L. E. (2014). Effect of applied water amounts at various fractions of evapotranspiration on productivity and water footprint of chardonnay grapevines. *Am J Enol Vitic* 65, 215–221. doi: 10.5344/ajev.2014.12105.

Williams, L. E., and Ayars, J. E. (2005). Grapevine water use and the crop coefficient are linear functions of the shaded area measured beneath the canopy. *Agric For Meteorol* 132, 201 -211. doi: 10.1016/j.agrformet.2005.07.010.

Williams, L. E., Grimes, D. W., and Phene, C. J. (2010). The effects of applied water at various fractions of measured evapotranspiration on reproductive growth and water productivity of Thompson Seedless grapevines. *Irrig Sci* 28, 233–243. doi: 10.1007/s00271-009-0173 0.

Williams, L. E., and Heymann, H. (2017). Effects of applied water amounts and trellis/training system on grapevine water relations, berry characteristics, productivity and wine

composition of “Cabernet Sauvignon.” *Acta Hortic* 1150, 413–426. doi: 10.17660/ActaHortic.2017.1150.58.

Yu, R., Brillante, L., Torres, N., and Kurtural, S. K. (2021). Proximal sensing of vineyard soil and canopy vegetation for determining vineyard spatial variability in plant physiology and berry chemistry. *Oeno One* 55, 315–333. doi: 10.20870/oeno-one.2021.55.2.4598.

Yu, R., Torres, N., Tanner, J. D., Kacur, S. M., Marigliano, L. E., Zumkeller, M., et al. (2022). Adapting wine grape production to climate change through canopy architecture manipulation and irrigation in warm climates. *Front Plant Sci* 13. doi: 10.3389/fpls.2022.1015574.

Zotou, I., and Tsihrintzis, V. A. (2017). The water footprint of crops in the area of Mesogeia, Attiki, Greece. *Environmental Processes* 4, S63–S79. doi: 10.1007/s40710-017-0260-9.

Tables and Figures

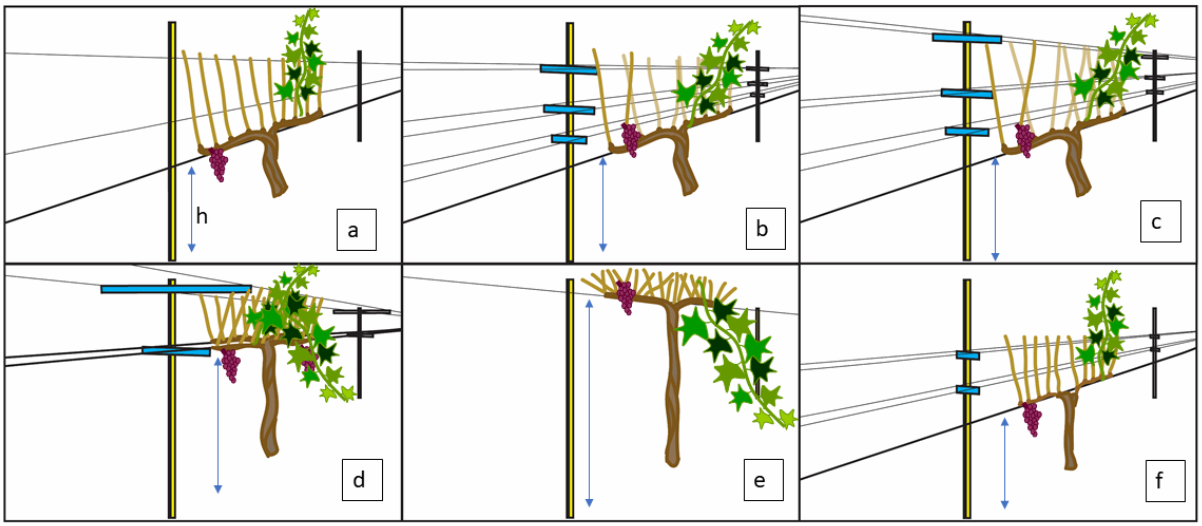

Figure 1. Illustrations of trellis systems established at Oakville Experimental Vineyard: (A) traditional vertical shoot position (VSP); (B) Vertical shoot position 60º (VSP60); (C) Vertical shoot position 80º (VSP80); (D) High quadrilateral (HQ); (E) Single high wire (SH); (F) Guyot-pruned vertical shoot position. "h" stands for the cordon height from the vineyard ground and the h for each trellis system was described in Materials and Methods. (Figure previously published in Yu et al., 2022)

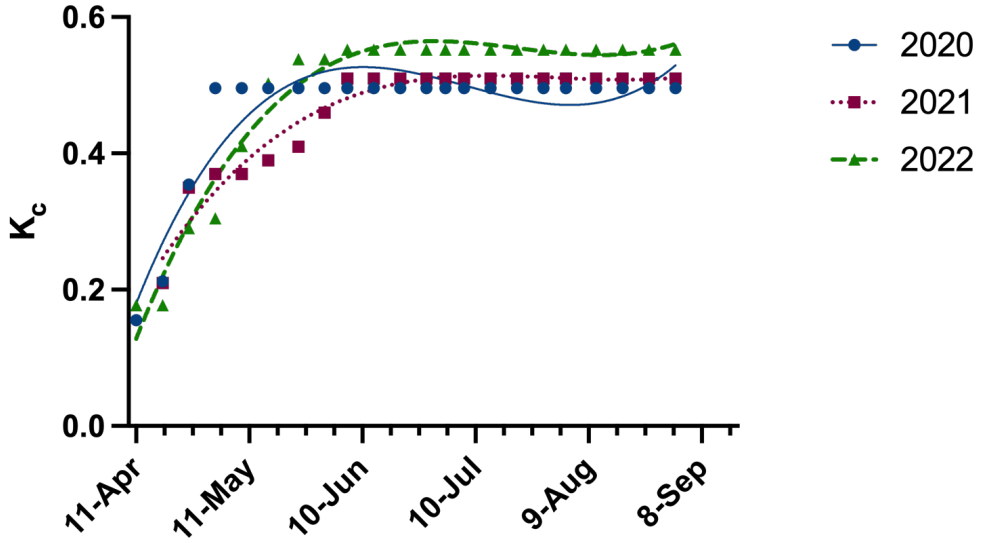

Figure 2. Regressions of crop coefficient (K_c) for each experimental year: 2020, 2021, 2022.

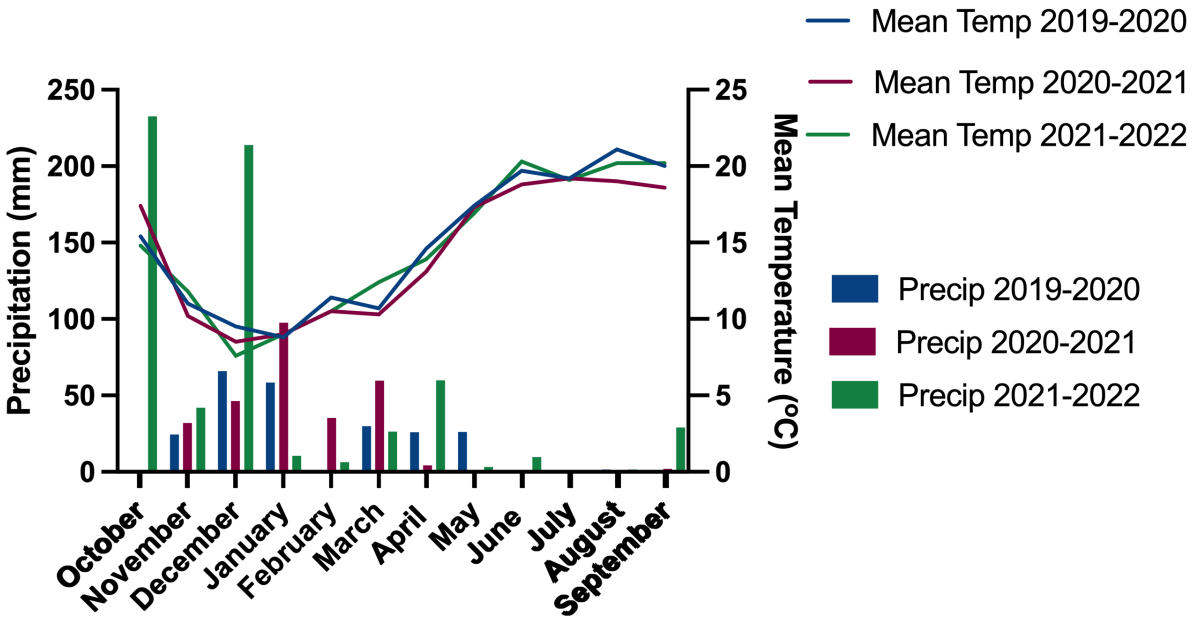

Figure 3. Mean air temperature (°C) and precipitation during the 2019-2020, 2020-2021 and 2021-2022 growing seasons. Weather data was obtained from CIMIS weather station #77 (Oakville, CA) located at the experimental site.

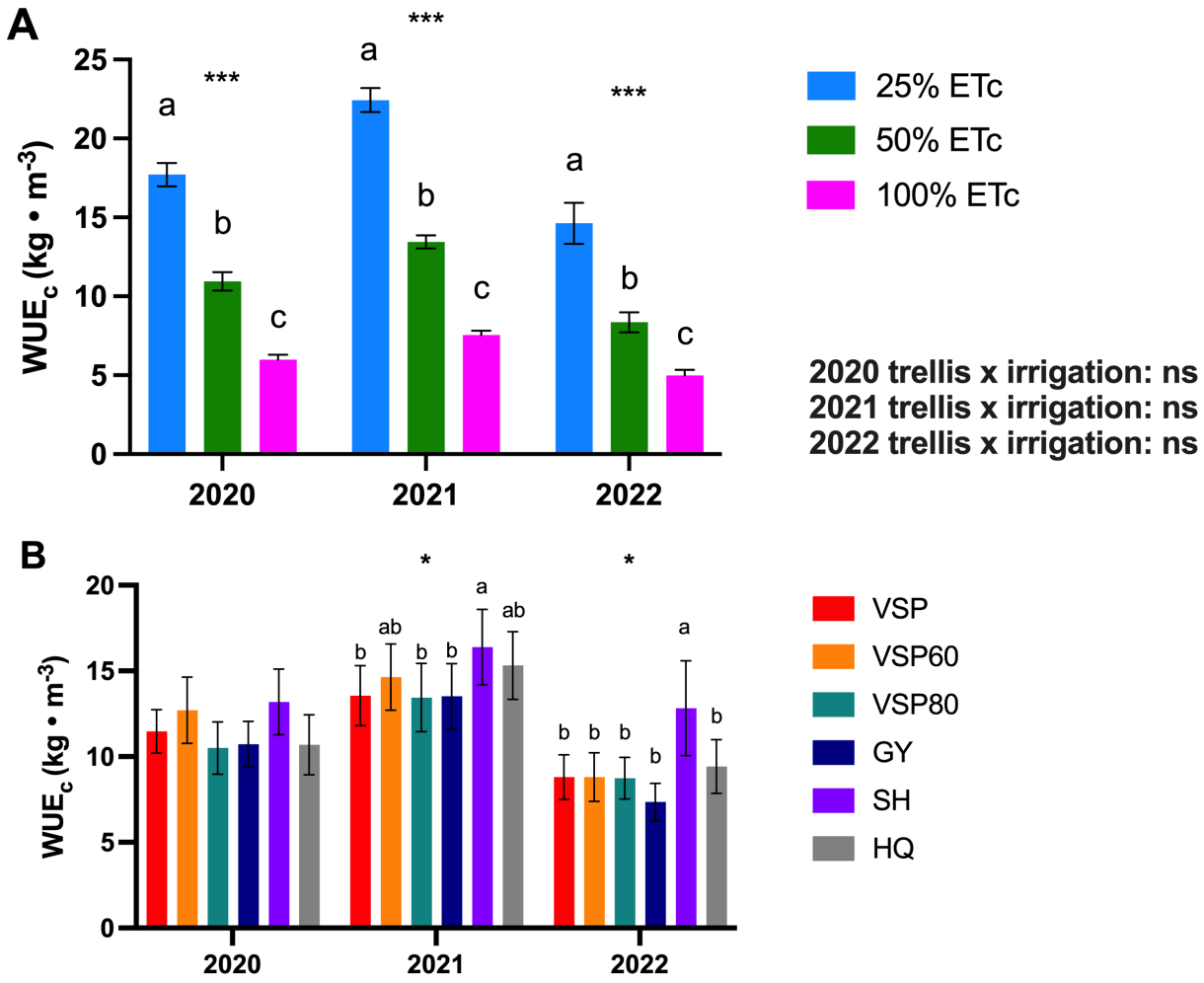

Figure 4. Crop WUE (WUE_c) of Cabernet Sauvignon grapevines (clone FPS08), subjected to (A) different replacements of crop evapotranspiration (25, 50, and 100% ET_c; n=3) and (B) six trellis systems (VSP, VSP60, VSP80, GY, SH, HQ; n=6) across three experimental years: 2020-2022. Values represent means ± SE. For each year, different letters indicate significant differences ($p \leq 0.05$) between irrigation treatments or trellis systems according to two-way ANOVA followed by Duncan's new multiple range *post-hoc* test. *, and *** indicate significance at 5, and 0.1% probability levels, respectively.

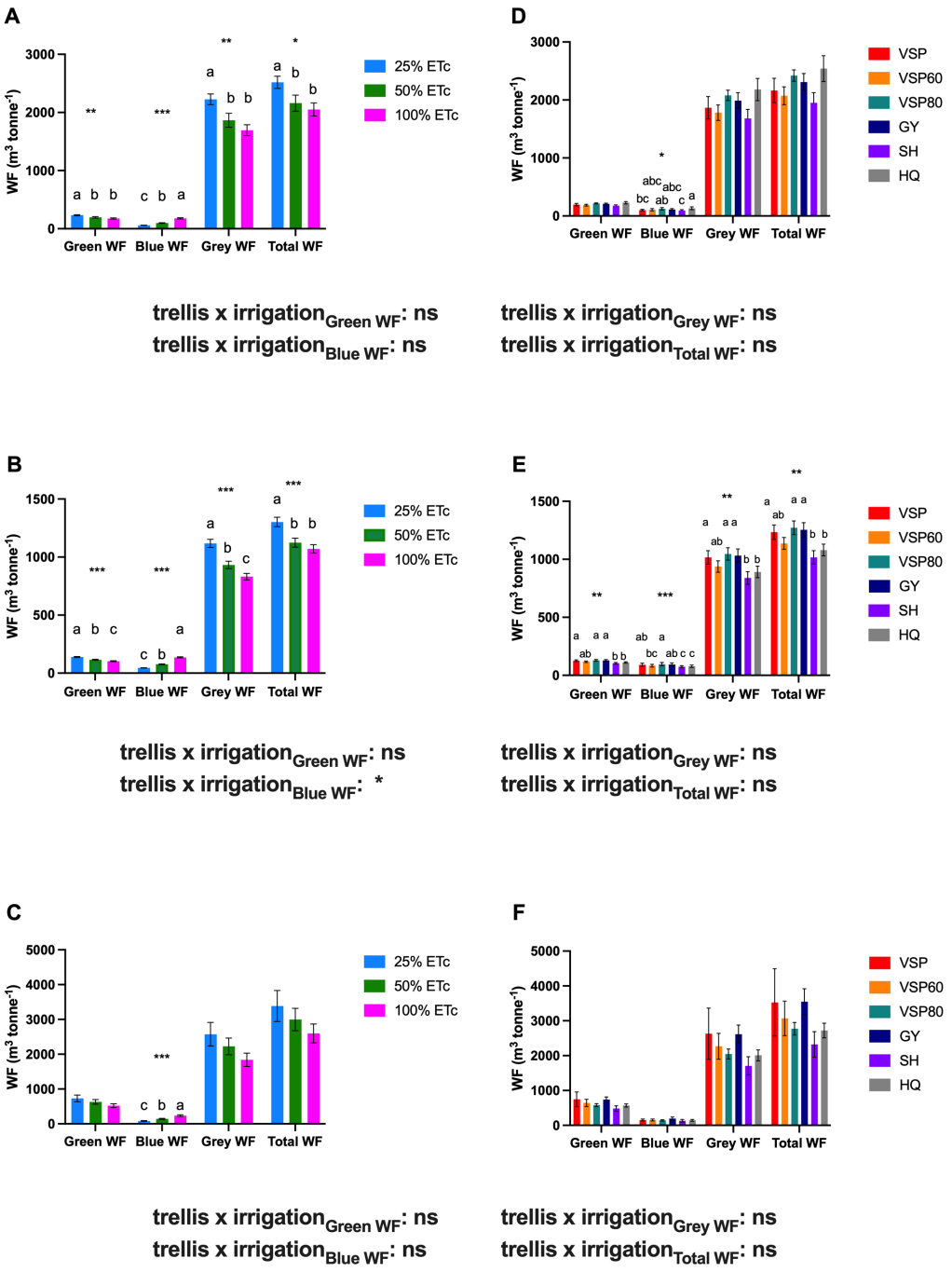

Figure 5. Water footprint (WF) components of Cabernet Sauvignon grapevines (clone FPS08) subjected to subjected to different replacements of crop evapotranspiration (25, 50, and 100% ET_c; *n*=3) and six trellis systems (VSP, VSP60, VSP80, GY, SH, HQ; *n*=6) over 2020 (A, F), 2021 (B, E) and 2022 (C, F) growing seasons. Values represent means ± SE. For each variable,

different letters indicate significant differences ($p \leq 0.05$) between irrigation treatments or trellis systems according to two-way ANOVA followed by Duncan's new multiple range *post-hoc* test. *, **, and *** indicate significance at 5, 1, and 0.1% probability levels, respectively.

Table 1. Reproductive and vegetative growth of Cabernet Sauvignon grapevines (clone FPS08) on six trellis systems subjected to different replacement of crop evapotranspiration (25, 50, and 100% ET_c) in Oakville, CA, USA, in 2020, 2021 and 2022 growing seasons

	Yield ($kg \cdot m^{-1}$ linear row)	Cluster mass (g)	Leaf Area Index (LAI)	Leaf Area: Fruit ($m2 \cdot kg^{-1}$)
2020				
Trellis				
VSP	4.15 ± 0.34 ab	132.76 ± 10.71 a	1.25 ± 0.07	1.02 ± 0.09
VSP60	4.22 ± 0.32 ab	133.40 ± 5.63 a	1.43 ± 0.07	1.11 ± 0.07
VSP80	3.47 ± 0.16 b	120.48 ± 7.04. a	1.21 ± 0.05	1.11 ± 0.05
GY	3.76 ± 0.29 ab	138.97 ± 6.98 a	1.49 ± 0.08	1.30 ± 0.08
SH	4.58 ± 0.38 a	74.18 ± 2.99 c	1.35 ± 0.10	0.97 ± 0.07
HQ	3.47 ± 0.26 b	97.24 ± 6.53 b	1.34 ± 0.10	1.36 ± 0.21
p-value	*	***	ns	ns
Irrigation				
25% ET_c	3.30 ± 0.14 b	100.00 ± 5.17 b	1.18 ± 0.04 b	1.15 ± 0.05
50% ET_c	4.08 ± 0.22 a	118.39 ± 6.51 a	1.42 ± 0.05 a	1.19 ± 0.10
100% ET_c	4.46 ± 0.24 a	130.12 ± 7.21 a	1.44 ± 0.06 a	1.10 ± 0.09
p-value	***	***	***	ns
trellis x irrigation	ns	ns	ns	ns
2021				
Trellis				
VSP	7.19 ± 0.39 c	161.60 ± 6.49 ab	1.54 ± 0.09	0.69 ± 0.04
VSP60	7.79 ± 0.46 bc	166.29 ± 5.86 ab	1.48 ± 0.08	0.61 ± 0.04
VSP80	6.93 ± 0.33 c	163.00 ± 7.54 ab	1.50 ± 0.08	0.69 ± 0.05
GY	7.06 ± 0.37 c	183.37 ± 6.71 a	1.32 ± 0.08	0.60 ± 0.04
SH	8.76 ± 0.49 a	106.05 ± 8.19 c	1.77 ± 0.17	0.64 ± 0.06
HQ	8.21 ± 0.47 ab	132.79 ± 28.26 bc	1.44 ± 0.12	0.53 ± 0.05
p-value	***	***	ns	ns
Irrigation				
25% ET_c	6.47 ± 0.22 c	133.21 ± 7.95 b	1.34 ± 0.05 b	0.66 ± 0.03
50% ET_c	7.76 ± 0.24 b	167.90 ± 13.96 a	1.64 ± 0.09 a	0.64 ± 0.04
100% ET_c	8.73 ± 0.31 a	155.43 ± 7.00 ab	1.55 ±0.08 a	0.57 ± 0.04
p-value	***	*	*	ns

trellis x irrigation	ns	ns	ns	ns
2022				
Trellis				
VSP	3.99 ± 0.51 ab	95.39 ± 10.07 a	1.28 ± 0.06 bc	1.48 ± 0.40
VSP60	3.64 ± 0.33 b	92.88 ± 5.71 a	1.59 ± 0.12 a	1.56 ± 0.23
VSP80	3.64 ± 0.27 b	98.71 ± 7.13 a	1.66 ± 0.08 a	1.48 ± 0.07
GY	3.00 ± 0.31 b	96.89 ± 4.82 a	1.64 ± 0.11 a	1.89 ± 0.21
SH	5.03 ± 0.60 a	48.98 ± 6.67 b	1.55 ± 0.11 ab	1.12 ± 0.14
HQ	3.84 ± 0.40 ab	55.11 ± 4.21 b	1.23 ± 0.07 c	1.08 ± 0.09
p-value	*	***	**	ns
Irrigation				
25% ET_c	3.30 ± 0.29 b	74.71 ± 5.60 b	1.42 ± 0.06	1.58 ± 0.19
50% ET_c	3.77 ± 0.29 ab	78.39 ± 5.69 b	1.52 ± 0.06	1.50 ± 0.15
100% ET_c	4.50 ± 0.32 a	90.88 ± 7.17 a	1.55 ± 0.09	1.22 ± 0.14
p-value	*	*	ns	ns
trellis x irrigation	ns	ns	ns	ns